INFORMATION TO USERS

This manuscript has been reproduced from the microfilm master. UMI films the text directly from the original or copy submitted. Thus, some thesis and dissertation copies are in typewriter face, while others may be from any type of computer printer.

The quality of this reproduction is dependent upon the quality of the copy submitted. Broken or indistinct print, colored or poor quality illustrations and photographs, print bleedthrough, substandard margins, and improper alignment can adversely affect reproduction.

In the unlikely event that the author did not send UMI a complete manuscript and there are missing pages, these will be noted. Also, if unauthorized copyright material had to be removed, a note will indicate the deletion.

Oversize materials (e.g., maps, drawings, charts) are reproduced by sectioning the original, beginning at the upper left-hand corner and continuing from left to right in equal sections with small overlaps.

Photographs included in the original manuscript have been reproduced xerographically in this copy. Higher quality 6" x 9" black and white photographic prints are available for any photographs or illustrations appearing in this copy for an additional charge. Contact UMI directly to order.

ProQuest Information and Learning
300 North Zeeb Road, Ann Arbor, MI 48106-1346 USA
800-521-0600

Characterisation of Phenol Hydroxylase and its Auxiliary Proteins, DmpM and DmpK, from *Pseudomonas* sp. Strain CF600

Elisabeth Cadieux

A Thesis

in

The Department

of

Chemistry and Biochemistry

Presented in partial Fulfillment of the Requirements

For the Degree of Doctor of Philosophy at

Concordia University

Montreal, Quebec, Canada

January 2002

ABSTRACT

Characterisation of Accessory Proteins, DmpK and DmpM, Associated with Multicomponent Phenol Hydroxylase

Elisabeth Cadieux, Ph. D.

Concordia University, 2002

Phenol hydroxylase from *Pseudomonas* sp. strain CF600 is an enzyme comprising three components: DmpP, a reductase containing an FAD and a [2Fe-2S] cluster; DmpM, an activator protein required for efficient catalysis; and DmpLNO, an oxygenase containing a binuclear iron cluster. The oxygenase requires an accessory protein, DmpK, for diiron cluster assembly. This thesis describes the characterisation of DmpM, DmpK, and DmpLNO.

DmpM was found to exist in two forms. DmpM purified from the native strain was active in stimulating phenol hydroxylase activity, whereas an inactive dimeric form accumulated when DmpM was expressed in *E. coli* Various treatments readily activated dimeric DmpM. Dissociation of the dimeric form of DmpM was shown to precede denaturation at low protein concentrations resulting in activation.

Assembly of the binuclear iron center in the oxygenase component of phenol hydroxylase was examined in the presence and absence of DmpK, a protein required for *in vivo* synthesis of active oxygenase. DmpK had an effect on reconstitution of apo-oxygenase only at lower ratios of Fe^{2+}/apo-oxygenase and it accelerated reconstitution. DmpK did not stably bind Fe^{2+}, and could not donate Fe^{2+} in the presence of chelators, suggesting that its primary role is not to deliver Fe^{2+} to the active site. When the

binuclear iron site was occupied by Mn^{2+}, DmpK and Fe^{2+} were required for reconstitution. This suggests a role for DmpK in metal ion discrimination.

The oxygenase is made up of three copurifying polypeptides, DmpLNO. Single turnover experiments confirm that DmpLNO contains the active site, but requires DmpM for efficient turnover. Mössbauer, EPR and UV/vis spectroscopy data, demonstrated the presence of two types of binuclear iron centers in DmpLNO. Treatment of the oxygenase with hydrogen peroxide and/or DTT was investigated in order to understand why a significant proportion of the enzyme was inactive.

Site-directed and random mutagenesis were performed on DmpM to identify residues involved in its interaction with the oxygenase. Although mutation of six conserved residues activated phenol hydroxylase in steady-state assays, the double mutant M37T/V77A, resulting from random mutagenesis, did not activate phenol hydroxylase. These results suggest that multiple substitutions are necessary to affect DmpM's interaction with the oxygenase component.

ACKNOWLEDGMENTS

First and foremost, I want to thank Justin Powlowski. His supervision and support are the source of this text. I want to thank him in particular for his constant, careful and thoughtful criticisms. He has taught me much more than the mechanics and techniques of research. He has given me a perspective of science that gives meaning to what I do.

Next I want to thank my committee members: Judith Kornblatt, who was the first person to encourage me on the path that led here. She was always supportive and enthusiastic about the journey. Next, Joanne Turnbull: every doctoral student should have a Joanne on their team. Joanne is, most importantly a good friend and an inspiration.

The faculty of Concordia's Chemistry and Biochemistry Department have all enriched this experience. I want to thank in particular Ann English, Paul Joyce and Jack Kornblatt.

Many thanks to my lab mates for their friendship, kindness and support, in particular, Roch, Nathalie, Jun, Dinesh, Sue, Pam, Lena and Kelly. Pascale Gaudet has been a constant support, a drinking buddy and a friend. Thanks to Alexander for formatting the text and graphics of this thesis.

Finally, I want to thank my family: Tiffany, Gregoire, Fred, William, Ann and Barry for their love and encouragement.

This thesis is dedicated to my mother and grandmother whose memory inspires me, and Alexander for his immense patience and love.

TABLE OF CONTENTS

LIST OF FIGURES

LIST OF TABLES

LIST OF ABREVIATIONS

ACP, acyl carrier protein

BCA, bicinchoninic acid

CD, circular dichroism

CoA, coenzyme A

Dmp, dimethyl phenol

DTT, dithiothreitol

E.coli, Escherichia coli

EDC, 1-ethyl-3-[3-dimethylaminopropyl]-carbodiimide hydrochloride

EPR, electron paramagnetic resonance

EXAFS, extended x-ray absorption fine structure

FAD, flavin adenine dinucleotide

IAEDANS, 5-((((2-iodoacetyl)amino)ethyl)amino)naphthalene-1-sulfonic acid

ICP-MS, inductively coupled plasma-mass spectrometry

IPTG, isopropyl-1-thio-β-D-galactopyranoside

ITC, isothermal titration calorimetry

MMO, methane monooxygenase

MMOB, activator protein of methane monooxygenase

MMOH, oxygenase component of methane monooxygenase

MMOR, reductase component of methane monooxygenase

MOPS, 3-[N-morpholino]propanesulfonic acid

NADH, dihrdronicotinamide adenine dinucleotide

NADPH, dihydronicotinamide adenine dinucleotide phosphate

NHS, N-hydroxysuccinimide

NMR, nuclear magnetic resonance

PAGE, polyacrylamide gel electrophoresis

PCR, polymerase chain reaction

R1, subunit 1 of ribonucleotide reductase

R2, subunit 2 of ribonucleotide reductase

RNR, ribonucleotide reductase

SDS, sodium dodecyl sulfate

TCA, trichloroacetic acid

TCEP, Tris(2-carboxyethyl)phosphine

TFE, trifluoroethanol

Thr, threonine

Tris, Tris[hydroxymethyl]aminomethane

UV/Vis, ultraviolet/visible

CONTRIBUTIONS OF AUTHORS

Chapter 2 is published in *Biochemistry* (1999) **38**, 10714-10722 with Justin Powlowski and I as co-authors. I performed all the experiments, and co-wrote the manuscript.

Chapter 3 is a manuscript submitted for publication with Justin Powlowski and I as co-authors. I performed all the experiments, and co-wrote the manuscript.

Chapter 4 is a manuscript submitted for publication with the following authors: Elisabeth Cadieux, Vladislav Vrajmasu, Catalina Achim, Eckard Münck, and Justin Powlowski. Vladislav Vrajmasu, Catalina Achim and Eckard Münck obtained and interpreted the Mössbauer and EPR data. I prepared the samples for them and performed all other experiments. The manuscript was written by Justin Powlowski and me except for the sections on the EPR and Mössbauer spectroscopies, which were written by the Mössbauer group: Vladislav Vrajmasu, Catalina Achim, Eckard Münck at the Carnegie Mellon Institute.

I authored Chapter 5 and the Introduction, with the indispensible editing advice of Dr. Justin Powlowski.

I prepared the first drafts of all the manuscripts.

Chapter 1

Introduction

1.1 INTRODUCTION

Billions of kilograms of phenol are produced annually by distillation of petroleum, oxidation of cumene or toluene, and by hydrolysis of chlorobenzene. The major use of phenol is in the production of phenolic resins that are used in the construction and appliance industries. It is also an ingredient in consumer products ranging from slimicide to mouthwash. However, phenol is a highly toxic substance for animals. Disposal of phenol is done by controlled burning but it can be degraded by microbes that use phenols as sole sources of carbon and energy.

Microbes capable of degrading phenol have been exposed to biologically-produced phenols and methyl-substituted phenols for a long time. Phenol degrading bacteria were isolated as long ago as 1932 (1). One of the best-studied phenol degrading bacteria is *Pseudomonas* sp. strain CF600 originally reported by Shingler *et al.* (2). This organism harbours the plasmid-encoded *dmp* operon that encodes phenol hydroxylase and associated *meta*-cleavage pathway enzymes. *Meta*-cleavage refers to ring cleavage by insertion of O_2 adjacent to the two hydroxyls of catechol (Fig 1.1). In contrast, other phenol degrading bacteria use an *ortho*-cleavage pathway where ring cleavage occurs between the hydroxyl groups of catechol. From this step on, the pathway relies on a completely different set of enzymes required for metabolizing the ring cleavage product (3).

The phenol/dimethylphenol (*dmp*) pathway of *Pseudomonas* sp. strain CF600 is encoded on a plasmid exceeding 200kb in size (2). There are fifteen genes in the *dmp* operon encoding the enzymes of the pathway. The first six genes, *dmpKLMNOP*, encode polypeptides associated with the first enzyme in the pathway, phenol hydroxylase. This

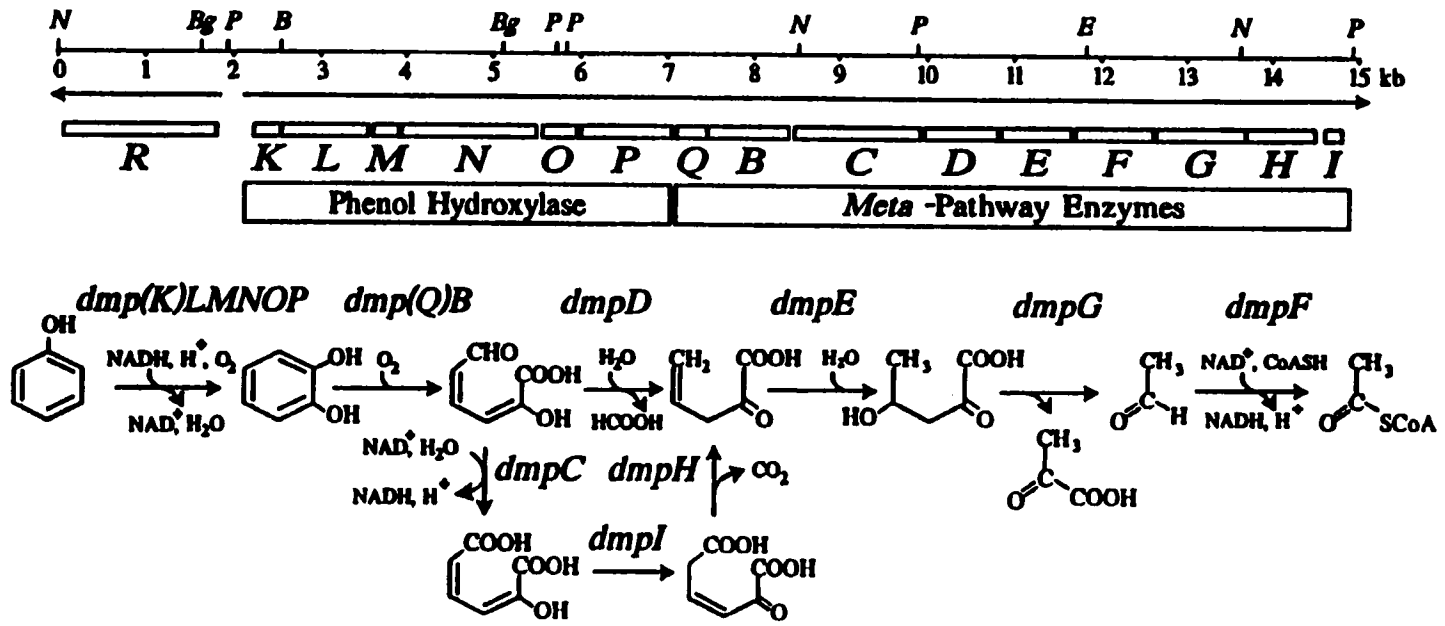

Figure 1.1 Phenol degradation pathway in P*seudomonas* sp. strain CF600. Adapted from reference 12.

enzyme catalyses the hydroxylation of phenol to form catechol. The remaining nine genes of the operon, *dmpQBCDEFGHI*, encode the *meta*-cleavage pathway enzymes for the conversion of catechol to pyruvate and acetyl-CoA (4, 5, 6).

The polypeptide products of *dmpLMNOP* are required for *in vitro* phenol hydroxylase activity (7). The enzyme is arranged as three components: DmpP is an FAD, [2Fe-2S]$^{+}$ center containing NADH-dependent reductase; DmpLNO are three polypeptides that copurify, where DmpN contains conserved ligands for a non-heme diiron containing active site; and DmpM is an activator protein lacking any metals or cofactors (Fig 1.2).

The multicomponent nature of the *Pseudomonas* sp. strain CF600 phenol hydroxylase is somewhat unusual. The first reported purification of a hydroxylase for phenol degradation was for the phenol hydroxylase from the yeast *Trichosporon cutaneum* (8). This is a single polypeptide hydroxylase that catalyses FAD-mediated activation of molecular oxygen, much like other bacterial monooxygenases for hydroxyl-containing aromatics (9). The 2-electron reduced flavin reacts initially with O_2 to form a flavin 4a-hydroxoperoxide intermediate, and delocalization of electrons into the ring from the hydroxyl group of the substrate aids in attack on the flavin-activated oxygen (10). Unlike flavoprotein monooxygenases, the multicomponent phenol hydroxylase from *Pseudomonas* sp. strain CF600 is more similar to methane and toluene monooxygenases, whose substrates are considerably less susceptible to oxygenation than phenol.

Methane monooxygenases from *Methylosinus trichosporium* and *Methylococcus capsulatus* (Bath) have been relatively well characterized (reviewed in ref 11). Both enzymes are made up of five polypeptides reminiscent of multicomponent phenol

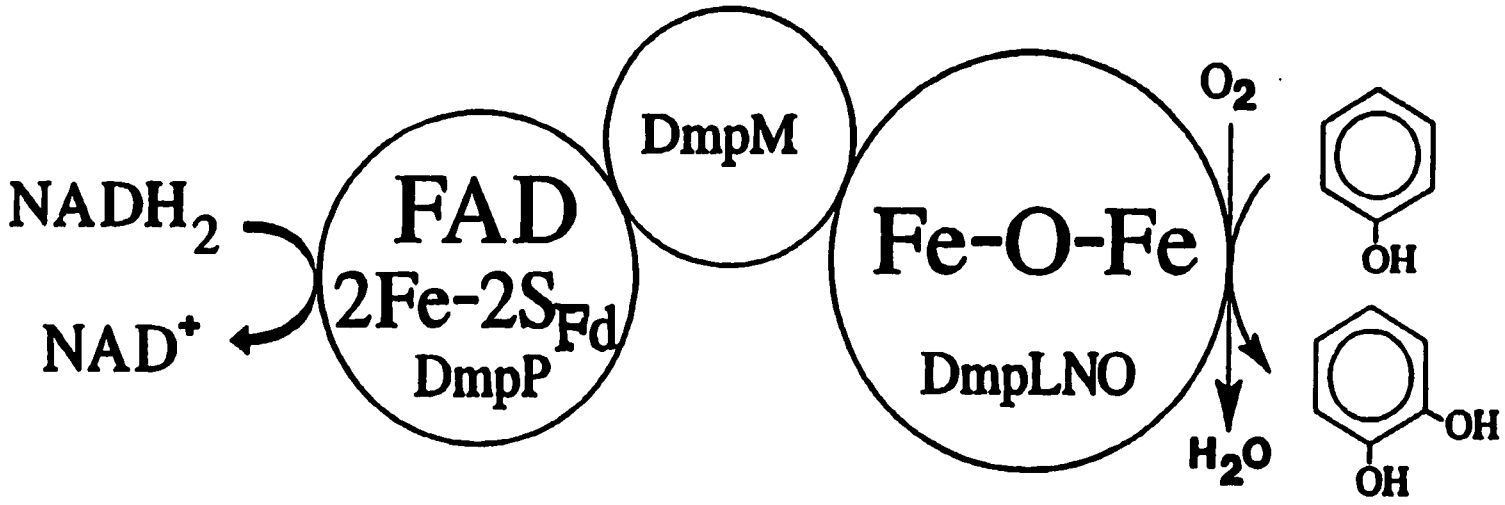

Figure 1.2 Cartoon representation of phenol hydroxylase. The figure is adapted from reference 67.

hydroxylase: one is a reductase with FAD and an iron-sulfur center; three polypeptides copurify and contain the diiron-binding motif; the other is a cofactorless protein essential for efficient catalysis. The reductases of phenol hydroxylase and methane monooxygenase share 28% identity at the amino acid level, while the activator proteins (MmoB for methane monooxygenase and DmpM for phenol hydroxylase) share 27% identity (12). There is very little overall identity between the amino acid sequences of the other three polypeptides of phenol hydroxylase and methane monooxygenase. Despite this, DmpN and MmoX appear to share identically spaced ligands for a diiron site (13). The crystal structure of methane monooxygenase shows that its binuclear iron center is ligated by two histidines and four glutamate residues (Fig 1.3) (14).

Another well-studied enzyme that contains a binuclear iron center is ribonucleotide reductase. Although it does not catalyze oxygenase chemistry, ribonucleotide reductase has a binuclear iron center ligated by two histidines, one aspartate, and three glutamate residues (Fig 1.3) (15). The spacing of these ligands in ribonucleotide reductase and methane monooxygenase is very similar, although they share very little overall sequence identity. Note the differences in the bridging ligand of the oxidized binuclear iron centers: it is hydroxo for methane monooxygenase and oxo for ribonuclotide reductase (Fig 1.3).

Other oxygenases either known or postulated on the basis of amino acid sequence to contain binuclear iron centers include toluene-2-monooxygenase (16), toluene-3-monoxygenase (17, 18), and toluene-4-monooxygenase (19). These enzymes are capable of hydroxylating toluene to the corresponding *o*-, *m*-, or *p*-cresols, respectively. Alkane monooxygenases can epoxidize various alkenes and alkynes: they too contain similar

Methane Monooxygenase

Ribonucleotide Reductase

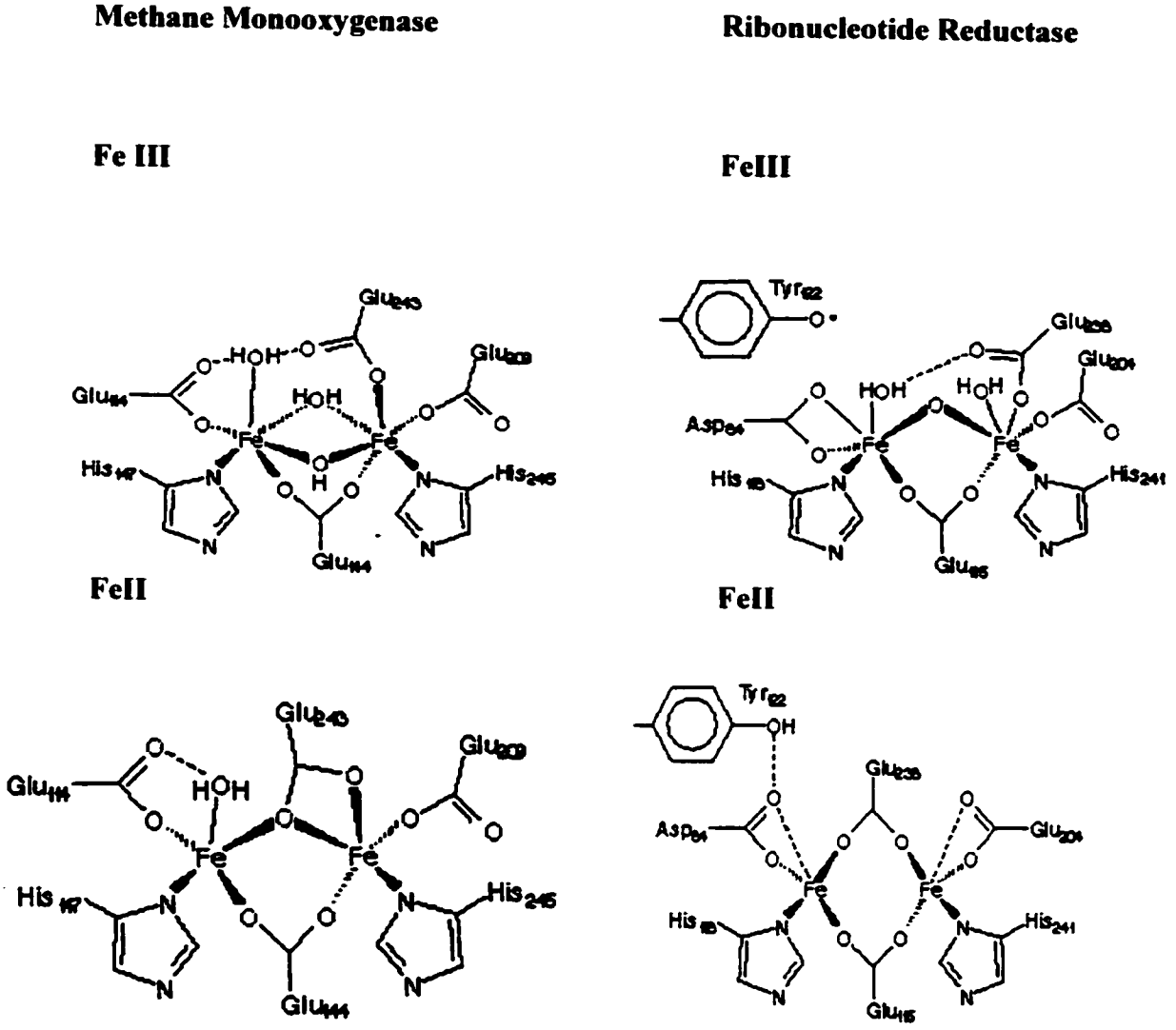

Figure 1.3 Active site of Methane Monooxygenase and Riboneucleotide Reductase. The figure is found at http://bmbsgi11.leeds.ac.uk/promise/FEFEMAIN.html#function.

components to phenol hydroxylase, with a non-heme carboxylate bridged diiron center predicted on the basis of sequence comparisons (20). However, none of these oxygenases are as well characterised as methane monooxygenase.

The scientific interest in studying diiron center containing proteins is that they can perform a variety of functions, and understanding the factors that tune diiron centers to perform a specific function is interesting and important. These various functions include: *hydroxylation* by oxygenases (21, 22); *iron storage* by ferritins (23); and *oxygen transport* by hemerythrin (24). Clearly, the protein environments around the diiron centers of these proteins must direct the center reactivity.

Since methane monooxygenase has been studied extensively in the past decade, and considering the apparent similarity between phenol hydroxylase and methane monooxygenase, methane monooxygenase is a useful starting point for understanding phenol hydroxylase. I will therefore describe the key features of methane monooxygenase in more detail.

1.1.2 Methane Monooxygenase

There are two well-characterized soluble methane monooxygenases, one from *M. trichosporium* and the other from *M. capsulatus* (Bath). They catalyse the oxygenation of methane to methanol (eq 1):

$$CH_4 + NADH + H^+ + O_2 \longrightarrow CH_3OH + NAD^+ + H_2O \qquad \text{(eq 1)}$$

Methanol is then converted to formaldehyde by methanol dehydrogenase. Carbon can either be assimilated at this point, or formaldehyde dehydrogenase and formate dehydrogenase catalyse the formation of CO_2 (25).

As described in the previous section, methane monooxygenase consists of three proteins, a hydroxylase (MMOH), a reductase (MMOR), and a regulatory protein (MMOB), all of which are required for optimal catalytic activity (22,26). The hydroxylase is comprised of three polypeptides arranged as an $\alpha_2\beta_2\gamma_2$ heterodimer (14). The structure and function of each component is considered in more detail below.

The Reductase Component : MMOR

MMOR, like DmpP, contains an FAD and an iron-sulfur cluster on a single polypeptide (22, 27). The iron-sulfur center of MMOR has been characterised by EPR and Mössbauer spectroscopies (13). The spectra are typical of [2Fe-2S]-type ferredoxins. Two electrons from NADH are stored in the flavin and Fe-S cluster of MMOR before transport to the diiron site of MMOH (27, 28, 29). Experiments have shown that MMOR also causes changes in the structure and reactivity of MMOH through the formation of a tight complex with the α subunit (29, 30).

The Activator Component : MMOB

MMOB is a 15.9 kDa protein lacking any prosthetic groups. Addition of MMOB to the other MMO components increases the turnover rate in steady-state assays by 150-fold (30). Maximum activity is reached at 2 moles MMOB per hydroxylase $\alpha\beta\gamma$ protomer, with a decrease in rate observed at higher concentrations of MMOB. Chemical cross-linking data indicate that MMOB interacts with the α subunit of the hydroxylase (30). Furthermore, MMOB has been shown to perturb the EPR spectra of the mixed

valent (Fe(II)-Fe(III)) and the reduced (Fe(II)-Fe(II)) forms of the hydroxylase, indicating that MMOB binding alters the environment of the diiron active site (30).

MMOB also affects the redox potential of the MMOH diiron center (31). In this study, reductive titrations of MMOH alone and complexed with MMOR and MMOB were done to determine the redox potential of the oxygenase component in each complex. MMOB was found to decrease the average midpoint potential value by 132 mV. It was also found that the dissociation constant for the MMOB-MMOH complex increases by 3-4 orders of magnitude upon reduction. Together, these two pieces of data provide evidence for a mechanism by which the affinity of the MMOB-MMOH complex may be coupled to the catalytic cycle. Thus, MMOB binds to oxidized MMOH, and upon reduction, the decrease in MMOB affinity would cause MMOB to dissociate.

MMOB also affects the regioslectivity of the methane monooxygenase reaction. This was shown by studying the oxygenation of isopentane, where hydroxylation can occur at the primary, secondary or tertiary carbons. In the absence of MMOB, hydroxylation at the tertiary carbon produced the major product whereas in the presence of MMOB the primary carbon was the dominant hydroxylation site (32).

MMOB was found to increase the rate of O_2 reactivity with diferrous MMOH, by 1000-fold, monitored by EPR spectroscopy (33). The significance of this effect is to maximize the rate of turnover and minimize the reactivity of O_2 with other species.

The NMR structures of MMOB from both *M.capsulatus* (Bath) and *M. trichosporium* OB3b have been reported (34, 35). The structure of DmpM of *Pseudomonas* sp. CF600 has also been solved by NMR although the resolution of the structure is lower than those of the MMOB proteins. (36). MMOB and DmpM appear to have similar overall structures. The main difference between the two structures is that

DmpM apparently has a hole in the middle of the protein big enough for phenol to fit, possibly allowing it to be involved in substrate binding and channelling. This hole is absent in MMOB. NMR and proteolysis experiments have shown that the N-terminus of MMOB is functionally important and is the region interacting with MMOH (37, 38). In this context, it is interesting to note that DmpM of phenol hydroxylase lacks the amino-terminal 33 residue extension of MMOB. NMR experiments carried out with MMOB in the presence of MMOH pinpointed other sites of interaction, such as : E53, E94, G97, F100, and D108 (35). These residues are conserved in other hydroxylase effector protein sequences, including DmpM of phenol hydroxylase, TbmC of toluene-2-monooxygenase, TmoD of toluene-4-monooxygenase, and TbuV of toluene-3-monooxygenase.

Despite these observations, the mechanism by which this small cofactorless protein regulates MMO hydroxylation are not well understood.

The Oxygenase Component : MMOH

High resolution crystal structures are available for MMOH proteins of *M. trichosporium* OB3b and *M. capsulatus* (Bath) in different crystal forms and oxidation states (14, 39, 40, 41).

Although the global conformation of the proteins in these different forms remains the same, some differences are observed at the diiron center. The structure of MMOH is an $\alpha_2\beta_2\gamma_2$ dimer, and consists mostly of α-helical secondary structure (14, 41). α-Helical contacts between the α and β subunits from each protomer are responsible for dimer formation. The γ subunits, positioned on the outer sides of the hydroxylase are not involved in protomer contacts. The diiron active site is situated in a four-helix bundle in the core of the α subunit. Other dioxygen activating enzymes such as the R2 subunit of

ribonucleotide reductase and stearoyl-ACP Δ^9 desaturase have a similar four helix-bundle surrounding the diiron center (15, 42, 43).

The diiron center of MMOH has been extensively examined by various techniques including EPR, Mössbauer, EXAFS, and Raman spectroscopies, as well as x-ray crystallography (13, 14, 41, 44, 45, 46, 47). The binuclear iron center of oxidized MMOH contains two antiferromagnetically spin-coupled irons, as observed by Mössbauer spectroscopy. This center exhibits no ground state EPR signal, but an integer spin EPR signal is observed upon reduction. Most of the spectroscopic techniques suggest that the as-isolated form of binuclear iron center has a protonated oxo-bridge between the two Fe atoms.

The interest in studying the binuclear iron centre of methane monooxygenase is to understand how the extremely stable C-H bond of methane is broken, and also how molecular oxygen is activated by the binuclear iron center. The ground state of the dioxygen molecule (O_2) has two unpaired electrons each located in the π^* antibonding orbital. The two unpaired electrons have the same spin quantum number, meaning that they have parallel spins, and therefore O_2 is in the triplet state. In order for O_2 to oxidize another atom or molecule, the atom or molecule must have two electrons in parallel spin to fit into the vacant π^* orbital of O_2. Most biomolecules have covalent bonds that consist of two electrons of opposite spins occupying the same orbital (hence, singlet state). The reaction of molecular oxygen with biomolecules is therefore referred to as "spin restricted" (48). One way of increasing the reactivity of dioxygen is to move one of the two electrons in a way as to alleviate the spin restriction, forming singlet O_2. However, singlet O_2 is extremely reactive and so Nature has found another way to make it react with

organic molecules : oxygen must be activated by complexation with a transition metal. The diiron center of methane monooxygenase, as well as other oxygenases with a binuclear iron center, provide the site for controlled O_2 activation.

INTERMEDIATES OF THE CATALYTIC CYCLE

Much work on MMOH during the last decade has been focused on elucidating steps in the activation of O_2. Early on, single turnover experiments showed that reduced MMO can react with O_2 and substrate to form hydroxylated products and oxidized MMO in the absence of the other MMO components. The single turnover reaction proves that activation of dioxygen and hydroxylation both take place on MMOH (22, 49). Figure 1.4 shows the intermediates in the catalytic cycle detected during single turnover in the absence of the other MMO components. These species have been detected by various techniques including stopped-flow optical spectroscopy, freeze-quench in combination with EPR, Mössbauer, and EXAFS spectroscopies.

Evidence for the existence of the Fe(II)-Fe(II) species in reduced samples was established by the observation of an EPR signal with g = 16 (30). The decay of Fe(II)-Fe(II) species can be followed by monitoring this signal, and the rate of decay is dependent on the presence of MMOB, and independent of the O_2 concentration (33, 49, 50, 51).

Following the decay of the diferrous intermediate, the next species that can be observed by Mössbauer and optical spectroscopies is the peroxo form of MMOH

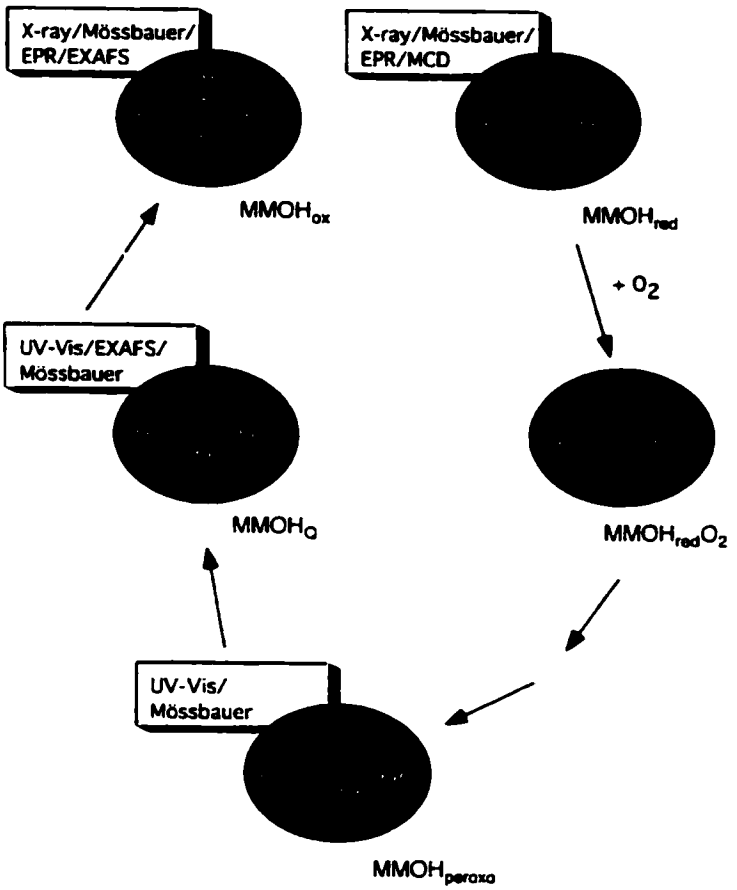

Figure 1.4 Catalytic intermediates observed for the single turnover reaction during Methane Monooxygenase catalysis. Techniques used to charecterise the intermediates are indicated. The figure was adapted from reference 11.

($MMOH_{peroxo}$). $MMOH_{peroxo}$ from *M. capsulatus* (Bath) has optical bands at 450 nm (ε = 4000 M^{-1} cm^{-1}) and 725 nm (ε = 1800 M^{-1} cm^{-1}) (49, 52, 53). A similar intermediate has been reported for the enzyme from *M. trichosprium* OB3b, with an optical band at 700 nm (ε = 2500 M^{-1} cm^{-1}) (54).

$MMOH_{peroxo}$ is converted to an oxo intermediate called $MMOH_Q$. The formation and decay of $MMOH_Q$ can be monitored by stopped-flow spectrophotometry due to its bright yellow color (53, 55). The decay rate of $MMOH_Q$ increases in the presence of hydrocarbon substrate, thus identifying $MMOH_Q$ as the oxygenating intermediate. $MMOH_Q$ has been characterized by rapid freeze-quench Mössbauer and EXAFS spectroscopies (49, 56, 57). The Mössbauer data suggest that $MMOH_Q$ has an Fe(IV)-Fe(IV) cluster with antiferromagnetic coupling between the two iron atoms. The EXAFS data indicate the presence of at least two single oxygen bridges between the irons. Whether the O-O bond is cleaved homolytically or heterolytically has been an important mechanistic question in the conversion of $MMOH_{peroxo}$ to $MMOH_Q$. The two possibilities are represented in Figure 1.5, but so far there is not enough evidence to distinguish which mechanism actually occurs.

The question of how $MMOH_Q$ hydroxylates methane and other substrates has been difficult to answer since no intermediates have been observed for this step by using rapid mixing spectroscopic methods. Substrate probes and theoretical studies heve been used to probe the mechanistic details (reviewed in 11). On the basis of these experiments, many mechanistic pathways have been proposed and are listed in Figure 1.6, but more experiments are needed to delineate the chemical characteristics of the hydroxylation step.

1.1.3 Toluene Monooxygenases

After methane monooxygenase, the next best characterized dinuclear iron centre monooxygenase is toluene 4-monooxygenase (T4MOH) from *Pseudomonas mendocina* KR1 (58). T4MOH hydroxylase comprises three polypeptides, TmoA, TmoB, and TmoE, with TmoA providing the diiron site. Other components required for toluene hydroxylation *in vitro* are TmoD, an effector protein; TmoC, a Reiske ferredoxin; and TmoF, an NADH oxidoreductase (59). Toluene-2-monooxygenase (T2MO) from *Burkholderia cepacia* G4 has been purified and characterised as a three-component oxygenase reminiscent of the three component system of methane monooxygenase and phenol hydroxylase (60). The low specific activity of 2 milliunits/mg for T2MO compared to 300 milliunits/mg for T4MO suggests that perhaps the T2MO system also requires a ferredoxin component like the T4MO four-component enzyme system described above (59, 60).

Single turnover experiments demonstrated that T4MOH alone could catalyze the conversion of toluene to *p*-cresol, with a product yield of 8%. Addition of TmoC or TmoD did not change the yield obtained from single-turnover of T4MOH. The effector protein, TmoD, shares 34% sequence identity with the activator protein DmpM of phenol hydroxylase and 29% identity with MMOB of methane monooxygenase (61). The solution structure of TmoD exhibits an N-terminal βαββ domain and a C-terminal βααβββ domain. Although the general structure is similar to the MMOB proteins from *M. capsulatus* and *M. trichosporium*, it differs from DmpM of phenol hydroxylase (61). Sub-stoichiometric TmoD was found in purified samples of T4MOH, suggesting that TmoD

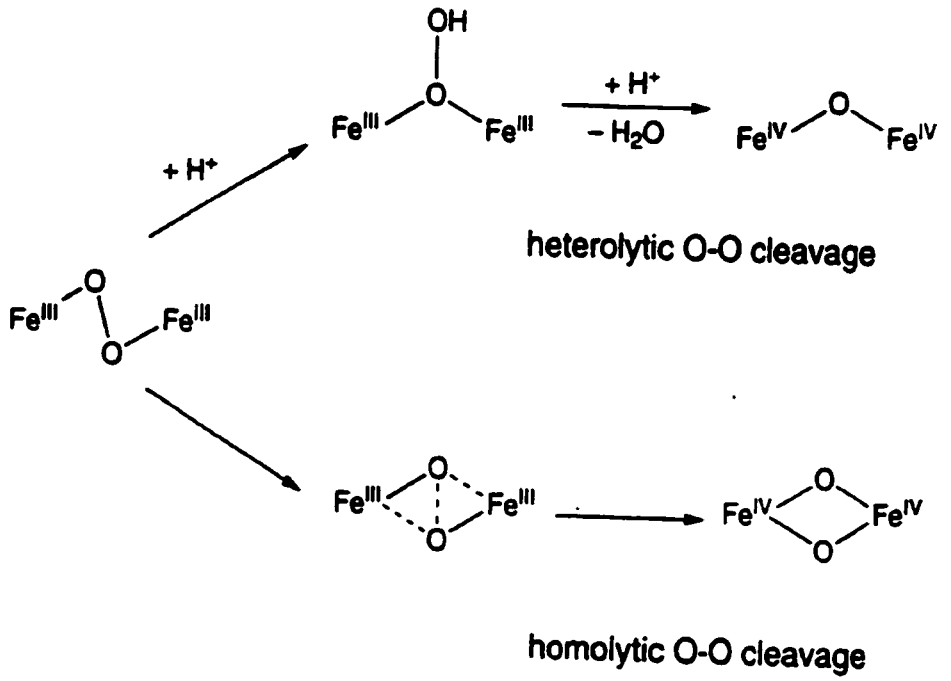

Figure 1.5 Heterolytic cleavage and homolytic cleavage proposed for methane monooxygenase. The figure was adapted from reference 11.

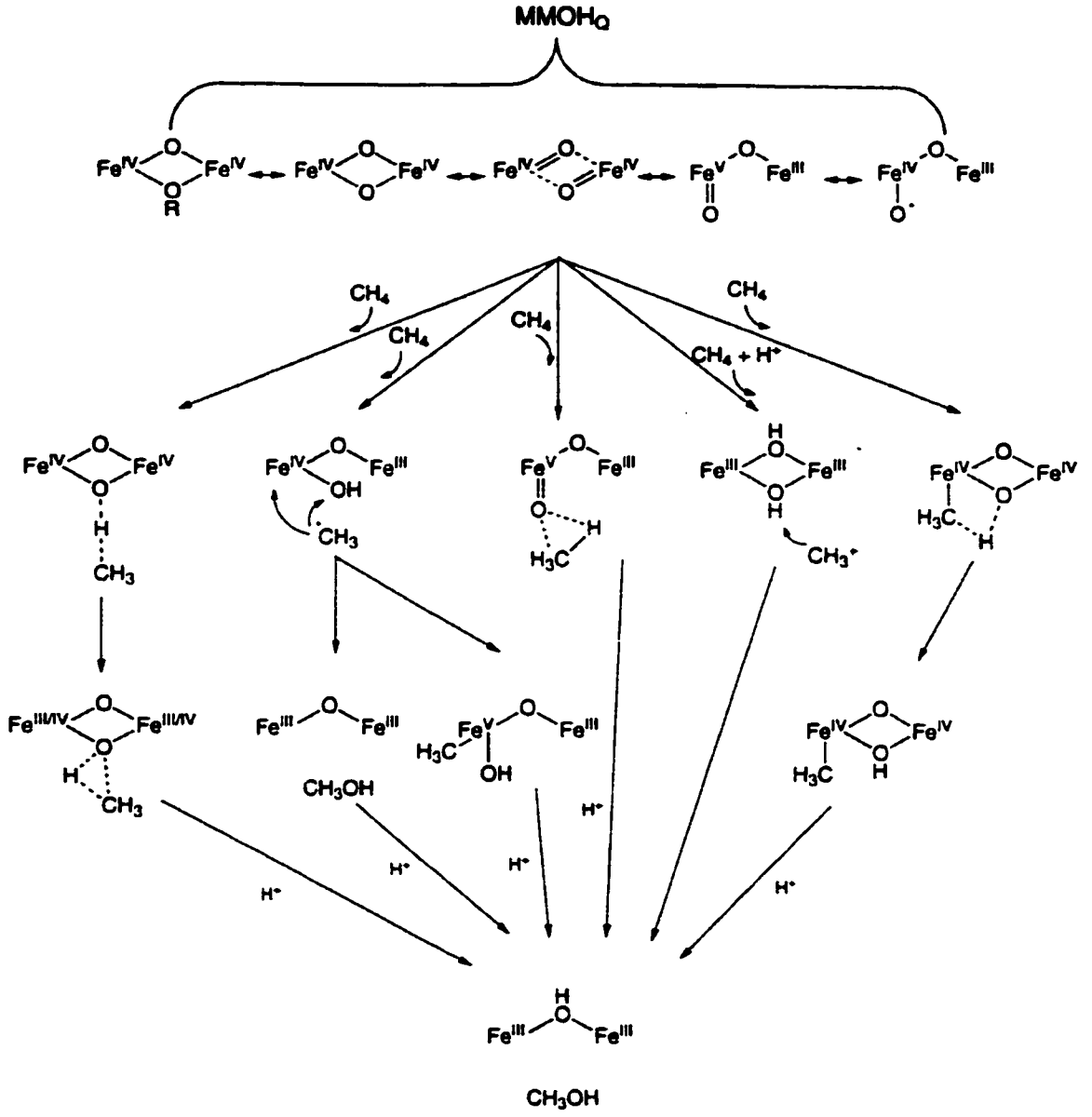

Figure 1.6 Mechanism of hydroxylation by methane monooxygenase. The figure was adapted from reference 11.

has a higher affinity for the differic state of T4MOH than does MMOB for diferric MMOH (59).

Heme-containing P-450 monooxygenases have provided a wealth of information about enzymatic iron-mediated oxygen activation. Sequence alignments of these enzymes show a conserved active-site Thr residue (62). The role of this conserved threonine has been investigated by mutagenesis of various P-450 monooxygenases. Protonation of dioxygen is believed to be required for the O-O bond to be cleaved during the catalytic cycle. The conserved threonine residue is thought to stabilize the oxygen-bound intermediate by forming a hydrogen bond to the iron-bound oxygen. Substitution of alanine for the conserved threonine in cytochrome P-450BM-3, a monooxygenase from *Bacillus megaterium*, resulted in impaired hydroxylation due to uncoupling of NADH consumption and substrate hydroxylation (63). The same substitution in neuronal nitric-oxide synthase caused an increase in catalytic activity compared to the wildtype (64).

Primary sequence alignments of diiron-containing oxygenases show that they also have a conserved threonine residue, and the x-ray structure of methane monooxygenase reveals that this residue, Thr-213 is located near the diiron active site (39). Thr-213 was proposed to have an important role in catalysis, possibly by acting as a proton donor during O_2 activation in the reaction cycle (39, 65). However, this hypothesis cannot be tested in methane monooxygenase since it cannot be expressed in recombinant form. Therefore, site directed mutagenesis on the conserved threonine residue in T4MOH, Thr-201, was done to investigate its role in catalysis (66). The catalytic activities, coupling efficiencies and regioselectivity of toluene hydroxylation were determined for these mutants and the results showed that Thr-201 is not essential for catalysis of toluene

hydroxylation by T4MOH (66). To date, no other reports of site-directed mutagenesis have appeared for other residues in this class of enzymes.

1.2 The Role of DmpK in Phenol Degradation

DmpK is located just upstream of the phenol hydroxylase genes in the *dmp* operon (Fig.1.1). The polypeptide product has been overexpressed and purified (67). The 10 kDa protein was devoid of any cofactors or metals. Gene deletion experiments showed that expression of *dmpK*, together with phenol hydroxylase and the enzymes required for catabolizing catechol, is essential for growth of cells on phenol via the multicomponent phenol hydroxylase. Paradoxically, DmpK is not necessary for *in vitro* phenol hydroxylase activity (68), and in fact it inhibits activity at relatively low concentrations (67).

The interaction of DmpK with phenol hydroxylase has been examined in some detail (67). Chemical cross-linking studies using purified proteins demonstrated that DmpK interacts with the two largest subunits of the oxygenase component of phenol hydroxylase (DmpLNO). In this study, the activities of the oxygenase component in crude extracts when expressed with or without *dmpK* gene product were also compared. It was found that crude extracts containing the oxygenase expressed in the absence of *dmpK* exhibited no phenol hydroxylase activity. In contrast, oxygenase expressed in the presence of *dmpK* was active in crude extracts. These results suggested that DmpK is involved in assembly of the oxygenase in an active form. Further hints about the mechanism of activation were gained by adding ferrous iron and purified DmpK to *in vitro* assays of hydroxylase activity in crude extracts. Adding ferrous iron to the crude extract from cells co-expressing *dmpLNO* and *dmpK* resulted in a 2-fold increase in

activity. This suggested that there was some inactive oxygenase present in the crude extract, probably apoenzyme, formed either because of sub-optimal expression of DmpK or iron loss from the oxygenase during cell breakage. In the absence of co-expression of DmpK, the crude extract contained inactive hydroxylase, and addition of ferrous iron alone resulted only in slight activation. Addition of ferrous iron *and purified DmpK* to crude extract from cells expressing *dmpLNO* but not *dmpK* resulted in activation of the oxygenase almost to levels observed in crude extracts from cells co-expressing DmpK and oxygenase. These results strongly suggested that DmpK plays an important role in iron incorporation into apo-oxygenase.

Based on amino acid sequence comparisons, there are DmpK-like proteins associated with multicomponent phenol hydroxylase from other organisms such as *Pseudomonas putida* P35X (69), *Pseudomonas putida* H (70), and *Pseudomonas stutzeri* (71). Also DmpK shares 61% identity with TomA associated with toluene-2-monooxygenase from *Burkholeria cepacia* G4. However, functions of these proteins is unknown. To investigate further how DmpK functions, it is essential to consider what is known about iron metabolism in bacteria.

1.2.1 Iron Transport and Storage in Bacteria

Iron storage and transport in bacteria and animals has been the topic of numerous review articles (23, 72). This section summarizes some relevant details.

Iron can exist in aqueous solution in two oxidation states: Fe^{2+} and Fe^{3+}. Ferric iron at physiological pH undergoes polymerization, forming insoluble ferric hydroxides. Since iron available in the environment is in the ferric form, microbes have developed mechanisms for iron solubilization and transport. Bacteria synthesize chelators derived

from catechols or hydroxamic acids that have high affinity for ferric iron (73). These chelators are called *siderophores*, and are secreted into the extracellular milieu. The Fe(III)-siderophore complex then enters the cell via a specific receptor. Once in the cell, Fe(III) is reduced to Fe(II) which dissociates from the siderophore. Alternative release mechanism involves hydrolysis of the Fe-siderophore, freeing Fe(III).

For multicellular organisms, iron assimilation is quite different. Proteins such as serum globulin and transferrin complex iron for transport in the circulation, from which the Fe-transferrin complex is taken up by cells via receptors. Iron release from the complex is pH dependent, and occurs due to the action of proton pumps. For example, there is evidence that the Fe-transferrin-receptor complex is internalized by endosomes where a proton pump acidifies the endosome vesicle to pH 5.5-5.0 (74, 75). Under these conditions, the iron is released from the transferrin-receptor complex and is delivered to the cytoplasm. The iron free transferrin-receptor is then targeted back to the plasma membrane and the extracellular alkaline pH releases the apo-transferrin into circulation for reutilisation.

Release of free iron in any cell type poses a potentially damaging problem. Oxidation of ferrous iron by molecular oxygen is represented by the following, known as the Fenton reaction:

$$Fe(II) + O_2 \longrightarrow Fe(III) + O_2^{\cdot-}$$

$$2O_2^{\cdot-} + 2H^+ \longrightarrow H_2O_2 + O_2^{\cdot-}$$

Free Fe(II) in solution within a cell would produce radical species which are highly toxic to the cell. Organisms therefore must protect themselves by having efficient iron storage proteins: in the case of bacteria, these are ferritin and bacterioferritin. These proteins can

hold up to 4500 Fe atoms per protein as solid ferric mineral in a large cavity of 0.8 nm in diameter in a cavity surrounded by 24 polypeptides (76).

A large number of proteins require iron for activity. The importance of iron in biological systems lies in its ability to cycle between Fe(III) and Fe(II) and to form various kinds of complexes, thus allowing a wide range of functions in catalysis and transport. There are reversible *oxygen binding* proteins, such as haemoglobin and myoglobin, in animals. *Oxygenases* include diiron mono-oxygenases, the haem P-450 oxygenases, and the mononuclear iron dioxygenases. There is a whole variety of iron-sulfur proteins involved in *electron transfer* and other types of reactions. Exactly how proteins aquire iron from intracellular stores is only just starting to be understood.

It has generally been thought that metal insertion into proteins and enzymes occurs *in vivo* simply by diffusion, due to lack of evidence suggesting otherwise and because metal centers can often be spontaneously reconstituted *in vitro*, (e.g. ribonucleotide reductase (77) and methane monooxygenase (78)). Since the discovery of accessory proteins involved in assembly of some metallocenters, this view is changing. While proteins assisting in metallocenter assembly are known to exist for a few enzymes, their mechanisms of action are surprisingly complex and often obscure. They include proteins involved in assembly of: the nickel-containing urease from *Klebsiella aerogenes;* the complex nitrogenases from *Azotobacter vinelandii* and *Klebsiella pneumoniae*; multicopper oxidase Fe3 from yeast; and copper-zinc superoxide dismutase from yeast. Examination of what is known about the mechanism of metal incorporation in these few examples may provide clues as to how DmpK functions. The uniqueness of DmpK precludes comparison with more closely related proteins.

1.2.2 PROTEIN-ASSISTED METALLOENZYME ASSEMBLY

UREASE

Urease from *Klebsiella aerogenes* consists of a trimer of trimers encoded by *ureA*, *ureB*, and *ureC*, with each UreC containing a bi-nickel metallocenter at the active site (79). One Ni^{2+} is co-ordinated to two histidine residues, an aspartate residue, and a carbamylated lysine residue. The other Ni^{2+} is co-ordinated to two other histidine residues, the same carbamylated lysine, and H_2O (also weakly liganded to the other Ni^{2+}). The gene cluster containing the *ureA*, *ureB* and *ureC* urease structural genes also includes the accessory genes *ureD* (upstream of *ureA*), and *ureEFG* which are contiguous and located downstream of *ureC*. The polypeptide products of the four accessory genes, *ureDEFG*, are required for formation of fully active urease *in vivo* (80). Urease purified after co-expression with the accessory genes possesses only nickel ions, but growth in media lacking Ni^{2+} results in production of apoenzyme. *In vitro* activation of apo-urease in the presence and absence of accessory proteins has been studied in order to further define the roles of the accessory proteins in metallocenter assembly. A proposed model for urease activation by accessory proteins is summarised in Fig. 1.7.

Apo-urease can be activated *in vitro* by the addition of bicarbonate and Ni^{2+}, but only 10-15% of the specific activity of native urease is attained (80). From the crystal structure of urease, the role of bicarbonate is clear: HCO_3^- reacts with a lysine residue, forming a carbamate, which is ligated to both nickel ions at the active site (79). The addition of nickel ion *prior* to the addition of bicarbonate prevents activation from occurring. Presumably, Ni^{2+} can bind to non-carbamylated apo-urease in the absence of accessory proteins, competing with the activation process *in vitro* (81).

Overexpression of *ureD* together with the structural genes of urease resulted in accumulation of apo-urease complexed with one, two or three molecules of UreD. The UreD-apourease complex was activated *in vitro* up to 24% in the presence of bicarbonate and Ni^{2+}, and activation was shown to be concomitant with dissociation of UreD from apo-urease. The interaction of the UreD-apo-urease complex with metal ions was further investigated in order to define the role of UreD (82). From this study, it was found that the presence of UreD appeared to reduce the rate of interaction of the noncarbamylated apoprotein with Ni^{2+}. It was also demonstrated that other metals can bind to apo-urease and UreD-apo-urease, some with higher affinity than observed for nickel. Since the UreD-apo-urease complex was not sufficient for full activation of urease *in vitro*, however, it is clear that additional factors are required for assembly of fully active urease. These factors include UreF and UreG accessory proteins required for activation of urease *in vivo*.

UreG is another accessory protein necessary for activation of urease *in vivo*. Amongst the three essential accessory proteins, UreD, UreF, UreG, it is the only one that has sequence similarity to other proteins. In particular, UreG has 25% sequence identity with HypB, an *E coli* protein which plays a role in nickel processing for a nickel-containing hydrogenase. HypB has been purified and found to bind and hydrolyze GTP (83). UreG contains a P-loop motif found in proteins that bind ATP and GTP, which led to the suggestion that UreG may bind and hydrolyse nucleotides as part of its role in facilitating metallocenter assembly (reviewed in ref. 84).

Purification of UreG, a UreDFG complex, and site-directed mutagenesis on the P-loop of UreG gave some insight into the role of UreG (85). Interestingly, it was found that although UreG by itself does not bind nucleotides (as evidenced by equilibrium dialysis,

and chromatography on ATP and GTP-linked resins), the wild-type UreDFG *complex* did bind to an ATP-linked agarose column. Furthermore, mutations in the P-loop yielded inactive urease *in vivo*, even when cells were grown in the presence of nickel; the UreDFG variant, where an alanine residue located in the P-loop was substituted by threonine or lysine, was unable to bind to the ATP-linked resin. Together, these results provided strong evidence that the P-loop motif in UreG, and hence nucleoside triphosphate hydrolysis, is likely to be necessary for *in vivo* incorporation of nickel into the active site of urease.

UreE is clustered together with the genes for the other accessory proteins. UreE is also thought to be an accessory protein, yet it is not essential for *in vivo* formation of active urease (86). UreE deletion mutants synthesized urease with decreased specific activity and reduced nickel content, although this could be suppressed by higher nickel content in the growth medium. UreE has been purified and shown to bind six Ni^{2+} suggesting a function as a nickel ion donor for the apo-urease (87). Spectroscopic and mutagenesis studies have shown that the histidine rich carboxyl terminus is not necessary for urease activation and that UreE can function with only two internal Ni^{2+} binding sites per dimer (88). Furthermore, some site-directed mutants of UreE showed a decreased rate of *in vivo* activation even though the purified variants had unperturbed Ni^{2+} binding/dissociation constants. These data suggest that UreE does more than just bind and release Ni^{2+}, and emphasises the importance of other proteins involved in urease assembly (89).

Adenosine deaminase possesses ligands comparable to the urease Ni^{2+}-ligands although Zn^{2+} is the functional metal in that protein (90). It is not known whether adenosine deaminase requires accessory proteins for proper assembly of the binuclear

metal center. Given the similarity of the active sites to that of urease, it would not be surprising if adenosine deaminase requires accessory proteins in order to ensure that the proper metal gets incorporated into the active site.

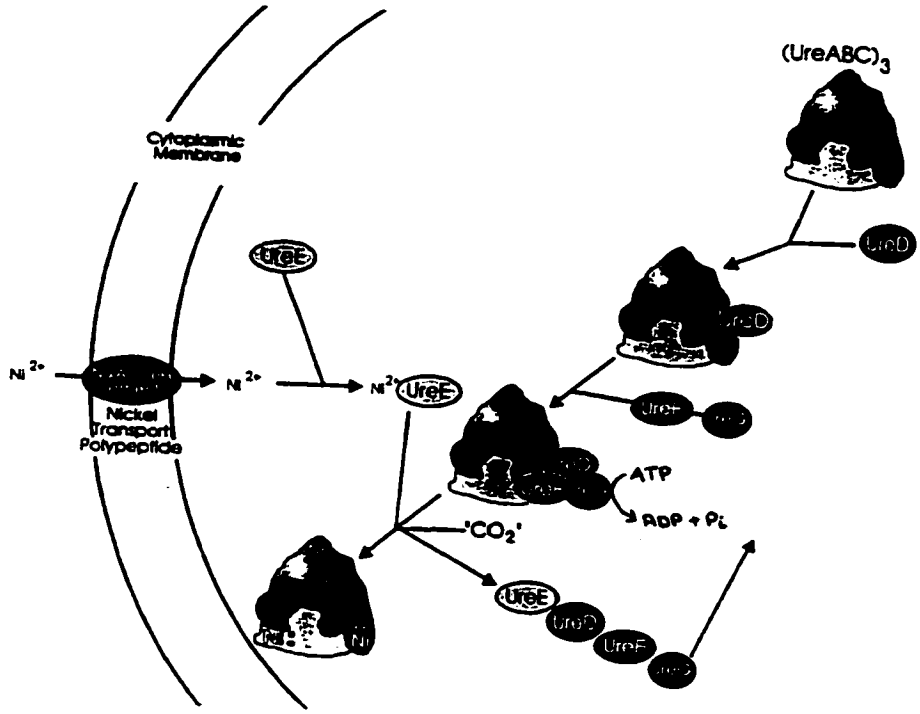

Figure 1.7 Model for Urease activation by accessory proteins. The figure was adapted from reference 85.

NITROGENASE AND ISC ASSEMBLY PROTEINS

Nitrogenases from *Azotobacter vinelandii* are associated with a number of accessory proteins involved in assembly of the nitrogenase metallocenters. Nitrogenase I is a two- component enzyme comprising an Fe-Mo active site component (NifDK) and an Fe-S reductase component (NifH) (91). The assembly of active nitrogenase enzyme involves many proteins, most of which have been characterised to some extent. NifH is the Fe protein component of the nitrogenase that plays a dual role: 1) it reduces nitrogenase during turnover; and 2) it is required for biosynthesis of the FeMo cofactor in some way (92). NifEN contains two iron-sulfur centres and has been postulated to act as a scaffold for incorporation of the Fe-Mo cofactor into the apoenzyme (93, 94). NifV is a homocitrate synthase necessary for biosynthesis of homocitrate, which is part of the FeMo cofactor (95). NifQ and NifB both have metal binding properties and are suspected to generate precursors to the FeMo cofactor (96, 97). NifS uses L-cysteine to release S^{2-} for incorporation into the nitrogenase Fe-S cluster (98). NifU was shown to contain a [2Fe-2S] cluster and serves as a scaffold for NifS-directed assembly of a transient cluster for nitrogenase (99). The roles of a few accessory proteins for nitrogenase assembly are still unknown. For example, NifY doesn't contain any metals, and it attaches to the apo-nitrogenase and dissociates from the FeMo form of the protein thus stabilising the apoenzyme form (100).

Recently, homologues of the nifS and nifU genes have been identified in *A. vinlandii* and *E. coli* (101). The homologues are termed IscA and IscU respectively, and are encoded within a highly conserved operon involved in general iron-sulfur cluster synthesis. IscA was shown to have cysteine desulfurase activity, and IscU contains only the N-terminal transient-cluster binding domain of NifU (101). Other genes in the *isc*

operon include *hscB*, *hscA*, and *fdx* located downstream of *iscS* and *iscU*. HscA and HscB are proposed to play a role in maturation of iron-sulfur containing proteins since they share sequence identity with heat shock molecular chaperones (101).

COPPER METALLOCHAPERONES

Other well-studied metalloprotein assembly proteins are those involved in copper metabolism. The concentration of 'free' copper inside a yeast cell is less than 10^{-18} M. which corresponds to less than one atom of free copper per cell (102). In spite of this very low concentration of copper, and the presence of high affinity copper chelators such as metallothioneins in the cell cytosol, enzymes and proteins that use copper as their cofactors manage to acquire it through specific metal chaperones. So far there are three well-documented copper chaperone systems, which are described briefly below.

COX17

Cytochrome oxidase is an important mitochondrial enzyme in the respiratory chain. It is made up of two subunits containing a total of three copper atoms. Two copper ions form a binuclear copper center located in the part of cytochrome oxidase exposed to the inter- membrane space, while a mononuclear copper site is buried in the inner membrane (103). Exactly how these copper atoms are inserted into this enzyme is still not clear, but two proteins were found to play a role in copper delivery to mitochondria. COX17 is localized both in the cytoplasm and in the inter-membrane space of the mitochondrion (104). COX17 can be expressed in *E.coli* and is isolated with Cu(I) bound by cysteine residues, with four out of six conserved cysteines required to coordinate the metal ion (105). Another protein, SCO1, located in the inner membrane of mitochondria, is required for copper insertion into yeast cytochrome oxidase (106). SCO1 and subunit 2

of cytochrome oxidase share sequence similarity, and both contain two copper-binding cysteinyl residues which may directly transfer copper from SCO1 to cytochrome oxidase (104, 107). COX17 may shuttle copper to mitochondria and deliver the ion to SCO1 before copper is delivered to cytochrome oxidase (108).

ATX1

ATX1 binds and delivers copper to a P-type copper transporter, CCC2, located in the Golgi compartment of yeast (109, 110, 111). ATX1 was found to bind Cu(I) via two cysteine residues, where the binding site is flexible enough to accommodate additional ligands (110). The copper loaded ATX1 donates the metal ion after first docking with an ATX1-like domain of the target protein through electrostatic interactions. Once the metallochaperone has docked with its target, a cysteine residue from the target domain is proposed to attack the Cu(I) of ATX1 (reviewed in ref. 108).

CCS

CCS is a chaperone protein that delivers copper to the apo form of copper and zinc-containing superoxide dismutase (SOD) (112). SOD is an enzyme that protects the cell from damage caused by toxic superoxide radicals by catalysing the conversion of superoxide radical to molecular oxygen and hydrogen peroxide. Deletion of the yeast CCS gene resulted in SOD lacking copper but still containing a zinc atom (113, 114). Yeast CCS is a large protein with three distinct domains (115, 116, 117). The N-terminal domain of CCS resembles the ATX1 metallochaperone, including the cysteinyl copper-binding site. The central domain of CCS is homologous to its target protein, SOD. This domain of CCS has been shown to interact with SOD, and the interaction is proposed to secure the enzyme during copper insertion (reviewed in ref. 108). SOD exists as a

homodimer in solution, and a proposed mechanism of copper insertion involves the formation of a heterodimer or a heterotetramer between CCS and SOD prior to copper transfer (117, 118, 119). The third domain, the C-terminal domain of CCS, is highly conserved among CCS of different species and includes a conserved CXC motif that can bind copper (120). Models of copper delivery to SOD have been proposed to involve both the C-terminal and the N-terminal domains of CCS, but the mechanism of copper transfer from the all-sulfur coordination in CCS to the all-nitrogen coordination in SOD remains obscure (121).

1.2.3 Assembly of Binuclear Iron Center-Containing Proteins

In vitro binuclear iron center assembly without the aid of accessory proteins has been studied quite extensively in ribonucleotide reductase (77). Ribonucleotide reductase catalyses the reduction of nucleoside diphosphates and is composed of two components, the R1 and R2 proteins. R1 protein contains the substrate binding site with redox- active thiols that participate in reduction of the ribose moiety of the substrate (122). R2 protein contains a tyrosyl radical-μ-oxodiiron(III) cofactor. The tyrosyl radical is essential for enzyme activity and is believed to participate in the catalytic reaction. Unlike methane monooxygenase and phenol hydroxylase, the role of the binuclear iron center of the R2 protein is believed to be to react with oxygen to generate a stable tyrosine radical, so the fully active form of RNR contains the oxidized diferric (Fe^{3+}-Fe^{3+}) center and a tyrosyl radical. Bollinger *et al.* have investigated the mechanism by which the iron cofactor of the R2 protein of *E. coli* RNR is assembled. They demonstrated that reconstitution of the holoenzyme from apo-RNR with Fe^{2+} and O_2 can be directed to either of two pathways depending on the availability of reducing equivalents. The kinetics of assembly were

examined using stopped-flow UV/VIS absorption spectroscopy, rapid freeze-quench EPR spectroscopy, and rapid freeze-quench Mössbauer spectroscopy (reviewed in ref. 77).

Under limiting Fe^{2+} conditions, tyrosyl radical-dinuclear iron cluster cofactor assembly involves the oxidation of the tyrosine before the formation of the diferric center. This pathway involves the initial accumulation of an intermediate suggested to be a μ-peroxodiferric complex (intermediate U). This intermediate undergoes one-electron reduction by tyrosine 122, simultaneously generating the tyrosyl radical and a second intermediate, a diferrric radical of unknown structure (intermediate X). The limiting Fe^{2+} then slowly reduces the second intermediate giving the final differric center (Fig 1.8. pathway A).

Under conditions where Fe^{2+} is in excess, the tyrosyl radical and the binuclear iron center are formed simultaneously. Under these conditions, the excess reductant, either Fe^{2+} or ascorbate (rather than Y122), rapidly converts intermediate U (the peroxo intermediate), forming a diferric radical intermediate (intermediate X) without the tyrosyl radical. Tyrosyl radical and diferric cluster are then produced by oxidation of the tyrosine by the diferric radical intermediate. More recently, the rate constant for the formation of intermediate X starting from the reduced holoenzyme was determined and found to be one order of magnitude greater than that observed in the apoR2 reconstitution experiments. The much slower rate of formation of species X from the apoR2 suggests a possible conformational change of apoR2 required for Fe binding (123).

There are no documented examples of protein-assisted assembly of diiron oxo bridged centres such as those found in methane monooxygenases, toluene monooxygenase, or ribonucleotide reductase. However, reconstitution experiments with the iron-depleted Protein A of methane monooxygenase from *M. capsulatus* (Bath)

suggested the possibility that a factor found in the crude extract may be involved in iron insertion (78). The experiments done with DmpK and phenol hydroxylase are so far the only evidence available suggesting the requirement for an accessory protein in this type of metallocenter assembly. How iron is specifically directed to the diiron site is a question raised by the work of Atta *et al.* (124,125). In these studies methane monooxygenase (MMO) and ribonucleotide reductase (RNR) binuclear iron sites were substituted with manganese. Two Mn(II) were inserted per apo-MMO molecule, as determined by EPR spectroscopy. To test the stability or the specificity of the metal binding site, the Mn substituted MMO was incubated with a 20-fold excess of Fe(II), under both aerobic and anaerobic conditions: none of the iron was incorporated. Conversely, native MMO was subjected to incubation with Mn(II) and more than 95% of the manganese ions remained unbound. These results indicated that Mn(II) has just as much affinity for the metal binding site as iron, if not more, since manganese can be incorporated into apo-MMO both aerobic and anaerobically whereas iron can only be incorporated anaerobically. Presumably, only Fe(II) gets inserted into the apo enzyme. In ribonucleotide reductase, Mn(II) was found to bind to apo-RNR and this form was stable, explaining why tyrosine 122 radical is never generated in the Mn(II)-substituted enzyme. These experiments demonstrate that metals other than iron can bind to the diiron site, leading to the question: what makes iron bind preferentially to these sites *in vivo*?

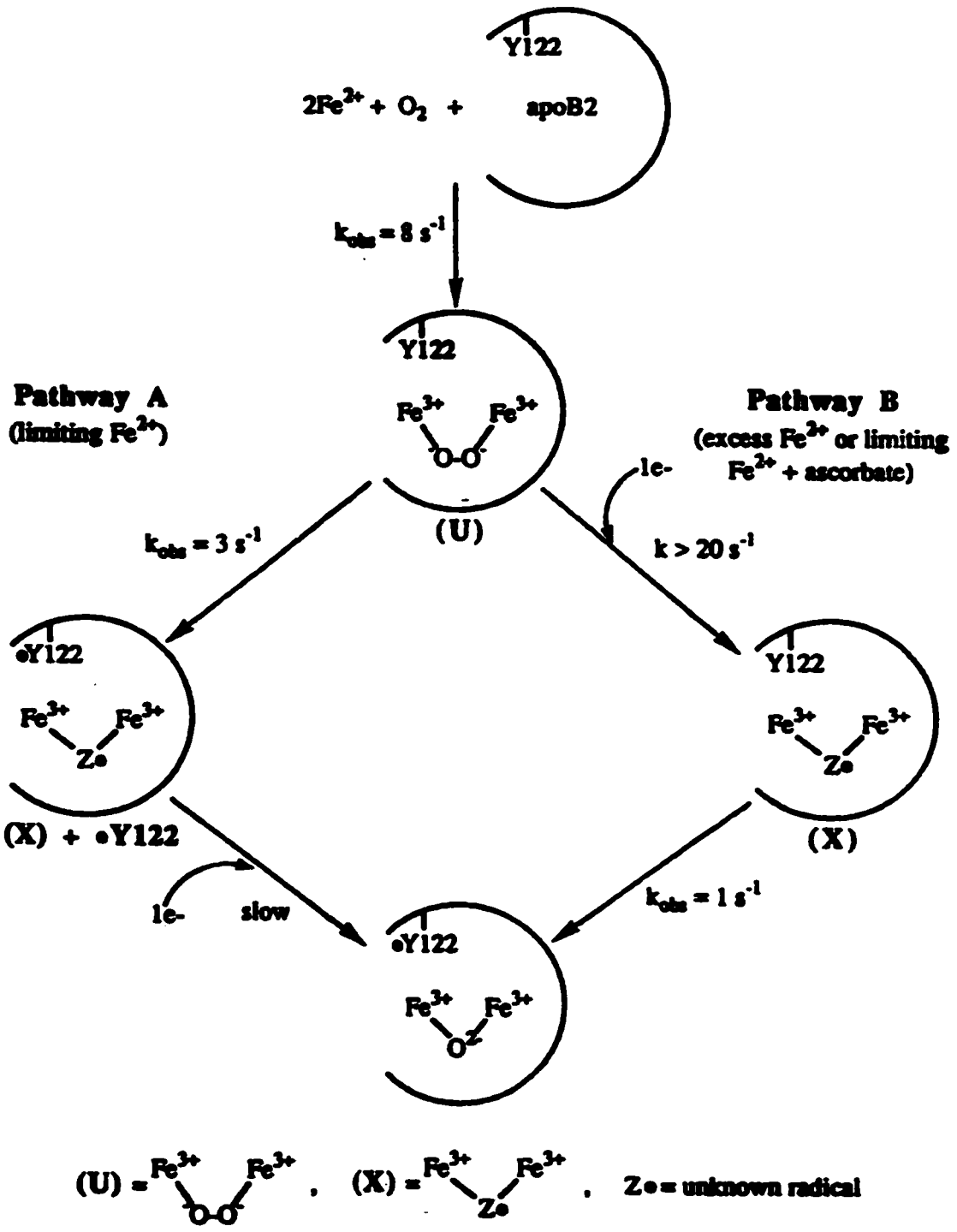

Figure 1.8 Assembly of the tyrosyl radical-dinuclear iron cluster of ribonucleotide reductase. The figure is adapted from reference 77.

1.3 AIMS OF THE THESIS

The study of multicomponent binuclear iron centre containing oxygenases is relatively new. It was only 17 years ago that the purification and characterisation of methane monooxygenase was first reported (126). Since then much work has been done on the methane and toluene monooxygenase systems, but the precise mode of interaction between the components to ensure a highly controlled oxygen activation reaction remains obscure. Phenol hydroxylase is an interesting new example of this class of enzymes. Examination of the roles of DmpM and DmpK of phenol hydroxylase from *Pseudomonas sp.* strain CF600 should provide insights into the control of reactivity of multicomponent oxygenases, and the process of binuclear iron center assembly.

DmpM is a component of phenol hydroxylase required for full activity. The recombinant form of DmpM was found to be expressed mainly as an inactive dimer. In order to do site-directed mutagenesis studies on this protein, it is essential to be able to reconstitute active DmpM from the inactive form. Characterisation of both the active and inactive forms, as well as procedures for activation, are described in Chapter 2. DmpM is similar to stimulatory proteins associated with other multicomponent oxygenases such as methane and toluene mono-oxygenases: although dimer forms of these proteins have been reported, their significance has not been investigated (22, 60).

Site-directed and random mutagenesis of DmpM was performed in order to try to identify residues involved in the interaction between DmpM and the oxygenase component (Chapter 5). Since DmpM shares sequence homology with MMOB and TmoD, residues conserved between these proteins were chosen for site-directed mutagenesis. Surprisingly, none of these substitutions had significant effect on multiple turnover activity of phenol hydroxylase. Random mutagenesesis using error-prone PCR

was attempted, and a double mutant was found to be unable to activate phenol hydroxylation in our standard activity assay. These results suggest that multiple substitutions are necessary to affect the interaction between DmpM and oxygenase components.

DmpK is an accessory protein involved in cofactor assembly of the oxygenase component of phenol hydroxylase. Very little is known about how metal cofactors are inserted into proteins and enzymes, but there is increasing evidence that it is assisted by other proteins. The mechanism of iron incorporation into apo-oxygenase in the presence of DmpK is examined in Chapter 3. Although many important enzymes contain diiron cofactors, no DmpK-like proteins involved in diiron center assembly have previously been reported in the literature. The work done on DmpK thus describes the investigation of a novel protein. Ramifications of this work for other binuclear iron centre containing proteins remain to be seen.

Purification and characterisation of the oxygenase component of phenol hydroxylase by Mössbauer, EPR and UV/vis spectroscopies are described in Chapter 4. Two major species of the diiron center of phenol hydroxylase were observed by Mössbauer spectroscopy. Heterogeneity in diiron centers of other proteins has been described previously, although the significance and the source of heterogeneity have not been determined. In a search for possible sources of active site modification, dithiothreitol and hydrogen peroxide were found to contribute to inactivation of phenol hydroxylase.

REFERENCES

1. Happold, F. C. and Key, A. (1932) *Journal of Hygiene* **32**,573-580

2. Shingler, V., Franklin, F. C. H., Tsuda, M., Holroyd, D. and Bagdasarian, M. (1989) *Journal of General Microbiology* **135**, 1083-1092

3. Dagley, S. (1986) *The Bacteria*, vol. X . *The Biology of Pseudomonas* (J. R. Sokatch, ed.), pp.527-556, Academic Press, Inc. London.Ltd., London

4. Bartilson, M. and Shingler, V. (1989) *Gene* **85**,233-238

5. Nordlund, I. and Shingler, V. (1990) *Biochimica et Biophysica Acta* **1049**,227-230

6. Shingler, V., Powlowski, J., and Marklund, U. (1992) *J. Bacteriol.* **174**, 711-724

7. Powlowski, J. and Shingler, V. (1990) *J. Bacteriol.* **172**, 6834-6840

8. Neujahr, H. Y. and Gaal, A. (1973) *Eur. J. Biochem.* **35**, 386-400

9. Detmer, K. and Massey, V. (1985) *J. Biol. Chem.* **260**, 5998-6005

10. Entsch, B., Ballou, D. P., and Massey, V. (1976) *J. Biol. Chem.* **251**,2550-2563

11. Merkx, M., Kopp, D.A., Sazinsky, M.H., Blazyk, J.L., Muller, J., Lippard, S.J. (2001) *Angew Chem Int Ed Engl* **40**, 2782-2807

12. Powlowski, J. and Shingler, V. (1994) *Biodegradation* **5**, 219-236

13. Fox, B. G., Shanklin, J., Somerville, C., and Münck, E. (1993) *Proc. Natl. Acad. Sci. U.S.A.* **90**, 2486-90.

14. Rosensweig, A. C., Fredrick, C. A., Lippard, S. J., and Nordlund, P. (1993) *Nature* **366**, 537-543

15. Nordlund, P., Sjoberg, B-M., and Eklund, H. (1990) *Nature* **345**, 593-598

16. Johnson, G. R. and Olsen, R. H. (1995) *Appl. Environ. Microbiol.* **61**, 3336-3346

17. Byrne, A. M., Kukor, J. J. and Olsen, R. H. (1995) *Gene* **154**, 65-70

18. Olsen, R. H., Kukor, J. J. and Kaphamer, B. (1994) *J. Bacteriol.* **176**, 3749-3756

19. Yen, K-M., Karl, M. R., Blat,t L. M., Simon, M. J., Winter, R. B., Fausset, P. R., Lu, H. S., Harcourt, A. A. and Chen, K. K. (1991) *J. Bacteriol.* **173**, 5315-5327

20. Miura, A. and Dalton, H. (1995) *Biosci. Biotech. Biochem.* **59**, 853-859

21. Dalton, H. (1980) *Adv. Appl. Microbiol.* **26**, 71-87

22. Fox, B. G., Froland, W. A., Dege, J. E. and Lipscomb, J. D. (1989) *J. Biol. Chem.* **264**, 10023-10033

23. Andrews, S.C. (1998) *Adv. Microb. Physiol.* **40**. 281-351

24. Holmes, M.A., Le Trong, I., Turley, S., Sieker, L.C., Stenkamp, R.E. (1991) *J. Mol. Biol.* **218**, 583-593

25. Murrell, J. C., McDonald, I. R., Gilbert, B. (2000) *Trends Microbiol.* **8**, 221-225

26. Colby, J. and Dalton, H. (1978) *J. Biochem.* **171**, 461-468

27. Lund, J. and Dalton H. (1985) *Eur. J. Biochem.* **147**, 291-296

28. Prince, R. C., Patel, R. N. (1986) *FEBS Lett.* **203**, 127-130

29. Gassner, G. T, and Lippard, S. J. (1999) *Biochemistry* **38**, 12768-12785

30. Fox, B. G., Liu, Y, Dege, J. E., and Lipscomb, J. D. (1991) *J. Biol. Chem.* **266**, 540-550

31. Paulsen, K. E., Lui, Y., Fox, B. G., Lipscomb, J. D., Münck, E., and Stankovich, M. T. (1994) *Biochemistry* **33**, 713-722

32. Froland, W. A, Andersson, K. K, Lee, S. K, Liu, Y, and Lipscomb, J. D. (1992) *J. Biol. Chem.* **267**, 17588-17597

33. Liu, Y., Nesheim, K. E., Paulsen, K. E., Stankovich, J. D. and Lipscomb, J. D. (1997) *Biochemistry* **36**, 5223-5233

34. Chang, S. L., Waller, B. J., Lipscomb, J. D., and Mayo, K. H. (1999) *Biochemistry* **38**, 5799-5812

35. Walters, K. J., Gassner, G. T., Lippard, S. J. and Wagner, G. (1999) *Proc. Natl. Acad. Sci. U.S.A.* **96**, 7877-7882

36. Qian, H., Edlund, U., Powlowski, J., Shingler V., and Sethson, I. (1997) *Biochemistry* **36**, 495-504

37. Chang, S. L., Wallar, B. J., Lipscomb, J. D., Mayo, K. H. (2001) *Biochemistry* **40**, 9539-51

38. Lloyd, J. S., Bhambra, A., Murrell, J. C. and Dalton, H. (1997) *Eur. J. Biochem.* **248**, 72-79

39. Rosensweig, A. C., Nordlund, P., Takahara, P. M., Frederick, C. A. and Lippard, S. J. (1995) *Chem. Biol.* **2**, 409-418

40. Whittington, D.A. and Lippard, S. J. (2001) *J. Am. Chem. Soc.* **123**, 827-838

41. Elangro, N., Radhakrishnan, R., Froland, W. A., Wallar, B. J., Earhart, C. A., Lipscomb, J. D., Ohlendorf, D. H. (1997) *Protein Science* **6**, 556-568

42. Lindquist, Y., Huang, W., Schneider G., Shanklin J. (1996) *EMBO J.* **15**, 4081-4092

43. Lombardi, A. Summa, C. M., Geremia, S., Randaccio, L., Pavone, V. and Degrado, W. F. (2000) *Proc. Natl. Acad. Sci. U.S.A.* **97**, 6298-6305

44. Fox, B. G, Surerus, K. K, Münck, E and Lipscomb, J. D. (1988) *J. Biol. Chem.* **263**, 10553-6.

45. DeWitt, J. G., Bentsen, J. G., Rosensweig, A. C., Hedman, B., Green, J., Pilkington, S., Papaefthymiou, G. C., Dalton, H., Hodgson, K. O., and Lippard, S. J. (1991) *J. Am. Chem. Soc.* **113**, 9219-9235

46. DeWitt, J. G., Rosensweig, A. C., Salifoglou, A., Hedman, B., Lippard, S. J. and Hodgson, K. O. (1995) *Inorg. Chem.* **34**, 2505-2515

47. Andersson, K. K., Elgren, T. E., Que, L. and Lipscomb, J. D., (1992) *J. Am. Chem. Soc.* **114**, 8711-8713

48. Halliwell, B. (1987) *FASEB J.* **1**, 358-364

49. Liu, K. E., Valentine, A. M., Wang, D. L., Huynh, B.-H, Edmondson, D. E., Salifoglou, A., Lippard, S. J. (1995) *J. Am. Chem. Soc.* **117**, 10174-10185

50. Liu, Y., Nesheim, J. C., Lee, J. D. and Lipscomb, J. D. (1995) *J. Biol. Chem.* **270**, 24662-24665

51. Lee, S. K., Nesheim, J. C. and Lipscomb, J. D. (1993) *J. Biol. Chem.* **268**, 21569-21577

52. Valentine, A. M., Stahl, S. S. and Lippard, S. J. (1999) *J. Am. Chem. Soc.* **121**, 3876-3887

53. Liu, K. E., Wang, D. L., Huynh, B.-H., Edmondston, D. E., Salifoglou, A. and Lippard, S. J. (1994) *J. Am. Chem. Soc.* **116**, 7465-7466

54. Lee, S. Y. and Lipscomb, J. D. (1999) *Biochemistry* **38**, 4423-4432

55. Brazou, B. J. and Lipscomb, J. D. (2000) *Biochemistry* **39**, 13503-13513

56. Lee, S. K., Fox, B. G., Froland, W. A., Lipscomb, J. D. and Münck, E. (1993) *J. Am. Chem. Soc.* **115**, 6450-6451

57. Shu, L. J., Nesheim, J. C., Kauffmann, K. Münck, E., Lipscomb, J. D. and Que, L. (1997) *Science* **275**, 515-518

58. Whited, G.M. and Gibson, D.T. (1991) *J. Bacteriol.* **173**, 3010-3016

59. Pikus, J. D., Studts, J. M., Achim, C., Kauffmann, K. E., Münck, E., Steffan, R. J., McClay, K. and Fox, B. G. (1996) *Biochemistry* **35**, 9106-9119

60. Newman, L., and Wackett, L. (1995) *Biochemistry* **34**, 14066-14076

61. Hemmi, H., Studts, J. M., Chae, Y. K., Song, J., Markely, J. L. and Fox, B. G. (2001) *Biochemistry* **40**, 3512-24

62. Nebert, D. W. and Nelson, D. R. (1991) *Methods Enzymol.* **206**, 3-11

63. Yeom, H., Sligar, SG, Li H, Poulos TL, Fulco AJ. (1995) *Biochemistry* **34**, 14733-40

64. Sagami, I. and Shimizu, T. (1998) *J. Biol. Chem.* **273**, 2105-2108

65. Fox, B.G., Shanklin, J., Ai, J., Loehr, T.M., Sanders-Loehr, J. (1994) *Biochemistry* **33**, 12776-86

66. Pikus, J.D., Mitchell, K.H., Studts, J.M., McClay, K., Steffan, R.J., Fox, B.G. (2000) *Biochemistry* **39**, 791-9

67. Powlowski, J., Sealy, J., Shingler, V., & Cadieux, E. (1997) *J. Biol. Chem.* **272**, 945-951

68. Nordlund, I., Powlowski, J., Shingler, V. (1990) *J. Bacteriol.* **172**, 6826-33

69. Ng, L.C., Shingler, V., Sze, C.C. and Poh, C.L. (1994) *Gene* **151**, 29-36

70. Herrmann, H., Muller, C., Schmidt, I., Mahnke, J., Petruschka, L. and Hahnke, K. (1995) *Mol. Gen. Genet.* **247**, 240-246

71. Arenghi, F.L., Berlanda, D., Galli, E., Sello, G. and Barbieri, P. (2001) *Appl. Environ. Microbiol.* **67**, 3304-3308

72. Crichton, R. R and Charloteaux-Wauters, M. (1987) *Eur. J. Biochem.* **164**, 485-506

73. Neilands, J. B. (1981) *Annu. Rev. Biochem.* **50**, 715-731

74. Dautry-Varsat, A., Ciechanover, A., Lodish, H.F. (1983) *Proc. Natl. Acad. Sci. U.S.A.* **80**, 2258-62

75. Klausner, R.D, Ashwell, G, van Renswoude, J, Harford, J.B, Bridges, K.R. (1983) *Proc. Natl. Acad. Sci. U.S.A* **80**, 2263-6

76. Banyard, S.H., Stammers, D.K., and Harrison, P.M. (1978) *Nature* **271**, 282-284

77. Bollinger, J. M. Jr., Tong, W. H., Ravi, N., Huynh, B. H., Edmonson, D. E., and Stubbe, J. (1995) *Methods in Enzymol.* **258**, 278-303

78. Green, J. and Dalton, H. (1988) *J. Biol. Chem.* **263**, 17561-17565

79. Jabri, E., Carr, M. B., Hausinger, R. P. and Karplus, P. A. (1995) *Science* **268**, 998-1004

80. Park, I-S. and Hausinger, R. P. (1996) *Biochem.* **35**, 5345-5352

81. Park, I.-S., M. B. Carr, and R. P. Hausinger. (1994) *Proc. Natl. Acad. Sci. U.S.A.* **91**, 3233-3237

82. Moncrief, MB. C. and Hausinger, R. P. (1996) *J. Bacteriol.* **178**, 5417-5421

83. Maier, T., Jacobi, A., Sauter, M., and Bock, A. (1993) *J. Bacteriol.* **175**, 630-635

84. Mobly, H. L. T., Island, M. D. and Hausinger, R. P. (1995) *Microbiol. Reviews* **59**, 451-480

85. Moncrief, MB. C., and Hausinger, R. P. (1997) *J. Bacteriol.* **179**, 4081-4086

86. Lee, M.H., Mulrooney, S.B., Renner, M.J., Markowicz, Y., Hausinger, R.P. (1992) *J. Bacteriol* **174**, 4324-30

87. Lee, M. H., Pankratz, H. S, Wang, S., Scott, R. A., Finnegan, M. G., Johnson, M. K., Ippolito, J. A., Christianson, D. W. and Hausinger, R. P. (1993) *Protein Science* **2**, 1042-1052

88. Brayman, T.G., and Hausinger, R.P. (1996) *J. Bacteriol.* **178**, 5410-5416

89. Colpas, G. J. and Hausinger, R. P. (2000) *J. Biol. Chem.* **275**, 10731-10737

90. Wilson, D. K., Rudolf, F.B., and Quiocho, F. A. (1991) *Science* **252**, 1278-1284

91. Dean, D., Bolin, J. and Zheng, L. (1993) *J. Bacteriol.* **175**, 6737-6744

92. Robinson, A. C., Dean, D. R., and Burgess, B. K. (1987) *J. Biol. Chem.* **262**, 14327-14332

93. Allen, R. M., Chatterjee, R., Ludden, P. W., and Shah, V. K. (1995) *J. Biol. Chem.* **270**, 26890-26896

94. Roll, J. T., Shah, V. K., Dean, D. R., and Roberts, G. P. (1995) *J. Biol. Chem.* **270**, 4432-4437

95. Hoover, T. R., Imperial, J., Ludden, P. W., and Shah, V. K. (1989) *Biochemistry* **28**, 2768-2771

96. Shah, V. K., Allen, J. R., Spangler, N. J., and Ludden, P. W. (1994) *J. Biol. Chem.* **269**, 1154-1158

97. Imperial, J., Ugalde, R. A., Shah, V. K., and Brill, W. J. (1984) *J. Bacteriol.* **158**, 187-194

98. Zheng, L., White, R. H., Cash, V. L., Jack, R. F., and Dean, D. R. (1993) *Proc. Natl. Acad. Sci. U.S.A.* **90**, 2754-2758

99. Yuvaniyama, P., Agar J.N., Cash, V.L., Johnson, M.K., Dean, D.R. (2000) *Proc. Natl. Acad. Sci. U.S.A.* **97**, 599-604

100. Homer, M. J., Paustian, T. D., Shah, V. K., and Roberts, G. P. (1993) *J. Bacteriol.* **175**, 4907-4910

101. Zheng, L, Cash, V.L, Flint, D.H., Dean D.R. (1998) *J. Biol. Chem.* **273**, 13264-72

102. Rae, T. D., Schmidt, P. J., Pufhal, R. A., Culotta, V. C., and O'Halloran, T. V. (1999) *Science* **284**, 805-808

103. Tsukihara, T., Aoyama, H., Yamashita, E., Tomizaki, T., Yamaguchi, H., Shinzawa-Itho, K., Hakashima, R., Yaono, R., and Yoshikawa, S. (1995) *Science* **269**,1069-1074

104. Beers, J., Glerum, D. M., and Tzagoloff, A. (1997) *J. Biol. Chem.* **272**, 33191-33196

105. Srinivasan, C., Posewitz, M. C., George, G. N., and Winge, D. R. (1998) *Biochemistry* **37**, 7572-7577

106. Schulze, M., and Rodel, G. (1989) *Mol. Gen. Genet.* **216**, 37-43

107. Glerum, D. M., Shtanko, A., and Tzagoloff, A. (1996) *J. Biol. Chem.* **271**, 20531-5

108. O'Halloran T.V., Culotta V.C. (2000) *J. Biol. Chem.* **275**, 25057-60

109. Lin, S. J., Pufahl, R., Dancis, A., O'Halloran, T. V., and Culotta, V. C. (1997) *J. Biol. Chem.* **272**, 9215-9220

110. Pufahl, R., Singer, C., Peariso, K. L., Lin, S. J., Schmidt, P., Fahrni, C., Culotta, V. C., Penner-Hahn, J. E., and O'Halloran, T. V. (1997) *Science* **278**, 853-856

111. Valentine, J. S., and Gralla, E. B. (1997) *Science* **278**, 817-818

112. McCord, J. M., and Fridovich, I. (1969) *J. Biol. Chem.* **244**, 6049-6055

113. Culotta, V. C., Klomp, L., Strain, J., Casareno, R., Krems, B., and Gitlin, J. D. (1997) *J. Biol. Chem.* **272**, 23469-23472

114. Lyons, T. J., Nerissian, A., Goto, J. J., Zhu, H., Gralla, E. B., and Valentine, J. S. (1998) *JBIC* **3**, 650-662

115. Schmidt, P., Rae, T. D., Pufahl, R. A., Hamma, T., Strain, J., O'Halloran, T. V., and Culotta, V. C. (1999) *J. Biol. Chem.* **274**, 23719-23725

116. Lamb, A. L., Wernimont, A. K., Pufahl, R. A., Culotta, V. C., O'Halloran, T. V., and Rosenzweig, A. C. (1999) *Nature Struc. Biol.* **6**, 724-729

117. Hall, L. T., Sanchez, R. J., Holloway, S. P., Zhu, H., Stine, J. E., Lyons, T. J., Demeler, B., Schirf, V., Hansen, J. C., Nersissian, A. M., Valentine, J. S., and Hart, P. J.(2000) *Biochemistry* **39**, 3611-3623

118. Lamb, A. L., Wernimont, A. K., Pufahl, R. A., O'Halloran, T. V., and Rosenzweig, A. C. (2000) *Biochemistry* **39**, 1589-95

119. Casareno, R. L., Waggoner, D., and Gitlin, J. D. (1998) *J. Biol. Chem.* **273**, 23625-23628

120. Schmidt, P. J., Ramos-Gomez, M., and Culotta, V. C. (1999) *J. Biol. Chem.* **274**, 36952-36956

121. Zhu, H., Shipp, E., Sanchez, R. J., Liba, A., Stine, J. E., Hart, P. J., Gralla, E. B., Nersissian, A. M., and Valentine, J. S. (2000) *Biochemistry* **39**, 5413-5421

122. Fontecave, M., Nordlund, P., Eklund, H., and Reichard, P., (1992) *Adv. Enzymol.* **65**, 147-183

123. Tong W. H., Chen S., Lloyd S. G., Edmonston D. E., Huynh B. H. and Stubbe J. (1996) *J. Am. Chem. Soc.* **118**, 2107-2108

124. Atta, M., Nordlund, P., Aberg, A., Eklund, H.and Fontecave, M. (1992) *J. Biol. Chem.* **267**, 20682-20688

125. Atta, M., Fontecave, M., Wilkins, P. C. and Dalton, H. (1993) *Eur. J. Biochem.* **217**, 217-223

126. Woodland M. P. and Dalton H. (1984) *J. Biol. Chem.* **259**, 53-59

Chapter 2

Characterization of Active and Inactive Forms of the Phenol Hydroxylase Stimulatory Protein, DmpM

ABSTRACT

The stimulatory protein, DmpM, of phenol hydroxylase from methylphenol-degrading *Pseudomonas* CF600 has been found to exist in two forms. DmpM purified from the native strain was mostly active in stimulating phenol hydroxylase activity, whereas an inactive form accumulated in a recombinant strain. Both forms exhibited M_r = 10,361.3 ± 1.3Da by electrospray mass spectrometry, but non-denaturing gel filtration showed M_r = 31,600 Da for the inactive form and 11,500 Da for the active form. Cross-linking and sedimentation velocity results were consistent with the inactive form being a dimer. Partial thermal or chemical denaturation, or treatment with trifluoroethanol, readily activated dimeric DmpM. A combination of circular dichroism and fluorescence spectroscopies, activity assays, and native and urea gel electrophoresis were used to further characterize reactivation with urea. These results showed that dissociation of the dimeric form of DmpM precedes denaturation at low protein concentrations and results in activation. The same concentration of urea that effects dissociation also converts the monomeric form to a different conformation.

INTRODUCTION

The *meta*-cleavage pathway encoded by the *dmp* operon of *Pseudomonas* strain CF600 efficiently degrades phenol and methyl-substituted phenols. Phenol hydroxylase is the first enzyme in the pathway and hydroxylates phenol to form catechol, which is then further degraded. Five polypeptides, encoded by *dmpLMNOP*, are required for phenol hydroxylase activity (1,2). These five polypeptides are arranged as 3 components: *dmpP* encodes a reductase containing a ferredoxin type [2Fe-2S] center and an FAD cofactor; *dmpLNO* encodes an oxygenase component with a binuclear iron center; and *dmpM* encodes a protein lacking any cofactors or metal (3). An additional polypeptide, DmpK, is required for the production of active oxygenase (4).

The reductase (DmpP) apparently accepts electrons from NADH and transfers them to the oxygenase component (DmpLNO) where they are required for insertion of oxygen into phenol (2). D*mpM* encodes a polypeptide with a molecular mass of 10.4 kDa that is essential for efficient catalysis of phenol hydroxylation (4), but its mechanism of activation has not previously been studied in any detail.

The components of phenol hydroxylase from *Pseudomonas* CF600 are similar to the components of methane and toluene monooxygenases (5,6). Amino acid sequence analyses show strong similarity between DmpM, MmoB and the small component of toluene monooxygenase (7, 8). These proteins appear to have similar roles in catalysis, with by far the best-studied example being MmoB. Its effects include: stimulation of methane monooxygenase activity by up to 150 fold (9); alteration of the regioselectivity of the hydroxylase component (10); changes in the environment of the binuclear iron center (11); and increases in the O_2 reactivity of the oxygenase (12).

Reports in the literature suggest that the methane monooxygenase regulatory protein, MmoB, can exist in multiple forms. Although MmoB from *M. trichosporium* OB3b has been shown by sedimentation velocity experiments to have a molecular mass of 15 kDa, other evidence suggests that MmoB can also exist as a dimer (5,9). The existence of a dimer form has also been suggested for MmoB from *M. capulatus* (Bath) (13). These authors also reported that MmoB is subject to proteolysis and requires protease inhibitors to prevent its degradation to two inactive forms, B' and B''. The physiological significance of this observation is not clear.

We have found that DmpM, the activator protein of phenol hydroxylase from *Pseudomonas sp.* strain CF600, can also exist in more than one form. While DmpM purified from the native strain is mostly in the active form, recombinant DmpM tends to accumulate in an inactive form. In this report, we have compared the properties of the inactive and active forms. Reconstitution of active DmpM from inactive preparations is also described.

MATERIALS AND METHODS

Materials: EDC was purchased from Sigma Chemical Co. DTT and NADH were obtained from Roche Molecular Biochemicals; phenol, urea, guandinium hydrochloride and glycerol (Ultra Pure grade) were from ICN Biomedicals. Catechol 2,3-dioxygenase was purified as described previously (4). Purification of the oxygenase component (DmpLNO) of phenol hydroxylase will be described elsewhere, and the reductase (DmpP) was purified using a previously published protocol (2). All restriction enzymes were purchased from Promega.

Analytical methods: Protein concentrations were estimated using the bicinchoninic acid (BCA) method (Pierce) following the 60°C protocol supplied by the manufacturer. Interfering substances such as DTT were removed using a modification of this method (14). Fluorescence measurements were carried out on an Aminco Bowman series 2 spectrofluorometer. Circular dichroism spectra were collected using a Jasco J-710 CD spectrometer. Electrospray mass spectrometry was done using a Finnigan SSQ 7000 single quadrupole mass spectrometer. All samples were passed through a 1 cm C-18 small molecule cartridge (Michrom BioResources) interfaced to the mass spectrometer. Initially the cartridge was equilibrated with 95% water-5% acetonitrile-0.05% trifluoroacetic acid, and elution was with 35% water-65% acetonitrile-0.05% trifluoroactic acid. Sedimentation velocity experiments were performed using a Beckman XL-A analytical ultracentrifuge. SDS-polyacrylamide gel electrophoresis was carried out using a Tris-glycine buffer (15) or Tricine buffer system (16). Native gels were purchased precast from ICN (CAP-Gels, 10-20% Tris/Borate/ EDTA, pH 8.3, native format, 8 x 10cm), or from BioRad Laboratories (Ready Gels, 10-20% Tris-HCl, native format, 8 x 10cm).

DNA manipulations: DNA manipulations were done according to standard techniques (17). DNA was purified using Wizard Miniprep kits, and DNA sequencing was performed using the Silver Stain sequencing kit (Promega).

The strategy for cloning *dmpM* into pET3a, a T7-polymerase based expression vector (18), was essentially as described previously (7). First, *dmpM* was amplified from pVI258 (1) using PCR. The 5'-end primer, 5'-GCCGCGAGGAATAACATATGTCATCAC -3', introduced an *Nde*I restriction enzyme site at the ATG start codon of *dmpM*, while the 3'-end primer 5'-CTTGTTGTGGGGATCCATGAGCTTG-3' introduced a *Bam*HI restriction enzyme site after the stop codon. The amplified PCR fragment was incorporated directly into the pCRII vector (Invitrogen). DmpM was then subcloned into pET3a on an *Nde*I-*Bam*HI restriction enzyme fragment. Thus, pCRII-*dmpM* and pET3a were digested using *Nde*I and *Bam*HI, and the fragments were purified from agarose gels using a Sephaglas kit (Pharmacia). After ligation, the resulting plasmids were transformed into *E. coli* DH5. Successful subcloning was verified by restriction digest followed by agarose gel electrophoresis, and the sequence was confirmed.

Bacterial growth and DmpM expression: The pET3a-*dmpM* construct was transformed into *E. coli* BL21(DE3) (18). Cells were grown either in LB or M9 minimal medium (17), using ampicillin or carbenecillin selection (100 μg/ml). IPTG (0.5 mM) was added when the OD_{600} of the culture reached 0.6-0.9 and growth was continued for an additional 1-4 hours. Cells were collected by centrifugation, and the cell paste was stored at -80°C until used.

Purification of native DmpM from phenol-grown Pseudomonas sp. *strain CF600*: The buffer used was 0.05 M Tris-HCl, pH 8.0, containing glycerol (10%) and DTT (1 mM) (referred to as "TGD"). *Pseudomonas sp.* strain CF600 was grown in a fermenter in M9 minimal medium (16 L) supplemented with metals (2). Phenol was used as the carbon source and was added (3-5 mM) whenever culture oxygen demand decreased abruptly. The pH of the growth medium was maintained at 7.0-7.5 by addition of NH_4OH. When an OD_{650} of approximately 5 was reached, cells were concentrated using a tangential-flow filtration unit (Millipore) and then collected by centrifugation at 3800 x g for 20 minutes. Cell pastes were stored at -80°C until used.

Cell paste was suspended in TGD (2 volumes), and then a spatula tip of DNase was added to the thawed cells prior to sonication. Aliquots (30 ml) were sonicated in 10 bursts of 15 sec each, maintaining a temperature of less than 10°C by immersion in a salt-ice water bath. The sonicated cell suspension was centrifuged at 70,400 x g for 60 minutes. The supernatant ("crude extract") was collected and centrifuged again for 5 minutes at 3800 x g before loading onto the first column.

Crude extract was loaded (6 ml/min) onto a Fast-Flow DEAE Sepharose column (30 x 2.6 cm) which was then washed with TGD buffer containing 75 mM NaCl for 40 min. The oxygenase component and DmpM eluted in the middle of a 75 mM to 275 mM NaCl gradient. Fractions (12 ml) containing DmpM and the oxygenase component were combined and loaded onto a Phenyl Sepharose High Performance column (36 x 2.6 cm) equilibrated with TGD buffer containing 0.15 M NaCl. DmpM eluted in the first few fractions following a wash with 0.15 M NaCl, whereas the oxygenase component eluted when the column was washed with 5 mM TGD. Fractions containing DmpM were

combined and stored at -80°C until purification of the more labile oxygenase component was completed.

DmpM-containing fractions were thawed, centrifuged for 5 min at 3800 x g and brought to 1 M ammonium sulfate. This solution was centrifuged for 5 min at 3800 x g before loading (1.5 ml/min) onto a Phenyl-Sepharose High Performance column (36 x 2.6 cm) equilibrated with TGD buffer containing 1 M ammonium sulfate. Then the column was washed with 1 M ammonium sulfate in TGD for approximately 10 min, prior to eluting the column with a gradient of 1 M to 0 M ammonium sulfate in TGD (600 ml).

Fractions (6 ml) containing DmpM were identified by SDS-PAGE, combined, and brought to 80% saturation with ammonium sulfate. After 30 min on ice the mixture was centrifuged at 7000 x g for 30 minutes. The precipitate was collected, redissolved in TGD (10 ml), and then centrifuged for 5 min at 3800 x g. This sample was then loaded (1ml/min) onto a Sephacryl S-300HR column (78 x 2.6 cm), which was subsequently eluted with TGD buffer, collecting 6 ml per fraction.

Fractions that contained DmpM were combined and loaded (6 ml/min) onto a Fast-Flow DEAE Sepharose column (18 x 1.6 cm) previously equilibrated with TGD buffer. The column was eluted (1 ml/min) with a gradient of 0 M to 0.3 M NaCl (600 ml). Fractions (6 ml) containing DmpM were combined and concentrated using an Amicon PM10 ultrafiltration membrane. The concentrated protein was passed through a desalting column equilibrated with TGD before storing it at -80°C.

Purification of recombinant DmpM: Purification of recombinant DmpM was carried out essentially as described previously (7), except that a Phenyl-Sepharose chromatography

step (see below) was usually necessary in order to obtain good yields of homogeneous protein. In addition, ammonium sulfate precipitation at 80% saturation was used to concentrate the protein between ion exchange and gel filtration chromatography steps.

After gel filtration chromatography (7), ammonium sulfate was added to the DmpM preparation to a final concentration of approximately 1 M. After centrifugation for 5 min at 3800 x g, the supernatant was loaded (3 ml/min) onto a Phenyl-Sepharose High Performance column (36 x 2.6 cm) previously equilibrated with TGD buffer containing 1 M ammonium sulfate. The column was then eluted (2 ml/min) with a gradient of 1-0.075 M ammonium sulfate in TGD (600 ml), collecting 6 ml fractions. Fractions containing DmpM, which eluted at the end of the gradient, were combined and concentrated by ultrafiltration using an Amicon PM-10 membrane. The concentrated protein was then aliquoted and stored at -80°C. Before use, samples were dialyzed against an appropriate buffer.

Phenol hydroxylase activity assays: Phenol hydroxylase activity was assayed essentially as described earlier (4) by coupling phenol hydroxylase with catechol 2,3-oxygenase: catechol 2,3-oxygenase catalyzes the *meta*-cleavage of catechol, the product of phenol hydroxylase, to form 2-hydroxymuconic semialdehyde. Formation of 2-hydroxymuconic semialdehyde was monitored by observing the increase in absorbance at 400 nm. Unless noted otherwise, assay mixtures (1 ml) contained: 50 mM MOPS buffer (pH 7.4), DmpM (0.12 μM), NADH (300 μM), DmpP (0.38 μM), catechol 2,3-oxygenase (4-5 Units), and varying amounts of oxygenase component. The background rate was recorded for 30 seconds and the reaction was initiated by adding phenol to 1.25 mM. An extinction

coefficient for 2-hydroxymuconic semialdehyde of 20,500 M^{-1} cm^{-1} at 400 nm was used in all calculations (4).

Chemical cross linking of DmpM using EDC:

Crosslinking reactions using EDC were carried out according to the protocol described by Grabarek and Gergley (19). Prior to cross-linking, samples of DmpM were dialyzed to exchange Tris buffer for 50 mM phosphate buffer, pH 7.5, containing 10% glycerol. DmpM (77 μM; 25 μg) was incubated for 60 min at 25°C in 50 mM phosphate buffer pH 7.5, containing glycerol (10%), EDC (2 mM) and NHS (5 mM), and then the reaction was terminated by the addition of β-mercaptoethanol (20 mM). More DmpM was then added at a 1:1 molar ratio with DmpM already in the reaction mixture, and the solution was further incubated for 1 hour at 25°C . Progress of the cross-linking reaction was monitored using SDS-polyacrylamide gel electrophoresis.

Denaturation of DmpM with urea: In early experiments, inactive recombinant DmpM (0.4 ml) was added to 10 M urea (1.6 ml) to a final DmpM concentration of 160 μM, and the solution was incubated on ice for 30 minutes. The sample was then dialyzed for 3 hours at 4°C against 20 mM MOPS buffer, pH 7.4 (1L). The dialysis buffer was replaced and dialysis was continued overnight, after which the buffer was replaced again and dialysis continued for an additional 3 hours.

When the concentrations of urea were varied, DmpM was first dialyzed as above, but using 50 mM phosphate buffer pH 7.5, containing 10% glycerol, prior to preparation of denatured samples. Non-denaturing gel electrophoresis of dialyzed samples was used

to confirm that the DmpM sample remained in its original form (monomer or oligomer) after dialysis treatment. Protein concentrations of the dialyzed samples were estimated using the BCA method, prior to addition of urea. A stock solution of urea (10 M) was freshly prepared in 50 mM phosphate buffer pH 7.5, with 10% glycerol, and the pH was adjusted to 7.5 after the urea dissolved. Stock solutions of DmpM were then added to diluted samples of the stock urea solution to generate concentrations of 0 to 7 M urea. Proteins in these samples were allowed to denature over 14 hours at room temperature prior to CD and fluorescence measurements.

CD spectra of all samples were scanned using a Jasco J-710 CD spectrometer. Spectra were acquired in the region 195-250 nm using a 0.1-cm path length cell (~ 200 µl) and a scan speed of 100 nm/min with a response time of 0.25 sec. The UV/CD spectra reported are the average of 5 scans at 0.5 nm resolution and a bandwidth of 1.0 nm.

Fluorescence emission spectra of protein samples were obtained using an Aminco Bowman Series 2 luminescence spectrometer. Spectra were collected from 300 to 400 nm following excitation at 290 nm with a bandwidth of 4 nm; samples were contained in a 400 µl quartz cuvette.

Analysis of the UV/CD and fluorescence transition curves: The unfolding of DmpM by urea was analyzed using the method of Pace et al. (20,21) assuming that unfolding of DmpM follows a two-state transition. A non-linear least-squares fitting procedure was used to obtain the unfolding parameters (22). These parameters were then used to calculate the fraction folded as a function of urea concentration (20). Transitions were

analyzed using the signals at 222 nm for circular dichroism data, and 315 nm for fluorescence data.

Urea gradient gels: Inactive recombinant and native DmpM samples were electrophoresed on discontinuous transverse urea gradient gels prepared using the method of Gentile et al. (23) with the buffers of Laemmli (15), including 10% glycerol (final concentration). Urea concentrations ranged from 0 to 7 M with an acrylamide counter-gradient of 16 to 10.4 %. Gels were run for 16 hours at 50V. Recombinant DmpM was also electrophoresed on urea gels with a gel buffer of pH 7.4. These gels were prepared following the protocol of McLellan (24), and included 10% glycerol.

Treatment of DmpM *with trifluoroethanol:* Inactive recombinant and native DmpM samples were dialyzed against 50 mM phosphate buffer pH 7.5, containing 10% glycerol, which insured that neither form of the protein was interconverted during dialysis (see *Results*). Retention of the different forms of the protein was monitored by using non-denaturing gel polyacrylamide gel electrophoresis. Protein-TFE samples were prepared by adding DmpM (27 μg) to 50 mM phosphate buffer, pH 7.5, with 10% glycerol and different TFE concentrations to a total volume of 200 μl (13 μM DmpM). CD spectra were acquired using the same instrument parameters as described above.

Temperature denaturation of DmpM: Thermal denaturation between 25-90°C was monitored at 222 nm using a heating rate of 1°C/min in a 0.1 cm jacketed cell in the circular dichroism instrument described above. Temperature was controlled using a

Neslab RTE-111 water bath. The concentrations of native and inactive recombinant DmpM during temperature denaturation were 13 and 15 μM, respectively, and the buffer used was 50 mM sodium phosphate, pH 7.5, containing 10% glycerol.

Gel filtration chromatography: A HiPrep S-100 (Pharmacia) gel filtration column (60 x 1.6 cm) was calibrated using proteins of known molecular weight. Each standard protein (4 mg), cytochrome c (M_r 12 500), chymotrypsin A (M_r 25 000), and albumin (M_r 45 000), was dissolved in 50 mM MOPS, pH 7.4, containing 0.15 M NaCl, (0.5 ml) and eluted from the column using this buffer. A flow rate of 0.4 ml/min was used, and 1.5 ml fractions were collected for analysis. Molecular masses of unknowns were estimated using the standard curve of log M_r vs elution time of the standard proteins.

Resolution of two forms of DmpM using gel filtration chromatography: Inactive recombinant DmpM (124 μM) was treated with 6 M guanidium-HCl and then loaded onto the S-100 column equilibrated with 50 mM MOPS, pH 7.4, containing 0.15 M NaCl. The column was then developed (0.3 ml/min) using this buffer, and 1.4 ml fractions were collected. Samples of fractions were analysed by electrophoresis on a native polyacrylamide gel. Fractions that contained the faster-migrating form were combined and concentrated using a Centricon 10 concentrator. Fractions containing the slower-migrating form were concentrated separately.

Analytical ultracentrifugation: Sedimentation velocity experiments were performed using a Beckman Coulter XL-A analytical ultracentrifuge at 20°C and a rotor speed of 56,000

rpm. Data processing was done using the computer program, Origin, provided by Beckman Coulter. The molecular mass of recombinant DmpM was calculated from the time derivative of the sedimentation velocity concentration profile according to the method of Stafford (25). The calculated molecular weight from this algorithm was corrected using values for the partial specific volume of the protein and solution density of 0.7291 mL/g (calculated using the program Sedinterp) and 1.029 g/mL (26), respectively. Protein solutions were dialyzed against 50 mM sodium phosphate buffer pH 7.5 + 10% glycerol and the protein concentration for the sedimentation velocity experiment was approximately 0.2 mg/ml.

RESULTS

Purification of DmpM from Pseudomonas sp. strain *CF600*: DmpM from phenol-grown *Pseudomonas* CF600 was purified according to the steps outlined in *Materials and Methods*. Purified protein migrated as a single band on SDS-polyacrylamide gels (data not shown). Identification as the *dmpM* gene product was confirmed by amino terminal sequencing in the case of native DmpM. Electrospray mass spectrometry revealed a single species in both recombinant and native samples, with identical masses of 10,361.3 ± 1.3 Da. This agrees well with the molecular mass of 10,359.55 Da calculated from the amino acid composition (1) minus the amino-terminal methionine residue.

Identification of two forms of DmpM : Under some conditions fast and slow-migrating forms of DmpM were distinguished using non-denaturing polyacrylamide gel electrophoresis (Fig 2.1). Although DmpM purified from phenol-grown *Pseudomonas sp.* strain CF600 was always isolated mainly as the faster-migrating form (Fig 2.1, Lane A), a slower-migrating form was isolated from *E. coli* overexpressing DmpM (Fig. 2.1, Lane B).

Both forms were present in crude extracts from *E. coli* overexpressing DmpM (Fig 2.2). The first step for purification of recombinant DmpM involved a DEAE-anion exchange column where these two forms separated (data not shown). Fractions containing each of the two forms were combined separately and then carried on through the purification procedure separately. The two forms did not appear to interchange substantially during further purification (data not shown). While the fast-migrating form was active in stimulating phenol hydroxylase activity, the slow-migrating form was not

Figure 2.1 Non-denaturing polyacrylamide gel of native and recombinant DmpM (2.2 μg). Samples were purified from *Pseudomonas sp.* CF600 (Lane A) or purified inactive recombinant DmpM (Lane B).


A B

Figure 2.2 Non-denaturing gel electrophoresis monitoring expression of recombinant DmpM after induction with 0.5 mM IPTG. Crude extracts (5 μg of protein) of cells from various time points after induction were loaded in each well. Lane 1; crude extract from uninduced cells; Lanes 2-6, crude extracts from cells at 15, 30, 60, 120 and 180 min after induction, respectively. Migration positions for fast (M) and slow (*) migrating DmpM are indicated.

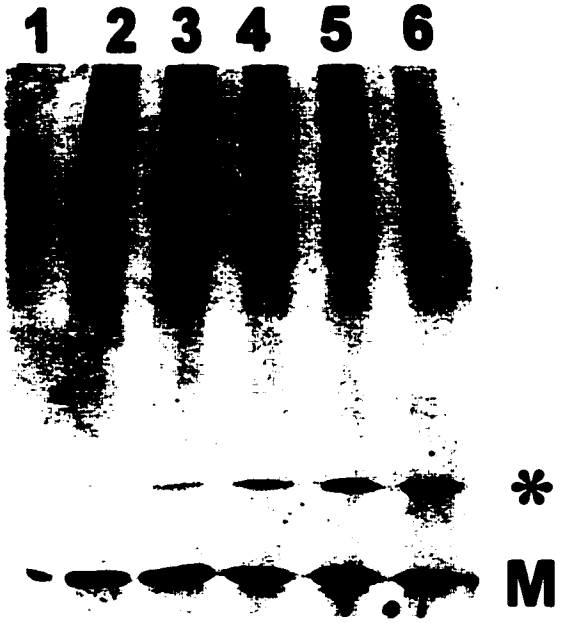
1 2 3 4 5 6
*
M

Table 2.1 Phenol hydroxylase activity with native and recombinant DmpM before and after urea denaturation

DmpM added to assay (μg)		2.5	0.5	0.25	0.125
Specific Activity (nmol/min)	Native DmpM	506	244	130	63.5
	Recombinant (+ urea)	527	123	71.5	31.5
	Recombinant (- urea)	11.7	—	—	—

Inactive recombinant DmpM was treated with 6 M urea followed by dialysis to remove the denaturant, as described in *Materials and Methods*. Non-denaturing gels indicated that equal amounts of fast and slow migrating forms were present after this treatment, while the native DmpM preparation contained only the faster- migrating species. A control recombinant sample was dialyzed, but not treated with urea.

(Table 2.1). In subsequent studies the properties of slow-migrating inactive recombinant DmpM are compared to the properties of active DmpM isolated from *Pseudomonas sp.* strain CF600.

In order to test whether inactive, slow-migrating, DmpM was formed in the cell or only during purification, recombinant DmpM production was monitored in aliquots of culture taken at different time points after induction. Cells were collected by centrifugation and sonicated to obtain crude extract. Crude extracts from each time point were subjected to non-denaturing polyacrylamide gel electrophoresis (Fig 2.2), which reveals that slow migrating DmpM is apparent at 60 min after induction, but not before. It has not been determined whether slow migrating DmpM is newly synthesized or derived from the faster-migrating form. However, it is clear that the inactive form of recombinant DmpM accumulates over time *in vivo*.

Activation of inactive DmpM: Initial attempts at activating inactive recombinant DmpM involved unfolding with 6 M urea, followed by dialysis to remove the denaturant. After this treatment, native gels showed 50% conversion to the faster-migrating band when the DmpM concentration was 124 μM (1.3 mg/ml) (data not shown). Phenol hydroxylase activity assays using the urea-treated recombinant DmpM sample showed 100% activity relative to the active (native) form when the amount of DmpM added (2.5 μg) was above that required to saturate the hydroxylase (Table 2.1). Under non-saturating conditions, the urea-treated recombinant sample, containing approximately 50% slower-migrating protein, exhibited exactly half the activity of native DmpM, which contained only fast

migrating protein (Table 2.1). Thus, incubation with urea activates DmpM by promoting conversion of the slow migrating form to the fast-migrating form.

Size exclusion chromatography: The non-denaturing gel electrophoresis results are consistent with the inactive form of DmpM being either an oligomer, or a different conformation of the native form that migrates more slowly. Since DmpM contains no cysteine residues, dithiol and disulfide forms are ruled out as a possible explanation for the two bands observed on non-denaturing, non-reducing, polyacrylamide gels. In order to estimate molecular masses of the two forms, size exclusion chromatography was performed.

The two forms in a denaturant-treated recombinant sample were successfully separated on a gel filtration column in which the elution buffer contained 0.15 M NaCl but lacked glycerol (Fig 2.3). Resolution of the peaks was dependent on the addition of 0.15 M NaCl to the elution buffer: omission of the salt resulted in elution patterns where the two peaks merged. Samples from the first peak were inactive, consisted of the slow migrating band on non-denaturing polyacrylamide gels (Fig 2.3A inset), and eluted at a position corresponding to a molecular mass of 32,000 Da. The second peak to elute from the gel filtration column eluted at a position corresponding to a molecular mass of 12,500 Da, contained active protein, and when analyzed on non-denaturing polyacrylamide gels consisted only of the faster migrating band (Fig 2.3A inset). Although the higher molecular weight species was the major component when the gel filtration column was run in the absence of glycerol (Fig 2.3A), the lower molecular weight form was predominant when glycerol was included in the dialysis and elution buffers (Fig 2.3B and

Figure 2.3 Gel filtration of recombinant DmpM in the absence (A) and presence (B) of glycerol. Non-denaturing gel electrophoresis of peak fractions is also shown (*inset*). **A**: Elution profile of inactive recombinant DmpM (1.3 mg/ml) treated with GdHCl (6M), dialysed against 50 mM MOPS, pH 7.4, lacking glycerol, and eluted through the S-100 column with the same buffer containing 0.15 M NaCl. **B**: Elution profile of inactive recombinant DmpM (1.3 mg/ml) treated with GdHCl (6M), dialysed against 50 mM MOPS, pH 7.4, +10% glycerol, and eluted as in A.

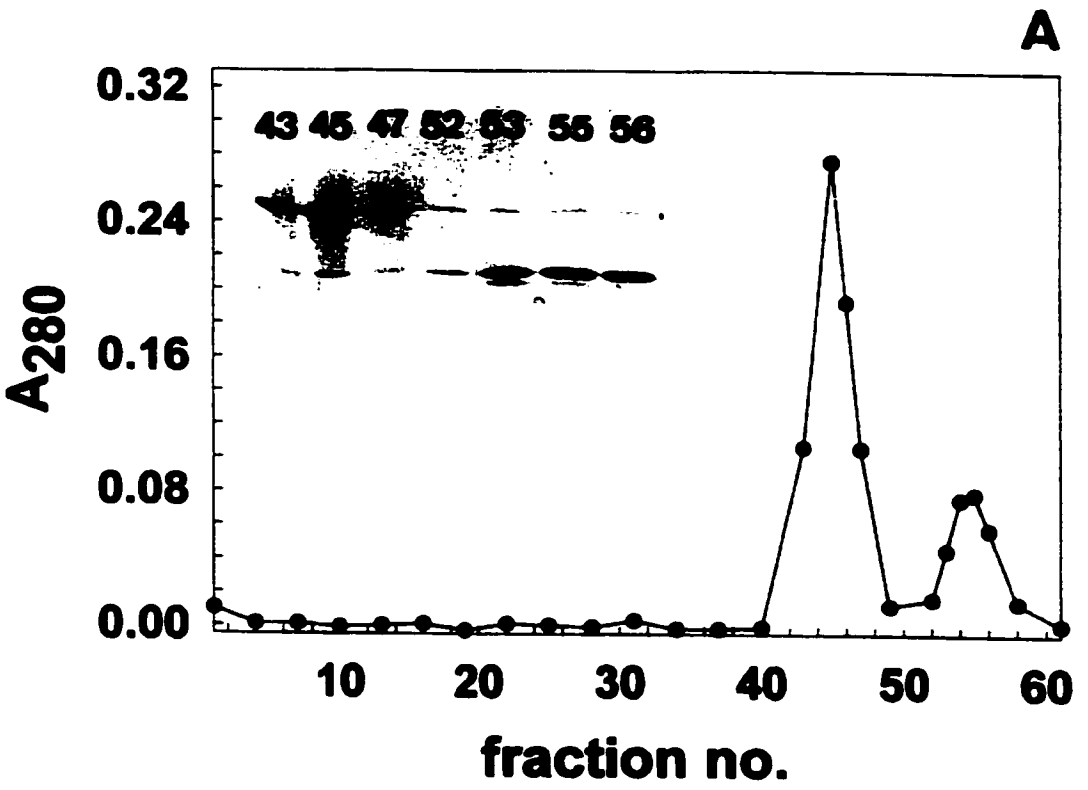
A
0.32
0.24
0.16
0.08
0.00
A280
43 45 47 52 53 55 56
10
20
30
40
50
60
fraction no.

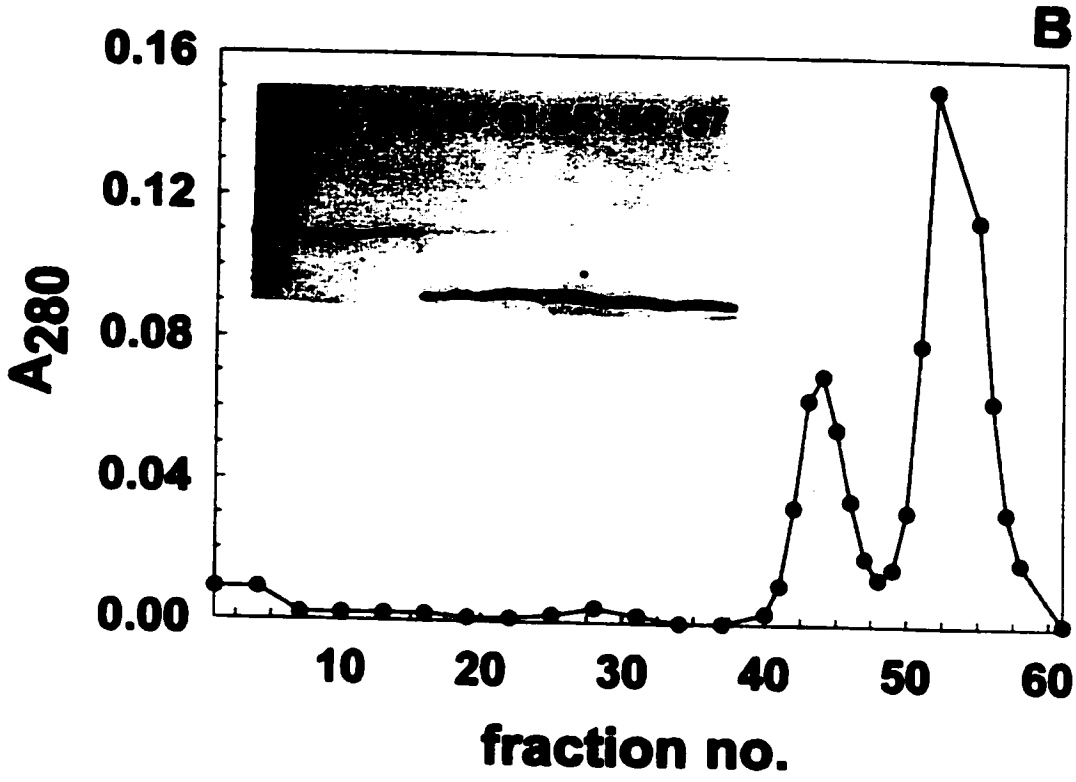
B
0.16
0.12
0.08
0.04
0.00
A280
10
20
30
40
50
60
fraction no.

inset). These data suggest that the active form of DmpM is monomeric, that the inactive form is an oligomer, and that glycerol affects the equilibrium between the two forms.

Interconversion between the two forms of DmpM is prevented by glycerol: The differing gel filtration profiles in the presence and absence of glycerol suggested that glycerol influences the distribution of DmpM between monomeric and oligomeric forms. Inactive recombinant DmpM was initially purified, like the native protein, using buffer containing 10% glycerol. Removal of glycerol by dialysis resulted in formation of active DmpM (Table 2.2): therefore glycerol appears to stabilize the inactive, slow migrating form of DmpM. Conversely, dialysis of native DmpM at against buffer lacking glycerol resulted in formation of the inactive, slow migrating form (Table 2.2). Therefore, both forms appear to be stabilized by the presence of glycerol.

Evidence that oligomeric DmpM is a dimer: Inactive recombinant and native DmpM preparations were exposed to various chemical cross-linkers in order to further characterize the oligomeric form. Figure 4 shows that inactive recombinant DmpM gave rise to bands corresponding to the molecular weight of dimeric DmpM when exposed to the cross-linker, EDC. These cross-linked products were not observed when native (fast-migrating) DmpM was incubated with the same cross-linkers (Fig 2.4). These results suggest that the inactive form is a dimer, rather than the trimer suggested by gel filtration experiments. This was confirmed in sedimentation velocity experiments, which gave a molecular weight of 20,913 Da for the inactive recombinant form of DmpM: a single boundary was observed, as would be expected for a homogeneous preparation.

Table 2.2 Relative phenol hydroxylase activity with native and recombinant DmpM after various treatments

Preparation	Treatment	Relative Activity (%)
Native DmpM (1.3 mg/ml)	None	100
	Dialysed against MOPS, pH 7.5	26
	Dialysed against MOPS pH 7.5 +10% glycerol	108
	Heating at 90°C [a]	96
Inactive recombinant DmpM (1.3 mg/ml)	None	ND[b]
	Dialysed against TGD	ND
	Dialysed against MOPS pH 7.5	29
	Dialysed against MOPS pH 7.5+ 10% glycerol	ND
	Heating at 90°C [a]	96

The phenol hydroxylase activity assays were carried out as described *in Methods and Materials* using 0.25 μg of DmpM. [a] The protein concentrations of native and recombinant DmpM in the heated samples were 0.13 and 0.15 mg/ml, respectively. [b] ND, not detectable.

Figure 2.4 Cross-linking of native (Lanes 1 and 2) and inactive recombinant (Lanes 3 and 4) DmpM with EDC at 25°C. Native DmpM without EDC (Lane 1); native DmpM + EDC (Lane 2) recombinant DmpM without EDC (Lane 3); recombinant DmpM + EDC (Lane 4)

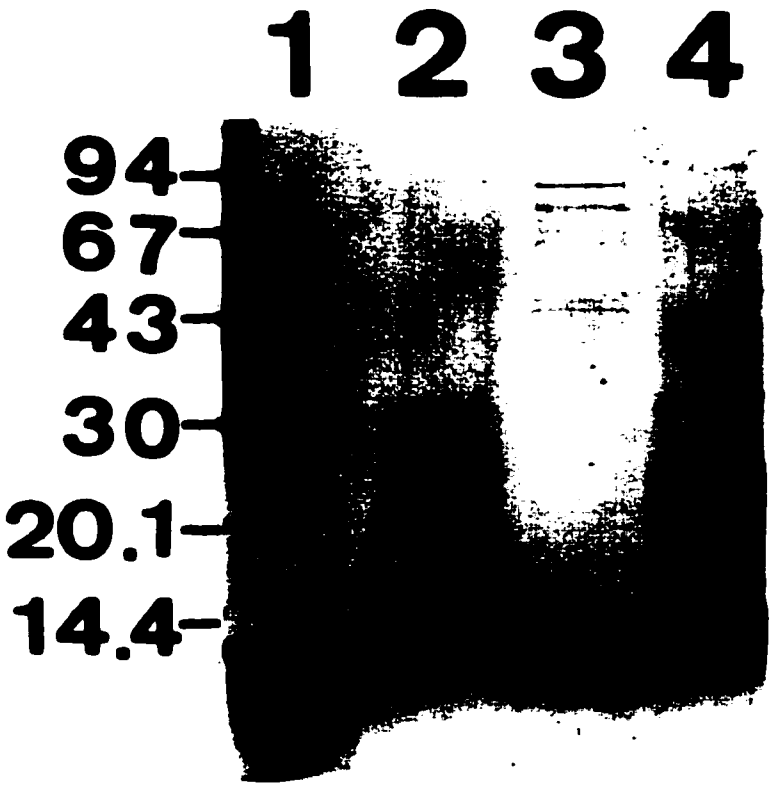
1 2 3 4
94
67
43
30
20.1
14.4

Activation of DmpM by heating: Inactive recombinant DmpM was also activated by heating to 90°C at a rate of 1°C/min. Table 2.2 shows that recombinant DmpM gained 96% activity relative to native DmpM activity after this treatment.

The state of DmpM resulting from heating was examined using both non-denaturing gel electrophoresis and CD spectroscopy. The CD spectrum of dimeric DmpM at 90°C indicated that the protein was not completely denatured at 90° (data not shown), suggesting that refolding from a completely unfolded form is not necessary for activation. Furthermore, non-denaturing polyacrylamide gel electrophoresis indicated that heat-activated recombinant DmpM migrated in the fast-migrating band characteristic of active protein (data not shown).

Activation with trifluoroethanol: The action of denaturants on the activation process was further probed by examining the effects of trifluoroethanol (TFE), which is known to affect secondary, tertiary and quaternary structures of proteins (27). As is shown in Fig 2.5, native DmpM remained active at all TFE concentrations tested. Inactive recombinant DmpM underwent a transition at 10-17.5% TFE, becoming fully active at the higher concentration of TFE (Fig 2.5). Non-denaturing polyacrylamide gel electrophoresis analysis of the samples at each TFE concentration showed a progressive increase in the proportion of the faster-migrating form over the same range of TFE concentrations, with essentially 100% in this form at 17.5% TFE (data not shown).

Although native DmpM maintained activity at all TFE concentrations, the far-UV CD spectrum of native DmpM indicated increasing α-helical content as TFE was added (data not shown). These structural changes may be reversed when DmpM is diluted into

Figure 2.5 Activation of dimeric DmpM by treatment with TFE. Phenol hydroxylase activity assays with DmpM (2.2 nmol) were as described in *Materials and Methods*. Dimeric recombinant (o) and native DmpM (•) were incubated at indicated TFE concentrations prior to activity assay.

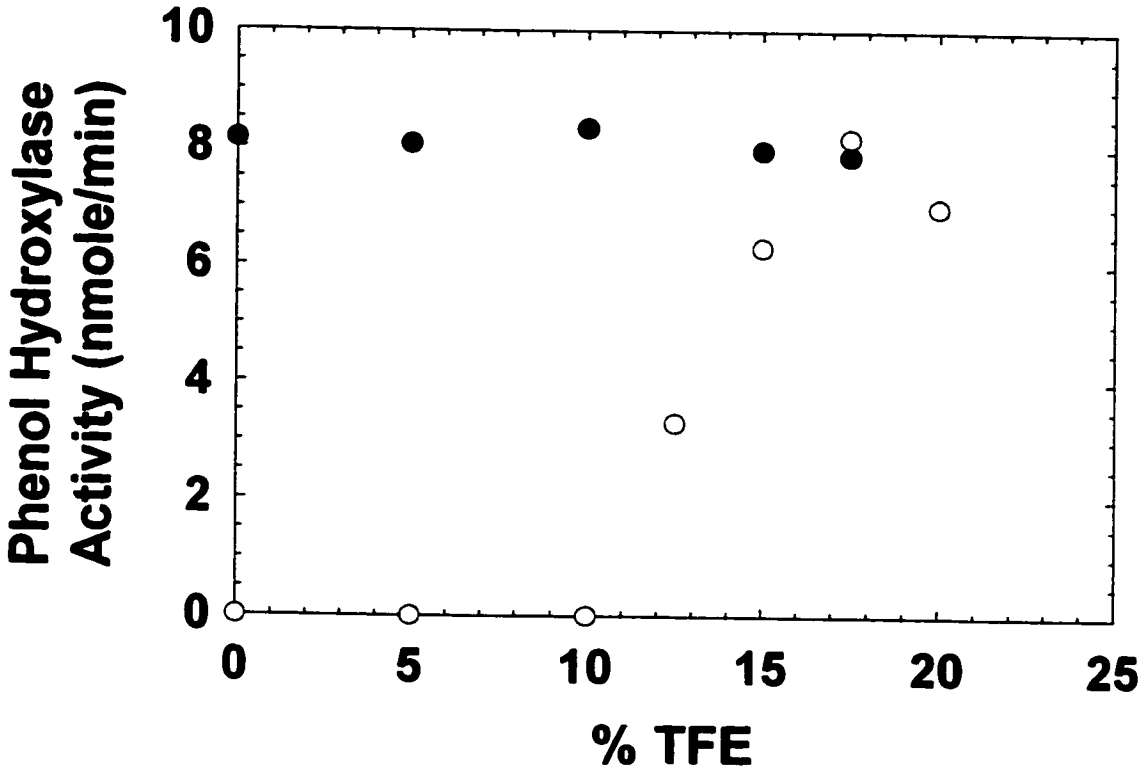
Phenol Hydroxylase Activity (nmole/min)
10
8
6
4
2
0
0
5
10
15
20
25
% TFE

assay mixtures lacking TFE, as activity is maintained (Fig 2.5). Increasing α-helical content was also observed when TFE was titrated into the inactive recombinant form (data not shown). Thus, addition of 17.5% TFE induces structural changes which result in activation of recombinant DmpM.

Dependence of activation on urea and protein concentrations: The effects of different concentrations of urea on inactive recombinant DmpM were examined both using activity assays and non-denaturing gel electrophoresis. DmpM samples were allowed to equilibrate overnight in buffer containing different concentrations of urea. Activation of DmpM by treatment with urea was dependent on protein concentration (Fig 2.6). Samples were incubated in the presence of urea at two different protein concentrations: 0.08 and 1.2 mg/ml (7.6 and 114 μM). The higher protein concentration required a greater concentration of urea for activation (Fig 2.6), as well as for the parallel conversion to the faster-migrating electrophoretic form (data not shown). The observed dependence on protein concentration is consistent with the existence of an inactive dimeric form of DmpM that is progressively dissociated as the urea concentration increases.

Urea-induced unfolding of DmpM monitored by CD spectroscopy: Denaturation of native (100% fast-migrating) and recombinant (100% slow-migrating) DmpM at different concentrations of urea was monitored by CD spectroscopy. The observed transitions were essentially identical when protein concentrations were kept at or below 29 μM (Fig 2.7).

Figure 2.6 Protein concentration dependence of recombinant DmpM activation with urea. DmpM (2.2 nmol) was used in phenol hydroxylase activity assays as described in *Materials and Methods*. Different concentrations of dimeric DmpM (0.08 mg/ml (•),1.2 mg/ml (Δ)) were incubated with various concentrations of urea prior to activity assays.

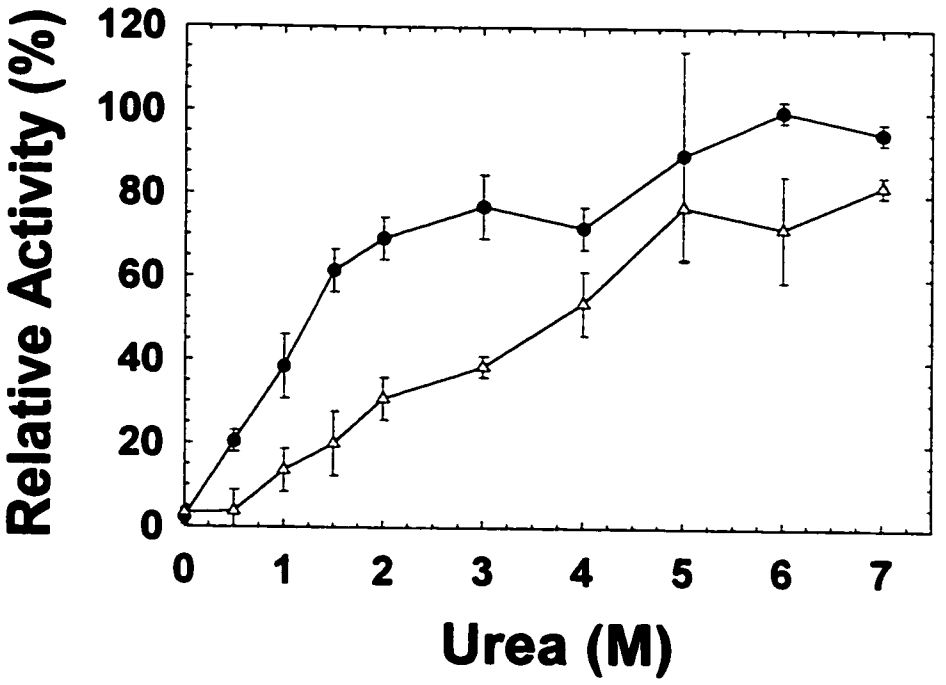
Relative Activity (%)
120
100
80
60
40
20
0
0
1
2
3
4
5
6
7
Urea (M)

Figure 2.7 Urea denaturation curves of native and recombinant dimeric DmpM monitored by circular dichroism and fluorescence spectroscopies at 25°C. **A**: Native DmpM (8.7 μM) in 50 mM sodium phosphate buffer pH 7.5 + 10% glycerol. **B**: Recombinant DmpM (9.1 μM) in 50 mM sodium phosphate buffer pH 7.5 + 10% glycerol. (•, CD data; —, fitted CD data; Δ, fluorescence data; · · ·, fitted fluorescence data). Fitted ΔG_{H2O} obtained from CD data: 3.67 ± 0.45 kcal/mol for native DmpM and 4.33 ± 0.54 kcal/mol for recombinant DmpM. ΔG_{H2O} obtained from fluorescence data; 3.74 ± 0.40 kcal/mol for native DmpM and 4.44 ± 0.37 kcal/mol for recombinant DmpM.

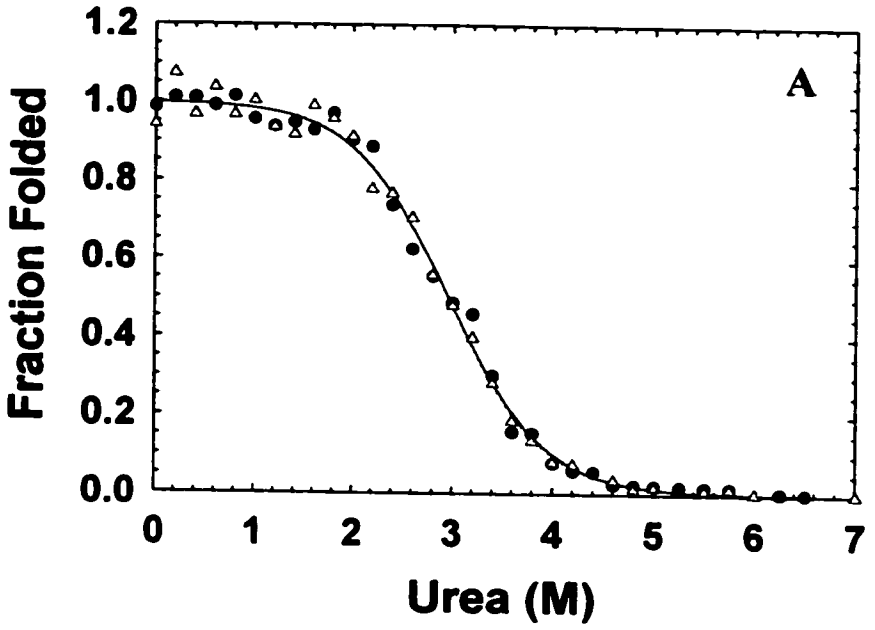
A
Fraction Folded
1.2
1.0
0.8
0.6
0.4
0.2
0.0
0
1
2
3
4
5
6
7
Urea (M)

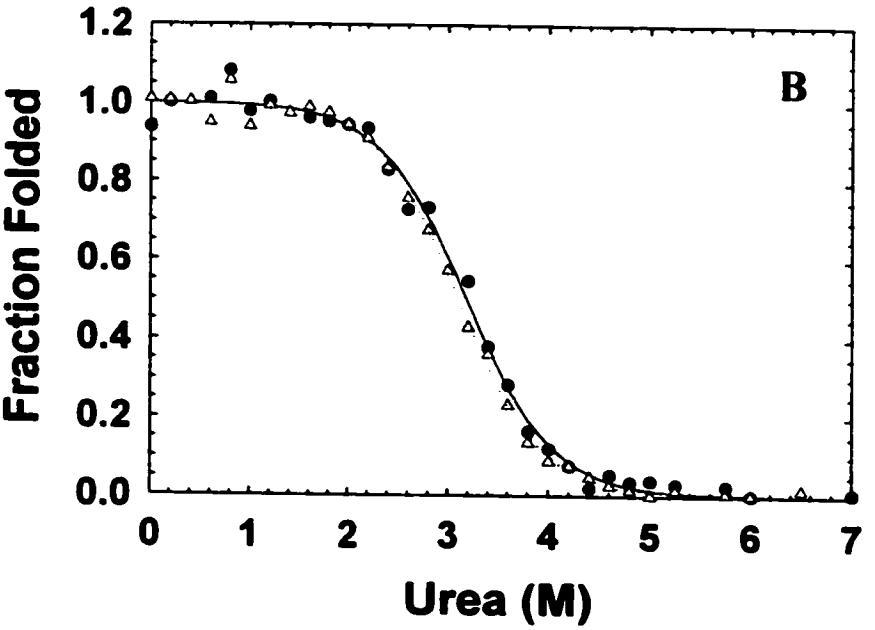
B
Fraction Folded
1.2
1.0
0.8
0.6
0.4
0.2
0.0
0
1
2
3
4
5
6
7
Urea (M)

Similar results were obtained using fluorescence spectroscopy (see below). At higher concentrations of recombinant DmpM, denaturation curves were protein concentration dependent (data not shown). These results suggest that at low protein concentrations the recombinant dimer dissociates before denaturation occurs, and that it is the monomeric form that denatures.

Urea gradient gel electrophoresis to monitor DmpM dissociation and unfolding: Urea gradient gels were used in order to obtain evidence for dissociation of oligomeric DmpM prior to unfolding. In the absence of urea, most of the sample is in the dimeric (slow-migrating) form, with a small amount of the monomer (faster migrating form) also present (Fig 2.8). Between 2 and 2.5 M urea, the slow-migrating form of DmpM is converted to the faster-migrating form characteristic of native DmpM monomer (Fig 2.8). The smear is indicative of slow equilibration between the two forms on the time-scale of the experiment (28). Denaturation then occurs between 3 and 4.5 M urea, producing the slowest-migrating, unfolded, form.

Figure 2.8 indicates a small shift, in both dissociation and denaturation, to a higher urea concentration compared with the CD and fluorescence denaturation data (Fig 2.7, and see below). This shift may be due to the difference in pH during electrophoresis, which is about 2 pH units higher than the pH of the solutions prepared for CD and fluorescence denaturation experiments. A urea gradient gel run using a buffer system at pH 7.5 (23) showed that at this pH, denaturation occurs between 2 and 4.5 M urea (data not shown), while dissociation occurs between 1 and 2 M urea. This behavior agrees more closely with the CD and fluorescence denaturation data, suggesting pH is indeed important.

Figure 2. 8 Discontinuous urea gradient gel electrophoresis of recombinant (dimeric) DmpM. Inactive recombinant DmpM (0.1 mg/ml) in 50 mM phosphate buffer pH 7.5 +10% glycerol was applied to urea gradient polyacrylamide gels ranging from 0 to 6.5 M urea.

UREA (M) 0 0.5 1 1.5 2 2.5 3 3.5 4 4.5 5 5.5 6 6.5

Fluorescence-monitored unfolding of DmpM: Denaturation of both native and recombinant DmpM above 2 M urea was also monitored using the red shift of the fluorescence emission maximum at 338 nm (Fig 2.9A). Fitting this data using a two-state unfolding model gave results almost identical to those obtained using CD spectroscopy to monitor unfolding (Fig 2.7).

Native DmpM, already in the monomer form, has a fluorescence spectrum which is less intense than that of the recombinant dimer when urea is not present (Fig 2.9B). Native DmpM undergoes a transition between 0 and 2 M urea resulting in an increase in fluorescence intensity at 338 nm (cf. Fig 2.9A and 2.9B), so that the fluorescence spectra of the two forms are identical in 2 M urea (Fig 2.9A). At 2-2.5 M urea, dissociation of the dimer has been shown to occur by urea gel electrophoresis (Fig 2.8). Interestingly, no significant fluorescence intensity changes were observed between 0 and 2M urea for the recombinant, dimeric, form of DmpM (Fig 2.9). These data are consistent with formation of an altered conformation of DmpM monomer, with the spectral characteristics of the dimeric form, produced from either native or recombinant DmpM in the presence of 2 M urea. It is this form of the monomer that is capable of undergoing dimerization.

Figure 2.9 : Fluorescence spectra of recombinant and native DmpM. **A**: Native (···) and recombinant (—) DmpM at 2 M urea and native (— —) and recombinant (– –) DmpM at 7 M urea. **B**: Native (···) and recombinant (—) DmpM in 0 M urea. A small correction factor was applied to account for different protein concentrations in recombinant and native samples by assuming that the spectra of native and recombinant DmpM should be the same in 7 M urea.

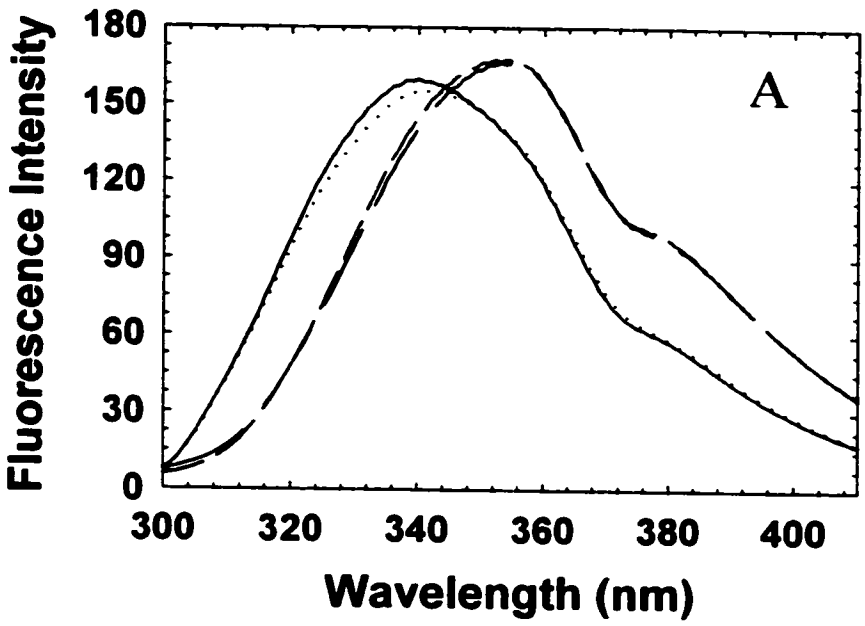
Fluorescence Intensity
180
150
120
90
60
30
0
300
320
340
360
380
400
Wavelength (nm)
A

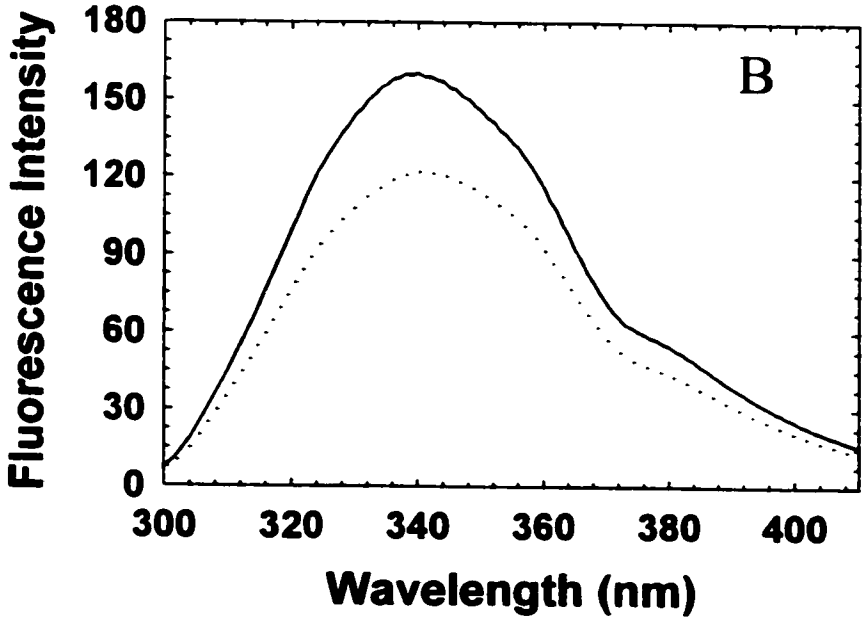
Fluorescence Intensity
180
150
120
90
60
30
0
300
320
340
360
380
400
Wavelength (nm)
B

DISCUSSION

Stimulatory proteins similar to DmpM are associated with multicomponent binuclear iron center-containing oxygenases such as toluene and methane monooxygenases. The best-studied example is MmoB, the stimulatory protein for methane monooxygenase. Studies of this protein have focussed on how interactions of the oxygenase with MmoB affect the reactivity of the oxygenase (5, 9-12). In the course of studying phenol hydroxylase, we found that recombinant DmpM could readily be isolated in an inactive form. In order to carry out site-directed mutagenesis studies of this protein, we needed to be able to obtain fully active preparations. In addition, we wanted to determine why these preparations were inactive, and whether this might be related to regulation of the oxygenase by this protein. Some of the impetus for this work came from recent findings that MmoB is converted to inactive forms by proteolytic events (13), although the physiological significance of this finding is uncertain.

No evidence was found for proteolysis of recombinant DmpM, which instead appeared to undergo dimerization to produce an inactive form. This form was readily distinguished from the active form by polyacrylamide gel electrophoresis under non-denaturing conditions. While some dimerization may occur during purification, it was also observed that the inactive form accumulated as induction progressed during cell growth. Thus, one way of minimizing the amount of the inactive form is to use relatively short induction times during expression.

The observation of a slower-migating form on non-denaturing polyacrylamide gels is consistent with dimer formation, but was not the sole piece of evidence for it. It was possible to separate the two forms of DmpM by gel filtration: the higher molecular weight form corresponded to the slower-migrating form and was inactive. The estimated

molecular mass was consistent with a trimeric structure, although cross-linking studies provided evidence only for a dimer. Sedimentation velocity experiments confirmed that the inactive slow-migrating form of DmpM is a dimer. The low molecular weight peak from the gel filtration column corresponded to the faster-migrating electrophoretic form and was active: the estimated molecular mass is consistent with a monomer. Finally, urea denaturation studies indicated a two-state transition for native DmpM, consistent with an equilibrium between folded and unfolded forms of the monomer. By contrast, the unfolding of recombinant DmpM was more complex and dependent on protein concentration, as would be expected for a dimeric form of the protein.

The observation that DmpM is active as a monomer, but inactive as a dimer, is interesting since similar proteins have been reported to exist in both forms (5, 6). The stimulatory activities of these different forms have not been reported. Since, like methane monooxygenase (5) phenol hydroxylase appears to be an $(\alpha\beta\gamma)_2$ complex (this laboratory, unpublished results) , it is likely that it is fully activated by 2 molecules of DmpM acting independently rather than by a DmpM dimer.

A number of methods for recovering the active form of DmpM were investigated. Heat denaturation successfully reactivated the protein and, as was evident from CD spectroscopy data, reactivation by this method did not involve full refolding. Incubation of inactive preparations with trifluoroethanol (10-20%) also activated inactive preparations, and reactivation correlated with the conversion of dimer to monomer. However, the effects of this denaturant on DmpM were complex. Non-denaturing concentrations of urea also activated recombinant DmpM, in a protein concentration-dependent manner. It was established that at a concentration of dimeric DmpM of 7.6 μM,

incubation with 3 M urea resulted in approximately 80% activity upon dilution in the assay cuvette (Fig 2.6). Furthermore, dissociation of the dimer to the monomer was observed to occur at 2-2.5 M urea by urea gradient gel electrophoresis, indicating that conversion to the monomer form can account for activation of the recombinant form.

Although inactive dimeric DmpM has not been observed in significant quantities after purification of native DmpM from *Pseudomonas sp.* strain CF600, simply removing glycerol allowed its partial conversion to the inactive form. Conversely, conversion of dimeric DmpM to monomer also occurred after removal of glycerol. Since glycerol stabilizes both the active monomer and inactive dimer forms of DmpM, the two species cannot be in direct equilibrium. Possibly, a conformational change allows DmpM to achieve a form which can dimerize. Evidence for this was obtained from urea-induced changes monitored by fluorescence spectroscopy. These data were consistent with the following scheme:

$$\begin{array}{ccccc} M & \rightleftharpoons & D & \rightleftharpoons & U \\ & & \Vert & & \\ & & DD & & \end{array}$$

where M is the native form, DD is the recombinant dimer, D is the monomer form present at 2-2.5 M urea, and U is the unfolded form of DmpM. In this model, glycerol binding to both M and DD may prevent interconversion of the two forms. In any event, it is only the D form of the monomer that can readily dimerize.

A number of possibilities can be entertained for how active DmpM is maintained in *Pseudomonas* CF600 growing at the expense of phenol. The most obvious explanation is that DmpM readily associates with the other components of phenol hydroxylase, thus

preventing the transition. Another factor may be that the concentration of DmpM in the cell remains low enough to favour folding into the monomeric, active form.

No evidence for significant inactive dimer formation in the native strain was obtained, yet it is possible that it does exist and could play a physiological role in the regulation of phenol hydroxylase activity. This might be required, for example, to prevent unnecessary oxidation of NADH by phenol hydroxylase in the absence of phenol. Interestingly, an inactivation event also occurs with the DmpM homologue, MmoB of soluble methane monooxygenase from *Methylococcus capsulatus* (Bath) (13). In this case, the inactive form of MmoB resulted from proteolysis between met12 and gly13. However, amino acid residues 2-34 of MmoB of methane monooxygenases are lacking in DmpM, and we have never observed any proteolysis in samples of DmpM that have been subjected to mass spectrometry analysis.

ACKNOWLEDGMENTS

This work was supported by an operating grant from the Natural Sciences and Engineering Research Council of Canada to JP. We thank Dr. Peter White from Boehringer Ingelheim (Canada), Ltd, Bioméga Research Division, for running the sedimentation velocity experiment and for analysis of the data. We thank Judith Kornblatt and Joanne Turnbull for their valuable advice, and Lena Sahlman for critical reading of the manuscript

REFERENCES

1. Nordlund, I., Powlowski, J., and Shingler, V. (1990) *J. Bacteriol.* **172**, 6826-6833
2. Powlowski, J. and Shingler, V. (1990) *J. Bacteriol.* **172**, 6834-6840
3. Powlowski, J. and Shingler, V. (1994) *Biodegradation* **5**, 219-236
4. Powlowski, J., Sealy, J., Shingler, V., and Cadieux, E. (1997) *J. Biol. Chem* **272**, 945-951
5. Fox, B.G., Froland, W.A., Dege, J.E., and Lipscomb, J.D. (1989) *J. Biol. Chem.* **264**, 10023-10033
6. Newman, L., and Wackett, L. (1995) *Biochemistry* **34**, 14066-14076
7. Qian, H., Edlund, U., Powlowski, J., Shingler, V., and Sethson, I. (1997) *Biochemistry* **36**, 495-504
8. Johnson, G.R. and Olsen, R.H. (1995) *Appl. Environ. Microbiol.* **61**, 3336-3346
9. Fox, B., Liu, Y., Dege, J.E., and Lipscomb, J.D. (1991) *J. Biol. Chem.* **266**, 540-550
10. Froland, W.A., Andersson, K.K., Lee, S., Liu, Y., and Lipscomb, J.D. (1992) *J. Biol. Chem.* **267**, 17588-17597
11. Davydov, A., Davydov, R., Graslund, A., Lipscomb, J.D., and Andersson, K.K. (1997) *J. Biol. Chem.* **272**, 7022-7026
12. Liu, Y., Nesheim, J.C., Lee, S., and Lipscomb, J.D. (1995) *J. Biol. Chem.* **270**, 24662-24665
13. Lloyd, J.S., Bhambra, A., Murrell, J.C., and Dalton, H. (1997) *Eur. J. Biochem.* **248**, 72-79
14. Brown R.E., Jarvis K.L., and Hyland K.J. (1989) *Anal. Biochem.* **180**, 136-138
15. Laemmli, U. K., (1970) *Nature (London)* **227**, 680-685

16. Schagger, H. and von Jagow,G. (1987) *Anal. Biochem.* **166**, 368-379

17. Sambrook, J., Fritsch, E.F., and Maniatis, T. (1989) *Molecular Cloning: A Laboratory Manual*, 2nd ed., Cold Spring Harbor Laboratory, Cold Spring Harbor, New York

18. Rosenburg, A.H., Lade, B.N., Chui, D.-S., Lin, S.W., Dunn, J.J., and Studier, F.W. (1987) *Gene (Amst.)* **56**, 125-135

19. Grabarek, Z., & Gergely, J. (1990) *Analytical Biochem.* **185**, 131-135

20. Pace, C.N., Shirley, B.R., & Thomson, J.A. (1990) in Protein Structure. A Practical Approach (Creighton, T. E., Ed.,) pp 311-330, IRL Press at Oxford University: Oxford, England.

21. Pace, C.N. (1986) *Methods Enzymol.* **131**, 266

22. Santoro, M.M. and Bolen, D.W. (1988) *Biochemistry* **27**, 8063-8068

23. Gentile, F., Veneziani, B. M., and Sellitto, C. (1997) *Analytical Biochem.* **244**, 228-232

24. McLellen, T., (1982) *Analytical Biochem.* **126**, 94-99

25. Stafford, W. F.III (1992) *Analytical Biochem.* **203**, 295-301

26. CRC Handbook of Chemistry and Physics, 59th edition, p D-278

27. Sonnichsen, F. D., Van Eyk, J. E., Hodges, R. S., and Sykes, B. D., (1992) *Biochemistry* **31**, 8790-8798

28. Creighton, T. E., (1979) *J. Mol. Biol.* **129**, 235-264

Chapter 3

The Role of DmpK in the Assembly of the Binuclear Iron Centre in Phenol Hydroxylase

ABSTRACT

Assembly of the binuclear iron centre in the oxygenase component of phenol hydroxylase was examined in the presence and absence of DmpK, a protein previously shown to be required for *in vivo* synthesis of active oxygenase. Apo-oxygenase was fully reconstituted in the presence of two or more Fe^{2+} per active site in the absence of DmpK. However, reconstitution was incomplete at lower ratios of Fe^{2+}/apo-oxygenase. Catalytic quantities of DmpK were found to accelerate reconstitution, and appeared to ensure that all of the apoenzyme was reconstituted. However, DmpK itself did not stably bind Fe^{2+}, and could not donate Fe^{2+} in the presence of chelators, suggesting that its primary role is not to deliver Fe^{2+} to the active site. When the oxygenase binuclear iron site was occupied by Mn^{2+}, DmpK was required for significant levels of reconstitution in the presence of added Fe^{2+}. This suggests a role for DmpK in metal ion discrimination. Binding experiments indicated that DmpK interacts tightly with both holo- and apo-forms of the oxygenase. Taken together, these results are consistent with binding of DmpK to the oxygenase to promote a conformational change that allows the enzyme to preferentially and efficiently bind Fe^{2+} under conditions when iron is limiting.

INTRODUCTION

There is increasing evidence that incorporation of metals into proteins and enzymes in organisms is protein-assisted. For example, while bacterial iron-sulfur centers may be assembled *in vitro* by incubation of ferric iron, thiol and sulfide (1), a battery of proteins encoded by the *isc* operon is required *in vivo* (2). Other examples include yCCS, a copper-binding protein that delivers copper to copper-zinc superoxide dismutase (3), and proteins associated with delivery of nickel to urease (4). Although detailed mechanisms for assisted metalloprotein assembly are generally lacking, proposed or demonstrated roles for accessory proteins include: metal ion binding (5,6), metal ion delivery (5,7,8), provision of an assembly scaffold (9) or delivery of a non-metal component of the prosthetic group (such as S^{2-} for iron-sulfur centers (10)). In other cases, the roles of proteins implicated in metallocentre assembly are still obscure.

A requirement for metallocenter assembly proteins appears to reflect the very low intracellular availability of certain metal ions, and the need to direct metal ions to their appropriate binding sites in newly-synthesized proteins. For example, in a study of superoxide dismutase assembly, intracellular free copper was found to be virtually nonexistent (3,11). A battery of proteins demonstrated to be involved in copper transport and distribution in eukaryotes indicates that access to copper inside the cell is tightly controlled (reviewed in 7).

Intracellular concentrations of free iron must also be very low since ferric ion is insoluble and ferrous iron is toxic by virtue of its ready reactivity with oxygen to generate free radicals. While iron uptake and storage mechanisms have been well-documented, the form of the mobile iron pool in the bacterial cell remains obscure

(12,13). Although many examples can be found in the literature of successful re-activation of apoproteins by incubation with ferrous iron, the limited availability of intracellular iron suggests that it is unlikely such mechanisms could account for *in vivo* assembly at a rate compatible with growth. However, aside from the example of iron-sulfur cluster assembly, and the involvement of ferrochelatase in heme assembly (14), there is relatively little evidence that accessory proteins exist for assembly of other iron centers in proteins.

We have previously reported evidence of a role for DmpK in the assembly of the diiron cluster of phenol hydroxylase (15). Phenol hydroxylase is the first enzyme in the *meta*-cleavage phenol degradation pathway of *Pseudomonas* sp. strain CF600, and is a multicomponent enzyme comprising five polypeptides encoded by *dmpLMNOP* (16,17). DmpLNO is a diiron containing oxygenase; DmpP is a reductase containing an FAD cofactor and an iron-sulfur cluster; and DmpM is a regulatory protein without any metals or cofactors (18,19). Deletion of *dmpK*, which is just upstream of *dmpLMNOP*, abolished the ability of cells to grow on phenol as the sole carbon and energy source (16). No hydroxylase activity was detected in crude extracts of *E. coli* expressing the oxygenase (DmpLNO) in the absence of *dmpK*, but addition of ferrous iron to crude extract in the presence of *dmpK* activated the oxygenase: oxygenase expressed in the presence of DmpK was active (15). These results established an important role for DmpK in the assembly of an active oxygenase, but the nature of this role was not determined.

Of all the well-characterised diiron containing proteins and enzymes, DmpK is the only protein shown to be involved in the assembly of a diiron cluster reported so far. In

this report, we have further examined the role DmpK plays in activating the oxygenase component of phenol hydroxylase, using *in vitro* reconstitution procedures.

EXPERIMENTAL PROCEDURES

Materials. DTT was purchased from Bioshop. NADH was obtained from Roche Molecular Biochemicals; phenol, ferrous ammonium sulfate, glycerol (ultrapure), and Tris were from ICN Biochemicals. IAEDANS was purchased from Pierce. Catechol 2,3-dioxygenase was purified as described elsewhere (15). The reductase (DmpP) and the activator protein (DmpM) were purified as previously described (17,18).

Analytical Methods. Protein concentration was estimated by the BCA method (Pierce) using the 60°C protocol provided by the manufacturer. Interfering substances such as iron and DTT were removed by using a modification of this protocol (20). In some cases, the spectophotometric method of Gill and von Hippel (21) was used to estimate protein concentration and gave results essentially identical to those obtained with the BCA assay. Iron content was estimated using the method described by Percival (22) using a standard iron solution purchased from BDH. Fluorescence polarization measurements were carried out on a Shimadzu model RF 5000 spectrofluorometer equipped with quartz polarizers. Circular dichroism spectroscopy was done using a Jasco J-710 CD spectrometer. Electrospray mass spectrometry data were collected on a Finnigan SSQ 7000 single quadropole mass spectrometer. Samples were passed through a 1 cm C-18 column (Michrom Bioresources) interfaced to the mass spectrometer. The cartridge was initially equilibrated with 95% water-5% acetonitrile-0.05% trifluoroacetic acid, and elution was with 35% water-65% acetonitrile-0.05% trifluoroacetic acid.

Expression Conditions. Expression and purification of DmpK, as well as conditions for expression of the recombinant oxygenase component of phenol hydroxylase (DmpLNO) in the presence and absence of *dmpK* expression have also been described previously (15).

Purification from E. coli *of* dmpLNO *expressed in the absence of* dmpK. Recombinant oxygenase (DmpLNO) expressed in the absence of DmpK was purified following the purification protocol developed for phenol hydroxylase from *Pseudomonas* sp. strain CF600 (Chapter 4, this thesis). Two peaks from the phenyl-Sepharose column contained phenol hydroxylase, as judged by SDS-PAGE. Enzyme that eluted under the same conditions as native enzyme (with 5 mM Tris-HCl, pH 8, containing 10% glycerol) was carried on to the next purification step, and is referred to as "Form A". Oxygenase that eluted earlier, with 50 mM Tris-HCl pH 8.0 containing 10% glycerol, was combined and stored at –80°C until it was purified further using the same steps as for the native hydroxylase purification, resulting in "Form B". Further purification of Form A resulted in two peaks from the last column (Fast-Flow DEAE Sepharose), which were combined and concentrated separately. These are referred to as Forms A1 and A2.

Purification from E. coli *of* dmpLNO *expressed in the presence of* dmpK. Recombinant oxygenase expressed in the presence of DmpK was purified following the protocol for phenol hydroxylase from *Pseudomonas* sp. strain CF600 (Chapter 4, this thesis).

Phenol Hydroxylase Activity Assays. Phenol hydroxylase activity was monitored as described previously, using catechol 2,3-dioxygenase to convert the product, catechol, to its yellow-coloured ring cleavage product (15).

Preparation of Apo-oxygenase. Purified oxygenase (64 μM) was dialyzed against 50 mM imidazole pH 7.0, containing the chelator, 8-hydroxyquinoline-5-sulfonate (50 mM), for 2 hr. The dialyzed sample was then passed through an Econo-Pac 10DG desalting column (BioRad) equilibrated with 50 mM Tris-HCl pH 7.4, containing 10% glycerol. Sometimes, instead of the desalting column, dialysis against 50 mM Tris-HCl pH 8, containing 10% glycerol, was used to remove the chelator. The dialysis buffer was changed a total of 3 times.

Reconstitution with Fe^{2+}. Apo-oxygenase (1.1 nmole) diluted to 105 μl with 50 mM Tris-acetate pH 7.5 was added to ferrous ammonium sulfate (2 nmol) in the presence or absence of DmpK (0.06 nmole). The solutions were incubated for the times indicated before addition to a phenol hydroxylase assay mixture. Since DmpK has an inhibitory effect on phenol hydroxylase activity (15), DmpK was added to the activity assays containing the –DmpK reconstitution mix to compensate for the inhibitory effect. Aerobic reconstitution in the presence of DmpK was also done at various Fe: apo-oxygenase ratios. These mixtures were incubated at room temperature for 30 min before assaying for activity.

Reconstitution with Fe^{3+}. Reconstitution was done as described above using 10 mM $FeCl_3$ 1:1 citrate pH 7.53 instead of ferrous ammonium sulfate.

Inhibition with Mn^{2+} and Zn^{2+}. 1 nmole apo-oxygenase was mixed with 2 nmol $MnCl_2$ or 2 nmol $ZnCl_2$ in a total volume of 105 µl 50 mM Tris-acetate, pH 7.5, and incubated at room temperature. After 15 minutes, 2 nmol Fe^{2+} was added in the presence or absence of 0.48 nM DmpK. The two mixtures (+/- DmpK) were then incubated for various times until the phenol hydroxylase assay was performed.

Conjugation of DmpK with IAEDANS. A 10x molar excess of the reductant, TCEP, was added to a 2 mg/ml solution of DmpK in 50 mM Tris buffer pH 8.5 (1ml) and incubated on ice for 20 minutes. A 200 µl aliquot of IAEDANS solution (11 mg/ml, 20x molar excess) was added to the protein mixture and incubated in the dark at 4° C for 24 hours. The sample was then passed twice through an Econo-Pac 10-DG desalting column equilibrated with 50 mM Tris-HCl buffer pH 8.5. The conjugated sample was analyzed by mass spectrometry before use.

Fluorescence Polarization. Titrations of 86 nM DmpK-IAEDANS (400 µl) with apo and holo-oxygenase were carried out at 25°C in 50 mM Tris-HCl buffer pH 7.5. Excitation and emission wavelengths of 336 nm and 480 nm, respectively, were used to determine the polarization values during titration. Polarization (P) was calculated using the equation $P= (F0^{\circ} - GF90^{\circ})/(F0^{\circ} + GF90^{\circ})$ where $F0^{\circ}$ and $F90^{\circ}$ are the fluorescence intensities measured with the emission polarizer set parallel and perpendicular to the excitation

polarizer, respectively. G is the G factor, which corrects for the difference in transmission efficiencies of the detectors to vertically and horizontally polarized light. Kd's were estimated by fitting the data using the following equation:

$$\alpha = (([L]_T+[E]_T+K_d) -(([L]_T+[E]_T+K_d)^2-4*[L]_T*[E]_T)^{0.5})/(2*[E]_T)$$

where α is the degree of saturation ($\Delta F/\Delta F_M$), $[L]_T$ is the total amount of ligand added (holo or apo-oxygenase), $[E]_T$ is the total concentration of DmpK-IAEDANS, and K_d is the dissociation constant (23).

Iron binding to DmpK. A 5 x molar excess of ferrous ammonium sulfate was added to purified DmpK (72 μM) in 50 mM Tris-HCl pH 7.4. The mixture was allowed to incubate aerobically at room temperature for 30 min before removing the excess iron by passing the sample through a PD-10 desalting column (Pharmacia) previously equilibrated with 50 mM Tris-HCl pH 7.4. Samples eluting from the desalting column were analyzed by measuring absorbances at 280 nm, and iron assays were performed on all fractions.

Analytical Ultracentrifugation. Sedimentation velocity experiments were performed on a Beckman Coulter XL-I analytical ultracentrifuge at 20°C with a rotor speed of 45 000 rpm (An-60 Ti). Data processing was done with DCDT+ and Svedberg software written by John Philo (24, 25). Prior to ultracentrifugation, samples were dialyzed against 50 mM Tris-HCl pH 7.5, or the same buffer containing 150 mM NaCl.

Isothermal Titration Calorimetry. Calorimetric experiments were performed with a VP-ITC titration calorimeter (Microcal). Protein samples were dialysed against 50 mM Tris-HCl pH 8.0 at 4°C before use. The $MnCl_2$ solution was prepared in the same dialysis buffer used for the proteins. The reaction cell contained 1.4 mL of apo-oxygenase (25 μM) with or without DmpK (1.25 μM). The injection syringe was filled with 1.5 mM $MnCl_2$ and was rotating at 400 rpm during the titration. The titration experiments consisted of 40 injections, each of 4 μL and 6 sec duration with 720 sec interval between injections. Data were analysed using software provided by the manufacturer.

Manganese binding to apo-oxygenase. A 5x molar excess of $MnCl_2$ was added to apo-oxygenase (11 μM) in 50 mM MOPS buffer, pH 7.5. This mixture was incubated at room temperature for 15 minutes, after which excess Mn^{2+} was removed by passage through a PD-10 desalting column previously equilibrated with 50 mM MOPS buffer, pH 7.5. Fractions (1 ml) were collected and analyzed by measuring the absorbance at 280 nm. Fractions containing the oxygenase were then analyzed for manganese content using the protocol described by McCall (26).

ICP-MS. ICP-MS samples were run by Margaret Antler at McGill University. Samples were prepared using the protocol for acid digestion described by Kimbrough et al. (27).

RESULTS

Preparation of Apo-oxygenase

Iron-free oxygenase was prepared as described in *Experimental Procedures*, using a method described originally for removal of the binuclear iron center from ribonucleotide reductase (28). The iron content of holo-oxygenase preparations was 1.6-2.4 Fe/oxygenase active site, whereas apo-oxygenase preparations contained no detectable iron and were devoid of phenol hydroxylase activity. In addition, ICP-MS analysis of apoenzyme prepared using this method showed no Cu, Mn, Co or Zn present in quantities greater than those present in holoenzyme (0.5 Zn per oxygenase and less than 0.2 Cu, Mn, Co per oxygenase). No differences in migration of apo- and holo-oxygenases were observed during native gel electrophoresis or analytical ultracentrifugation, and far-UV circular dichroism spectra of the two forms were essentially identical (data not shown). However, there was a significant difference in the fluorescence spectra of apo- and holo-oxygenases (Fig 3.1). These results are consistent with the occurrence of a conformational change as a result of iron removal from the oxygenase.

Restoration of activity by Fe^{2+}

Oxygenase activity was restored upon incubation of apoenzyme with increasing concentrations of Fe^{2+} (Fig 3.2A). The maximum reconstituted activity, reached at 2 Fe^{2+}/active site, was generally 90-100% that of the original holoenzyme preparation. Reconstitution of phenol hydroxylase activity was not observed when Fe^{3+} was substituted for Fe^{2+} (data not shown). Control experiments done in the absence of

Figure 3.1 Fluorescence spectra of apo and holo phenol hydroxylase. Fluorescence spectra of 0.46 μM apo (—) and holo (– –) oxygenase in 50 mM Tris-HCl pH 7.5 at 25°C. Excitation wavelength was 280 nm. Activities were measured over a 60 min. incubation period.

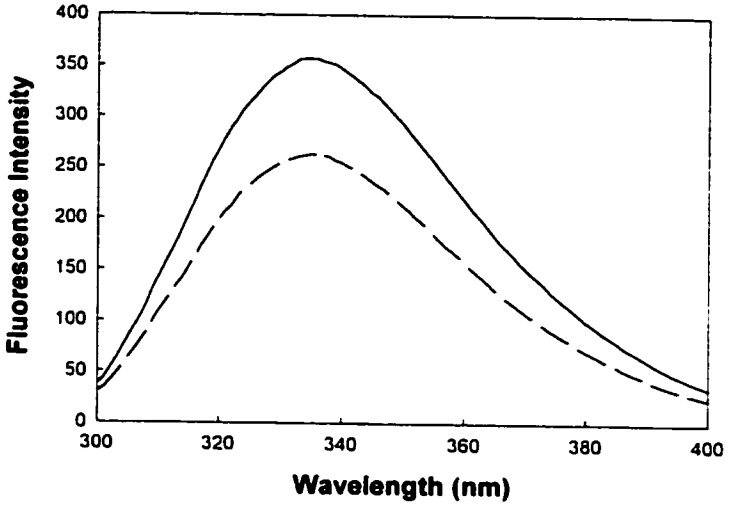
Fluorescence Intensity
400
350
300
250
200
150
100
50
0
300
320
340
360
380
400
Wavelength (nm)

apoenzyme showed that over the maximum time course of the reconstitution with Fe^{2+}, approximately 40% of the Fe^{2+} was oxidized to Fe^{3+}.

The presence of a 1:20 ratio of DmpK to apo-oxygenase enhanced the restoration of activity during titration with Fe^{2+} (Fig 3.2A). The concentration of DmpK was intentionally kept low to minimize the inhibitory effects when it is present at high concentration (15). DmpK increased the equilibrium proportion of active enzyme at the lowest Fe^{2+} concentrations, but at ratios of 2 Fe^{2+}/active site and higher, DmpK had little effect (Fig 3.2B). These data indicate that DmpK is important for the formation of active enzyme when Fe^{2+} is limiting, but not when there is enough to saturate the available binding sites. Furthermore, the direct dependence of activity on Fe^{2+} concentration in the presence of DmpK indicates that Fe^{2+} binding is highly co-operative, with little accumulation of inactive mononuclear Fe^{2+}-substituted oxygenase during the titration (29).

Kinetics of activity restoration in the presence and absence of DmpK

The effects of DmpK on the kinetics of apo-enzyme reconstitution were examined using limiting and non-limiting ratios of Fe^{2+}/apoenzyme. At all ratios, the presence of DmpK accelerated the appearance of active enzyme (Fig 3.3). The differences in rate become less pronounced as the Fe^{2+} to apoenzyme ratio increases. As was observed for the experiment shown in Fig 3.2, when Fe^{2+} was not saturating a lower proportion of the enzyme was activated. This could reflect either oxidation of iron during the longer time course in the absence of DmpK, or the incorporation of iron into mononuclear sites in the

Figure 3.2 Equilibrium reconstitution of phenol hydroxylase activity. **A** Apo-oxygenase was incubated with different ferrous ammonium sulfate concentrations in the presence (•) or absence (o) of DmpK as described in Experimental Procedures. Samples were incubated for 60 min at room temperature before activity assays were performed. **B**: Data from Figure 3.2A replotted as % difference in specific activity between +/- DmpK samples during reconstitution.

A

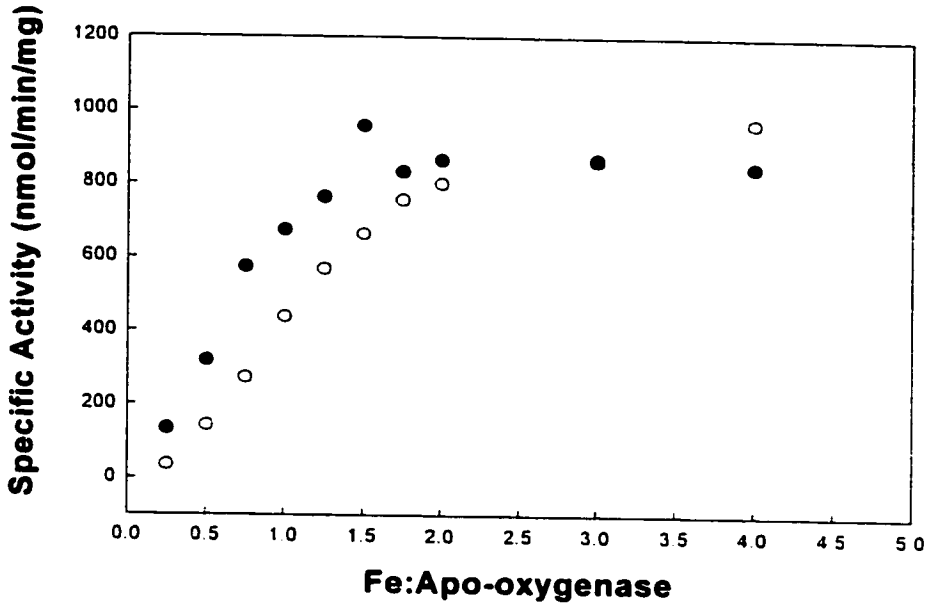
Specific Activity (nmol/min/mg)
1200
1000
800
600
400
200
0
0.0
0.5
1.0
1.5
2.0
2.5
3.0
3.5
4.0
4.5
5.0
Fe:Apo-oxygenase

B

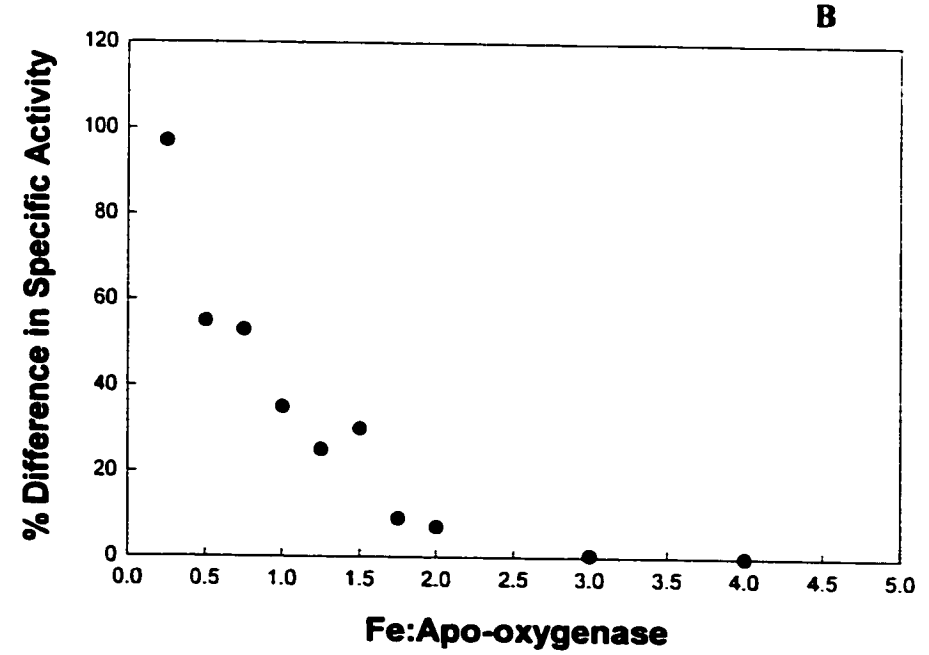
% Difference in Specific Activity
120
100
80
60
40
20
0
0.0
0.5
1.0
1.5
2.0
2.5
3.0
3.5
4.0
4.5
5.0
Fe:Apo-oxygenase

Figure 3.3 Kinetics of reconstitution at 0.5:1 (**A**), 1:1 (**B**), 2:1 (**C**), and 6:1 (**D**) Fe^{2+} to apo-oxygenase. Apooxygenase was incubated with varying concentrations of ferrous ammonium sulfate and assayed over time in the presence (•) and absence (o) of DmpK.

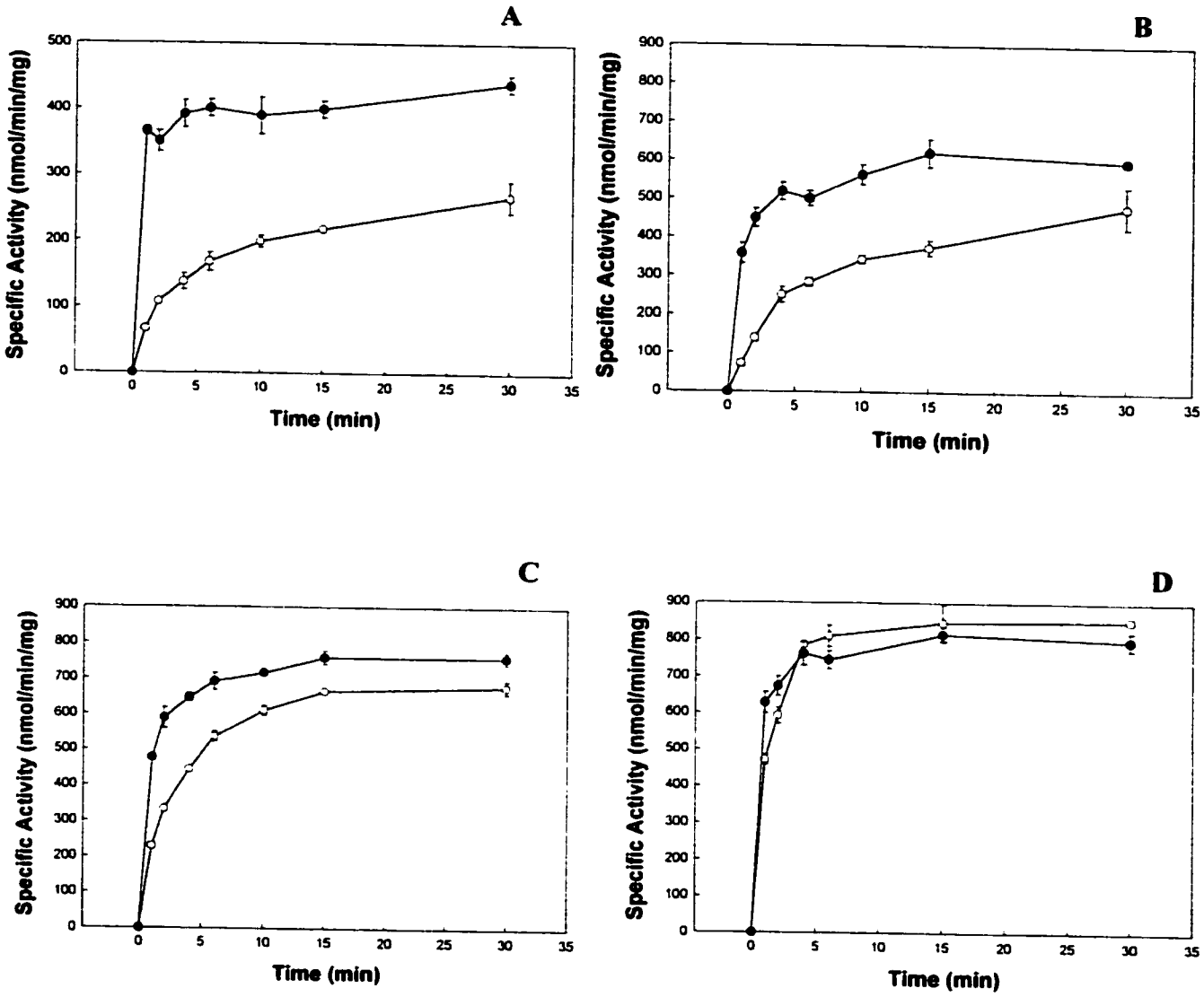
A
Specific Activity (nmol/min/mg)
Time (min)
B
Specific Activity (nmol/min/mg)
Time (min)
C
Specific Activity (nmol/min/mg)
Time (min)
D
Specific Activity (nmol/min/mg)
Time (min)

absence of DmpK, or both. Addition of DmpK *after* reconstitution with sub-saturating Fe^{2+} in the absence of DmpK failed to increase activity further (data not shown). The ratio of apo-oxygenase to DmpK was 20:1 in this experiment.

Inhibition of reconstitution by $MnCl_2$

Since it is likely that apo-oxygenase is exposed to a variety of divalent metal ions inside the cell, a role for DmpK in promoting metal ion discrimination was examined. These studies focussed initially on the effects of DmpK on holoenzyme reconstitution in the presence of competing Mn^{2+}. The binuclear iron binding sites of both ribonucleotide reductase and methane monoxygenase have been shown capable of binding Mn^{2+} in place of Fe^{2+} (30, 31).

Isothermal titration calorimetry experiments indicate that the apo-oxygenase of phenol hydroxylase binds Mn^{2+} at a ratio of 1 per oxygenase active site, but holoenzyme does not (Fig 3.4). It is thus reasonable to assume that Mn^{2+} binds at the Fe^{2+} binding sites, a conclusion supported by the observation that binding of Mn^{2+} severely inhibits activation by Fe^{2+} (see below). The Mn^{2+}:oxygenase binding ratio of 1 was verified by incubating the apo-oxygenase with $MnCl_2$, and removing the excess, as described in *Experimental Procedures*. The resulting preparation contained 0.7:1 Mn:oxygenase, as determined by the fluorescence manganese assay. This stoichiometry is curious, since with other apo-binuclear iron center proteins, incorporation of Mn^{2+} into both centers has been reported (30,31). The presence of DmpK did not affect the Mn^{2+} binding stoichiometry, but it did abolish a binding transient that was observed when the apo-oxygenase was titrated with Mn^{2+} in the absence of DmpK (Fig 3.4B).

Figure 3.4: Isothermal titration calorimetry of Mn^{2+} binding to apo- and holo-oxygenase. Apo-oxygenase was titrated with Mn^{2+} in the absence (**A**) and presence (**B**) of DmpK as described in the text, holooxygenase titrated with Mn^{2+} (**C**). The integrated data are also shown and fit to a one binding-site equation.

A

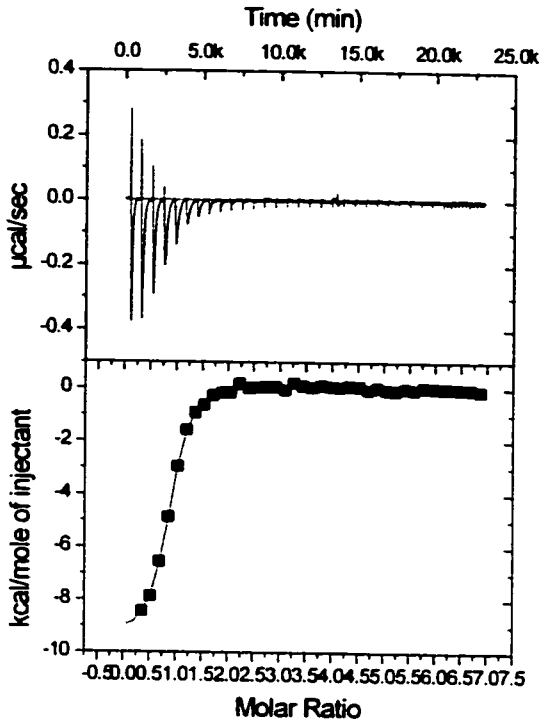
Time (min)
0.0
5.0k
10.0k
15.0k
20.0k
25.0k
µcal/sec
kcal/mole of injectant
Molar Ratio

B

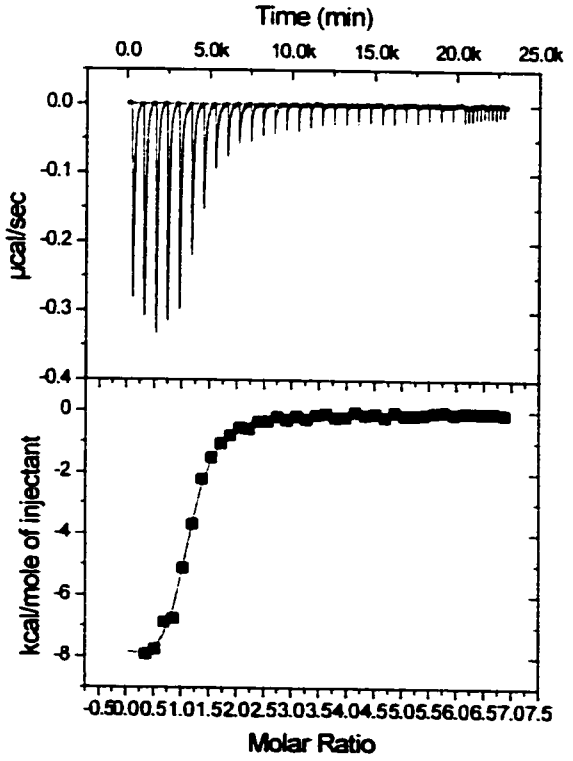
Time (min)
0.0
5.0k
10.0k
15.0k
20.0k
25.0k
µcal/sec
kcal/mole of injectant
Molar Ratio

C

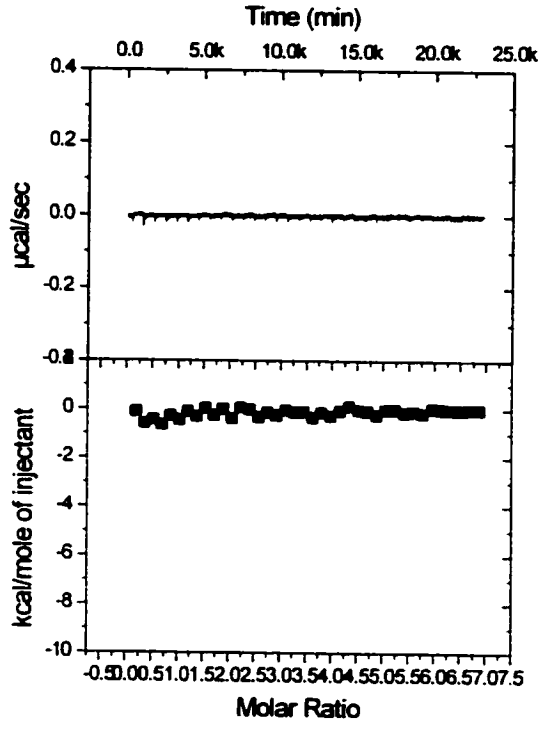
Time (min)
0.0
5.0k
10.0k
15.0k
20.0k
25.0k
0.4
0.2
0.0
-0.2
µcal/sec
0
-2
-4
-6
-8
-10
kcal/mole of injectant
-0.5 0.0 0.5 1.0 1.5 2.0 2.5 3.0 3.5 4.0 4.5 5.0 5.5 6.0 6.5 7.0 7.5
Molar Ratio

The effects of pre-incubation of apo-oxygenase with Mn^{2+} on the reconstitution of activity by Fe^{2+} were examined in the presence or absence of DmpK. Thus, apo-oxygenase with or without DmpK (20:1) was incubated with 2 equivalents of $MnCl_2$ for 15 min, followed by the addition of 2 equivalents of Fe^{2+}. After various times, activity assays were carried out. Pre-incubation with Mn^{2+} in the absence of DmpK resulted in only 7% activation 45 min after adding Fe^{2+} contrasting with 90-100% observed in the absence of Mn^{2+}. Pre-incubation with Mn^{2+} in the presence of DmpK yielded 51% activity compared to full activation in the absence of Mn^{2+}. These results suggest that DmpK may either prevent Mn^{2+} from binding to iron sites or DmpK may recognize Mn^{2+}-substituted oxygenase, and cause the Mn^{2+} to be removed so that iron can be incorporated. The ITC data demonstrate that Mn^{2+} can still bind to the apoenzyme in the presence of DmpK (Fig 3.4B), therefore, DmpK does not prevent Mn^{2+} from binding but perhaps it lowers the affinity for Mn^{2+} and/or increases the affinity for Fe^{2+}.

In order to test whether DmpK can act *after* Mn^{2+} has already bound to oxygenase, DmpK was added together with a two- or four-fold excess of Fe^{2+}/oxygenase active site, after a 15 min pre-incubation with 2 equivalents of $MnCl_2$. In the absence of added DmpK, very little reconstitution of activity was observed, presumably since Mn^{2+} is tightly bound to the Fe sites under these conditions (Fig 3.5, white symbols). However in the presence of DmpK, approximately half maximal activity was observed with 2 Fe/oxygenase, and full activity was gained with 4Fe/oxygenase (Fig 3.5, black symbols). These results suggest that the oxygenase has a lower affinity for Mn^{2+} when DmpK is present. Reconstitution was also tested under conditions where both Fe^{2+} and

Figure 3.5 Inhibition of reconstitution with Mn^{2+}. Inhibition was done as described in *Experimental Procedures*. Specific activity was monitored after addition of stoichiometric (squares) and 4:1 (circles) ferrous ammonium sulfate to the Mn-oxygenase in the presence (black) and absence (white) of DmpK.

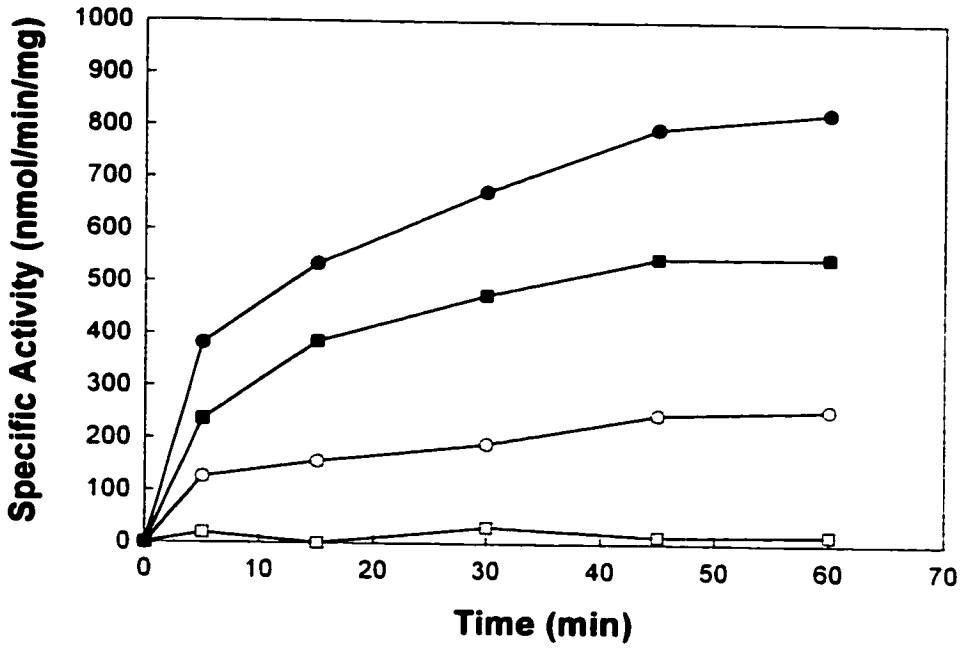
Specific Activity (nmol/min/mg)
1000
900
800
700
600
500
400
300
200
100
0
0
10
20
30
40
50
60
70
Time (min)

Mn^{2+} were present in equal concentrations. The presence of DmpK increased the activity approximately 2 fold compared to activation without DmpK (data not shown).

Release of Mn^{2+} from Mn-oxygenase is stimulated by DmpK

The ability of DmpK to stimulate metal ion release from Mn^{2+}-substituted oxygenase was directly examined in an experiment involving gel filtration chromatography. Mn^{2+}-substituted oxygenase was incubated with 1:20 of DmpK: apo-oxygenase for 30 min, after which the mixture was passed through a gel filtration column to separate the oxygenase from DmpK and free Mn^{2+}. Fractions containing the oxygenase were pooled and concentrated before reconstitution with 2 equivalents of Fe^{2+}, yielding a preparation with a specific activity of 209 nmol/min/mg. No activity was recoverable after a sample of Mn^{+2}-substituted oxygenase was subjected to gel filtration in the absence of pre-incubation with DmpK. These results provide supporting evidence for a role for DmpK in metal ion discrimination by altering the affinity for Mn^{2+}.

Purification of the oxygenase expressed in E. coli *with and without DmpK*

The results of the *in vitro* experiments are consistent with a role for DmpK in catalyzing Fe^{2+} insertion into apo-oxygenase and in allowing apo-oxygenase to discriminate between different metal ions. It was therefore of interest to examine whether oxygenase expressed in the absence of DmpK contains metal ions other than iron. Previous results indicated that oxygenase in crude extract from cells expressing it in

the absence of DmpK was not active (15), but this could be either because it lacks iron or because it contains another metal ion instead.

During purification, oxygenase expressed in *E. coli* in the absence of DmpK eluted as two separate peaks on a phenyl-Sepharose column, each of which was then further purified (see *Experimental Procedures*). The first peak from the phenyl-Sepharose column (Form B) yielded 50 mg of purified protein, from 6L of culture. The second peak eluting from the phenyl-Sepharose column separated into two peaks during a subsequent DEAE-Sepharose chromatography step. The first (Form A1) and second (Form A2) peak eluting from the DEAE column yielded 23 mg and 45 mg, respectively, of purified protein from 6L of cell culture. Forms A1 and B were both inactive and did not contain any significant quantities of iron. ICP-MS results showed that both of these forms contain significant amounts of zinc (see Table 3.1). Form A2 contained 0.3 Fe/oxygenase and the specific activity was 159 nmol/min/mg. By contrast, phenol hydroxylase purified from Pseudomonas CF600 elutes in a single peak from phenyl-Sepharose and mostly as a single peak upon elution from the subsequent DEAE column.

In a control experiment, recombinant oxygenase expressed in *E. coli* in the presence of DmpK was purified and found to have a specific activity comparable to that of purified native oxygenase, and contained 1.4 Fe/oxygenase (Table 3.1). In this case, 80 mg of protein was purified from 6L of cell culture.

Effects of added zinc on reconstitution of oxygenase by Fe^{2+}

The observation that only Zn^{2+} was associated with oxygenase purified from *E. coli* cells expressing it in the absence of DmpK prompted us to examine the effects of

zinc on Fe^{+2} uptake by apo-oxygenase. Apo-oxygenase with and without DmpK was incubated with 2 equivalents of Zn^{2+} for 15 min before addition of Fe^{2+} (Fig. 3.6). In this case, the presence of DmpK did not affect reconstitution and the low specific activity achieved indicates that very little of the enzyme was reactivated. When both Fe^{2+} and Zn^{2+} were incubated with apo-oxygenase simultaneously, DmpK allowed a larger percentage of the activity to be reconstituted, although the maximal activity was still very low (data not shown).

The possibility that Zn^{2+} binds at other sites and inhibits the oxygenase was investigated by examining its effects in steady-state phenol hydroxylase assays. Although pre-incubation of holooxygenase with $MnCl_2$ at a ratio of 2 Mn:1 holooxygenase did not affect activity, pre-incubation with $ZnCl_2$ (2:1 Zn:holooxygenase) for 45 min resulted in a 26% decrease in activity. These results suggest that Zn^{2+} may bind to an inhibitory site other than the diiron site on the oxygenase.

Binding of DmpK to apo- and holo-oxygenases

It has previously been shown using chemical cross-linkers that DmpK can bind to the large subunit (DmpN) of the oxygenase complex (15). Presumably DmpK binding to the oxygenase mediates the effects on metal ion incorporation reported above. Therefore, it was of interest to determine whether DmpK binding to the oxygenase is affected by the occupancy of the binuclear metal sites. Since DmpK is very small relative to the oxygenase, binding was conveniently monitored by fluorescence polarization using a fluorescent derivative of DmpK.

Table 3.1

Specific activity and metal content of recombinant phenol hydroxylase expressed ± DmpK

Purified Oxygenase from *E.coli*	Specific Activity (nmol/min/mg)	Metal Content (mol metal/mol oxygenase)
Expressed with DmpK	1400	1.4 Fe. 0.7 Zn
Expressed without DmpK:		
Form A1	[a]ND	[•] 0.8 Zn
Form A2	160	0.3 Fe. 0.8 Zn
Form B	[a]ND	[•]1.2 Zn

[•]No Fe was found in this sample when analyzed by colorimetric iron assay

[a]ND, not detectable

Figure 3.6 Inhibition of reconstitution with zinc. Inhibition was carried out as described in *Experimental Procedures*. Apo-oxygenase was incubated with stoichiometric zinc in the presence (•) and absence (o) DmpK for 15 min before addition of 4:1 iron per oxygenase. Specific activity was monitored after addition of iron.

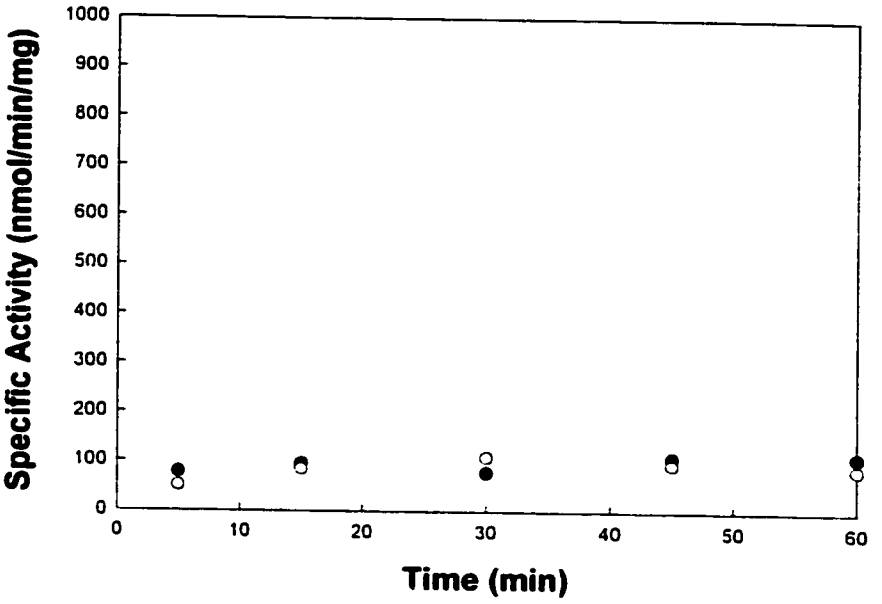
Specific Activity (nmol/min/mg)
1000
900
800
700
600
500
400
300
200
100
0
0
10
20
30
40
50
60
Time (min)

As described in *Experimental Procedures*, DmpK was modified with the cysteine-reactive reagent, IAEDANS. Analysis by electrospray mass spectrometry indicated the presence of a single species with a molecular mass of 10 755 Da, consistent with covalent modification of the single cysteine residue in DmpK by IAEDANS. DmpK labelled with IAEDANS retained the ability to stimulate reconstitution of apo-oxygenase when iron concentrations were limiting (data not shown). This result indicates that modification of the cysteine residue of DmpK does not impar its metal ion reconstitution properties.

Titrations of apo- and holo-oxygenases with IAEDANS-DmpK were monitored by fluorescence polarization. The binding curves are almost identical, indicating that DmpK has the same affinity for apo- and holo-oxygenases (Fig 3.7).

DmpK interaction with iron

In a number of cases, proteins involved in metallocenter assembly have been shown to bind the metal ions involved. Purified recombinant DmpK does not contain any significant quantity of iron (15), but it is possible that DmpK interacts with iron weakly and that iron is lost during purification. Another possibility is that since recombinant DmpK in our *E. coli* expression system is very highly expressed from the T7 promoter, perhaps the ability of the cell to supply iron is overwhelmed. Thus, previous results do not exclude the possibility that DmpK may interact with iron in the cell and mediate its donation to the oxygenase.

In order to test for iron binding, DmpK was incubated aerobically with Fe^{2+}, passed through a desalting column, and fractions were analysed for iron and protein content (Fig 4.8). DmpK eluting from the column was found to bind iron in a range of

Figure 3.7 Determination of dissociation constants for the interaction between DmpK and Apo and holo oxygenase. Fluorescence polarization experiments were done as described in the text. Fluorescence polarization of DmpK labelled with IADANS was monitored while titrating apo (Δ) and holo (•) oxygenase. Fitted data(—) resulted in Kd=190 nM for Apo-oxygenase and Kd=205 nM for holo-oxygenase interaction with DmpK.

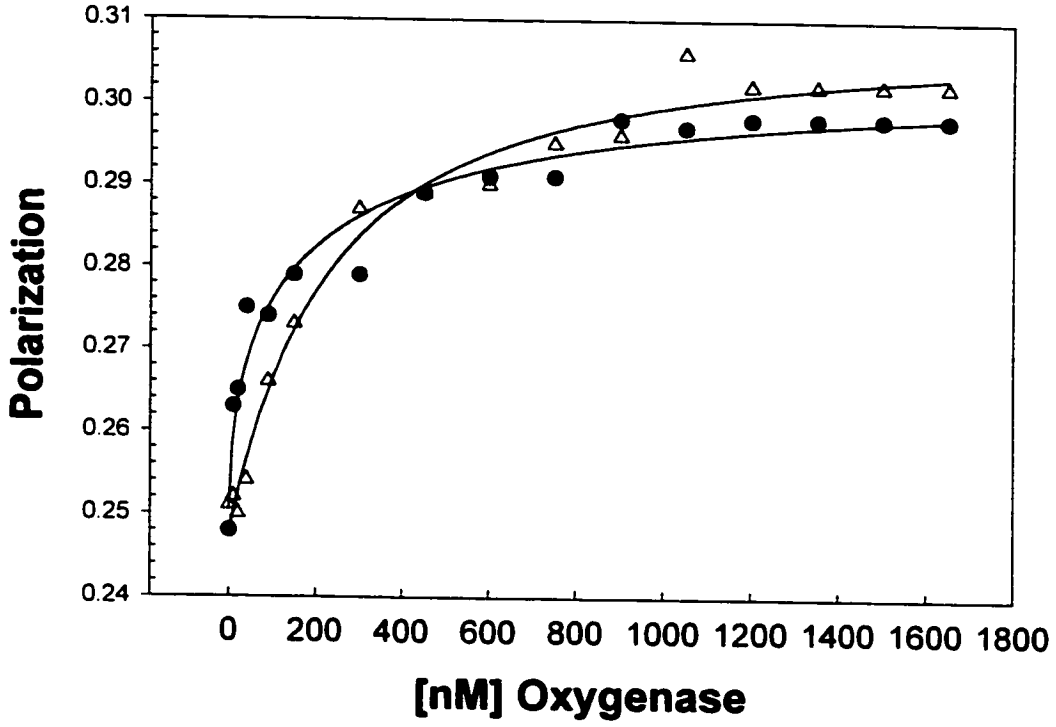
0.31
0.30
0.29
0.28
0.27
0.26
0.25
0.24
Polarization
0
200
400
600
800
1000
1200
1400
1600
1800
[nM] Oxygenase

1:1.6-2.5 iron to protein ratio. Fe^{3+} in solution seems to form complexes that elute from the desalting column at the same position as DmpK (data not shown). In order to confirm that the iron eluting with DmpK is actually bound to the protein and not oxidized iron complex eluting with DmpK, Fe^{2+} was incubated in aerobic 50 mM Tris-HCl buffer pH 7.5 without DmpK, and passed through a desalting column. The elution profile shows that under these conditions no iron elutes in fractions where DmpK elutes, hence any iron eluting with DmpK must be bound to it (Fig 3.8). The DmpK-Fe complex eluting from the desalting column was analyzed and found to contain 30% Fe^{2+} / 70% Fe^{3+} where the ratio of total iron to DmpK was 1:2.5. When DmpK was incubated with Fe^{2+} under anaerobic conditions and then desalted anaerobically, only about 1 mol Fe^{2+} / 7 mol protein was detected. Together, these results indicate that DmpK cannot stably bind Fe^{2+}.

Reconstitution of Apo-oxygenase using iron-loaded DmpK

Iron-loaded DmpK isolated as described above under aerobic conditions was incubated with apo-oxygenase at a ratio of 4:1 so that enough iron was present to potentially allow full reconstitution of the binuclear sites. After 10 min, oxygenase was separated from DmpK on an S-100 Sephacryl gel filtration column: fractions were monitored for protein content, and peaks corresponding to DmpK and oxygenase were well separated (data not shown). Fractions containing oxygenase were pooled, concentrated and assayed for iron content and activity. The specific activity of the recovered oxygenase was 100 nmol/min/mg (vs 590 nmol/min/mg for the original holoenzyme preparation) and the iron content corresponded to only about 11% compared to a holoenzyme containing 2 Fe/oxygenase monomer. Although some of the oxygenase

was reconstituted using the iron-loaded DmpK, we cannot exclude the possibility that some of the iron may have fallen off DmpK and been picked up by the oxygenase in solution, rather than being transferred directly from DmpK to the oxygenase. Furthermore, since only 30% of the iron from the DmpK-Fe complex was found to be in the ferrous form, it is not surprising that reconstitution with the DmpK-Fe complex resulted in low activity and iron content of the oxygenase since Fe^{3+} cannot reconstitute the oxygenase.

Inability of DmpK to reconstitute activity in the presence of Fe^{2+} chelator

Studies of copper and nickel accessory proteins involved in metallocentre assembly have shown that some of these proteins are able to mediate transfer of metal in the presence of efficient chelators. In order to test the ability of DmpK to mediate iron transfer in the presence of chelators, reconstitution experiments with Fe^{2+} (as described in *Experimental Procedures*) were performed in the presence of a 2-fold excess of 2,2'-bipyridyl over Fe^{2+}. Under these conditions, reconstitution was severely inhibited, and DmpK was unable to overcome this inhibition (results not shown).

Figure 3.8 PD-10 desalting column of DmpK and iron. Absorbance at 280 nm (—) and iron content (---) were measured for all fractions of the elution profile of a sample of DmpK (72uM) incubated with iron (5X molar excess) for 30 min prior to chromatography. The elution profile of Fe in 50mM Tris-HCl pH 7.5 without DmpK (— · · —) is also shown.

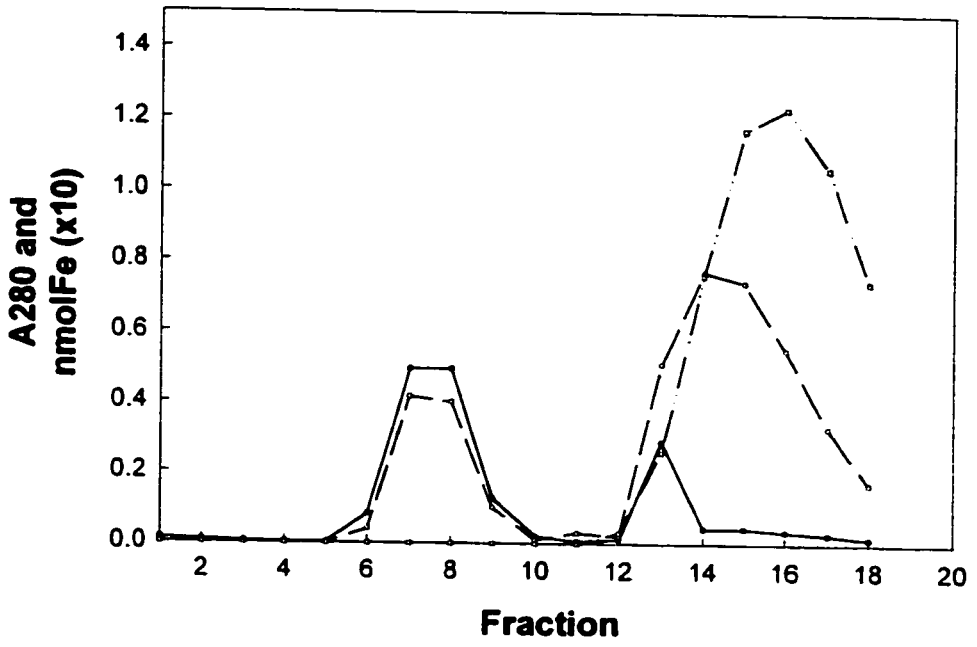
A280 and nmolFe (x10)
1.4
1.2
1.0
0.8
0.6
0.4
0.2
0.0
2
4
6
8
10
12
14
16
18
20
Fraction

DISCUSSION

The assembly of metals into metalloproteins is a topic of considerable current interest. Although thermodynamic and kinetic considerations govern the specificity of many of these assembly processes (32), a number of examples have been discovered recently where the assembly process is protein-assisted. Since the *in vivo* availability of metal ions is usually tightly controlled, it is perhaps not surprising that assembly mechanisms require the assistance of accessory proteins. At present, it is unclear how many metalloproteins require accessory proteins for assembly, and in cases where they are known to be required, mechanisms are often not well understood.

We previously reported that DmpK was required for the *in vivo* synthesis of an active phenol hydroxylase oxygenase component (15). The observation that reactivation of inactive oxygenase by crude extracts in the presence of Fe^{2+} was DmpK-dependent suggested a role for DmpK in assembly of the binuclear iron center of the oxygenase. In the present study we have examined the effects of DmpK on the reconstitution of apo-oxygenase by Fe^{2+}, in an attempt to understand how DmpK might assist in this process.

One of the complicating factors in these types of studies is the fact that the nature of the intracellular iron donor is unknown. Various high and low molecular weight iron complexes have been isolated from bacteria and are involved in intracellular iron homeostasis, but the sources of iron for metalloenzymes are not known (reviewed in 13). Furthermore, the nature of the intracellular iron pool in *Pseudomonas* sp. strain CF600 has not been studied. Therefore, in the present study we have supplied Fe^{2+} as ferrous ammonium sulfate, which is convenient but nevertheless represents a gross simplification of *in vivo* conditions.

In most of our studies, the effects of DmpK were especially evident when the concentration of Fe^{2+} was below the level required to saturate the available iron binding sites in apo-oxygenase. Observations at limiting Fe^{2+} concentrations are probably more relevant to the possible function of DmpK than the observations made in the presence of excess Fe^{2+}. Estimates of the size of the intracellular labile iron pool suggest that in *E. coli*, most of the available iron is in the reduced form at concentrations of approximately 10 μM (12, 33). In our *in vitro* reconstitution experiments, the highest concentration of Fe^{2+} was 20 μM. Since all of the labile iron is unlikely to be available for binding to apo-oxygenase, the effects that we observe are at iron concentrations likely to be physiologically relevant. It is also important to note that most experiments were done with a 20 to 1 molar excess of apo-oxygenase over DmpK. The main reason for doing this was to minimize the inhibitory effect of DmpK on oxygenase activity. The ratio of DmpK to oxygenase also appears to be quite low *in vivo* (15).

One of the major effects of DmpK on reconstitution of apo-oxygenase with Fe^{2+} was to accelerate the rate of appearance of active enzyme. It is also interesting to note that in the absence of DmpK, the level of reconstitution achieved when iron was limiting was significantly lower than that observed when DmpK was present. Addition of DmpK after the initial incubation period did not increase the activity further, suggesting that some of the iron was no longer available for activation of the remaining apoenzyme. One possibility consistent with this observation is that some of the iron oxidizes during the longer time-course in the absence of DmpK, effectively preventing it from taking part in further reconstitution. This would also explain the difference in the titration curves (Fig.

3.2): at low iron concentrations in the absence of DmpK, the apoenzyme never has a chance to become fully activated.

Reconstitution of apo-oxygenase with 2 Fe^{2+} per active site in the presence of DmpK resulted in a preparation of oxygenase with a specific activity very close to that of the original holoenzyme preparation used to generate apo-oxygenase. However, it is unlikely that the maximum specific activity represents fully active oxygenase. Mössbauer data indicate that preparations of purified oxygenase contain two species with different diiron centers whose proportion changes as the enzyme is inactivated (Chapter 4). On this basis, the most active preparations contain 20-30% of an inactive form of the binuclear iron centre. This may account for why the dependence of reconstitution on [Fe^{2+}] is not linear (Fig 3.2), as might be expected if a single set of sites were being populated.

A second major effect of DmpK was to help discriminate against Mn^{2+}, which can also bind to the apo-enzyme. Thus, in the presence of DmpK, Mn^{2+}-substituted oxygenase was fully reactivated in the presence of sufficient Fe^{2+}, whereas in the absence of DmpK it was not. This result could be explained by binding of DmpK to Mn^{2+}-substituted oxygenase, stimulating a conformational change in the oxygenase to allow it to release Mn^{2+}. Consistent with this, incubation of Mn^{2+}-substituted oxygenase with DmpK, followed by gel filtration, resulted in the loss of at least some of the Mn^{2+}. Interestingly, the same treatment did not result in loss of iron from active oxygenase. It is likely that oxidation of Fe^{2+} and formation of the binuclear iron centre is critical in preventing removal of iron from the holoenzyme when DmpK is present. Although these results suggest a role for DmpK in conferring metal ion binding specificity, the fact that

Mn^{2+} concentrations in cells are thought to be on the order of 1 μM suggests that iron should out-compete it *in vivo* (32, 33). In fact, oxygenase expressed in the absence of DmpK did not appear to contain stably bound Mn^{2+}, although a fraction contained Zn^{2+}.

The marked differences in the fluorescence spectra of holo- and apo-oxygenases (Fig 3.1) indicate that iron binding is accompanied by conformational change. It was therefore hypothesized that DmpK binding to the apo-oxygenase may induce this conformational change prior to metal binding. However, titration of the apoenzyme with DmpK did not effect the same fluorescence changes (results not shown). If DmpK stimulates a conformational change that facilitates Fe^{2+} binding, it might be expected to then dissociate readily from the holoenzyme. Several pieces of evidence indicate that this is not the case. First, we have previously shown that DmpK strongly inhibits the oxygenase in assays, even at an equimolar concentration (15). Second, fluorescence polarization data presented in this paper show that the binding constants for the interaction between DmpK are very similar for holo- and apo- forms of the oxygenase. However, the observation that DmpK is able to accelerate full activation of apo-oxygenase, even when present at 1/20 the concentration of the apo-oxygenase, suggests that DmpK is able to rapidly associate and dissociate from the two forms of the oxygenase. Since previous experiments suggest that the ratio of DmpK to oxygenase is quite low *in vivo* (15), the fact that DmpK can bind to the holoenzyme and inhibit it may not normally be a factor.

Metal transfer proteins, dubbed metallochaperones, have been identified in the transfer of Ni^{2+} to urease (UreE), and Cu^{1+} to apo-superoxide dismutase (CCS). Several pieces of experimental evidence suggest that DmpK is not the direct intracellular donor

of Fe^{2+} to apo-oxygenase. Binding of significant quantities of iron to DmpK was observed only under aerobic, non-reducing conditions, and most of the iron associated with DmpK was in the oxidized form. The iron-loaded form of DmpK was unable to reconstitute a significant fraction of the apooxygenase. DmpK was also unable to mediate iron donation in the presence of Fe^{2+} chelators, further distinguishing it from metallochaperones such as UreE and CCS, both of which have been demonstrated to mediate metal donation to apo-proteins in the presence of chelators (8, 34). However, these experiments do not rule out the possibility that DmpK, when bound to the oxygenase, may play a role in transient Fe^{2+} binding via an appropriate donor. Consistent with the idea that DmpK does not bind iron in a stable form is the observation that overexpression of DmpK does not appear to be particularly toxic to the host.

We also have collected some preliminary data in which potential iron-binding ligands, cysteine and histidine, have been modified in DmpK. Site-directed mutagenesis was used to examine whether each of two histidine residues in DmpK affected the ability to stimulate reconstitution of apoenzyme (E. Cadieux, unpublished data). The mutants were expressed, purified and tested in reconstitution assays under limiting iron conditions: both mutants behaved identically to the wild type protein. DmpK contains one cysteine residue that is conserved in other proteins associated with phenol hydroxylases from different organisms. This residue is not functionally important since the cysteine labelled with IAEDANS still had an effect on reconstitution under limiting iron conditions (this work).

The evidence presented in this paper is consistent with a role for DmpK in promoting a conformational change that allows the apo-oxygenase of phenol hydroxylase

to preferentially and efficiently bind Fe^{2+} under conditions when it is limiting. In common with other metallocentre assembly proteins, DmpK is not necessary when the required metal is abundant. Although work on other metallocentre assembly proteins has focussed on their metal-binding and donating activities, some of these proteins have also been proposed to facilitate metallocentre maturation via protein-protein interactions. Thus, variants of UreE with similar metal binding properties to the wild-type have drastically reduced ability to activate apo-urease (8). Another example is the human copper chaperone, hCCS, which is able to activate a denatured form of apo-superoxide dismutase (33).

One of the major differences between DmpK and other characterized metallocentre assembly proteins is that Fe^{2+}, unlike Cu^{+1} or Ni^{2+}, is not very stable in the presence of oxygen. Thus, if DmpK were a metallochaperone, it would have to be able to protect Fe^{2+} from reaction with oxygen. Since the labile iron pool appears to be mainly Fe^{2+}, DmpK may instead facilitate Fe^{2+} donation from a more general intracellular donor. A key requirement for further characterization of this process is the identification of the *in vivo* Fe^{2+} donor: experiments are underway to try to identify such a donor.

ACKNOWLEDGEMENTS

We thank Margaret Antler for running and analysing the ICP-MS samples and Lena Sahlman for critical reading of the manuscript. Elisabeth Cadieux was the recipient of a doctoral scholarship from Fonds pour la Formation de Chercheurs et l'Aide à la Recherche. This work was supported by a research grant from the Natural Sciences and Engineering Research Council of Canada.

REFERENCES

1. Hagen, K.S., Reynolds, J.G., and Holm, R.H. (1981) *J. Amer. Chem. Soc.* **103**, 4054-4063
2. Zheng, L., Cash, V.L., Flint, D.H., and Dean, D.R. (1998) *J. Biol. Chem.* **273**, 13264-13272
3. Rae, T.D., Schmidt, P.J., Pufahl, R.A., Culotta, V.C., and O'Halloran, T.V. (1999) *Science* **284**, 805-808
4. Lee, M.H, Mulrooney, S.B., Renner, M.J., Markowicz, Y., and Hausinger, R.B. (1992) *J. Bacteriol.* **174**, 4324-4330
5. Colpas, G.J., Brayman, T.G., Ming, L-J., and Hausinger, R.P. (1999) *Biochemistry* **38**, 4078-4088
6. Agar, J.N., Yuvaniyama, P., Jack, R.F., Cash, V.L., Smith, A.D., Dean, D.R., and Johnson, M.K. (2000) *J. Biol. Inorg. Chem.* **5**, 167-177
7. Huffman, D.L., and O'Halloran, T.V. (2001) *Ann. Rev. Biochem.* **70**, 677-701
8. G. J. Colpas and R. P. Hausinger (2000) *J. Biol. Chem.* **275**, 10731-10737
9. Yuvaniyama, P., Agar, J.N., Cash, V.L., Johnson, M.K., and Dean, D.R. (2000) *Proc. Natl. Acad. Sci. USA* **97**, 599-604
10. Zheng, L., and Dean D.R. (1994) *J. Biol. Chem.* **269**, 18723-18726
11. Lippard, S.J., (1999) *Science* **284**, 748-749
12. Bohnke, R. and Matzanke, B.F. (1995) *BioMetals* **8**, 223-230
13. Andrews, S.C., (1998) *Advances in Microbial Physiology* **40**, 283-351
14. Dailey, H.A. (1990) in *Biosynthesis of Heme and Chlorophylls* (Dailey, H.A., ed.) pp. 123-161, McGraw-Hill Publishing Co., New York

15. Powlowski, J., Sealy, J., Shingler, V., and Cadieux, E. (1997) *J. Biol. Chem.* **272**, 945-951

16. Nordlund, I., Powlowski, J., and Shingler, V. (1990) *J. Bacteriol.* **172**, 6826-6833

17. Powlowski, J., and Shingler, V. (1990) *J. Bacteriol.* **172**, 6834-6840

18. Cadieux, E. and Powlowski, J. (1999) *Biochemistry* **38**, 10714-10722

19. Quan, H., Edlund, U., Powlowski, J., Shingler, V., and Sethson, I. (1997) *Biochemistry* **36**, 495-504

20. Brown, R.E., Jarvis, K.L. and Hayland, K.J., (1989) *Anal. Biochem.* **180**, 136-138

21. Gill, S.C. and von Hippel, P.H. (1989) *Anal. Biochem.* **182,** 319-326

22. Percival, M.D. (1991) *J. Biol. Chem.* **266**, 10058-10061

23. Clarke, A.R., (1996) in Labfax Enzymology, (Engel, P.C., ed.) pp 203, Academic Press, Inc and BIOS Scientific Publishers Limited, Oxford

24. Philo, J.S., (1997) *Biophys. J.* **72**, 435-444

25. Philo, J.S.,(2000) *Anal. Biochem.* **179**, 151-163

26. McCall K.A. and Fierke C.A. (2000) *Anal. Biochem.* **284**, 307-315

27. Kimbrough, D.E. and Wakakuwa, J.R. (1991) Solid Waste Testing and Quality Assurance, Third Volume, ASTM STP 1075, p231, C.E. Tatsch, Ed., American Society for Testing and Materials, Philidelphia.

28. Atkin, C.L., Thelander, L., Reichard, P., and Lang, G. (1973) *J. Biol. Chem.* **248**, 7464-7472

29. Shim, H. and Raushel, F.M.(2000) *Biochemistry* **39**, 7357-7364

30. Atta, M., Nordlund, P., Aberg, A., Eklund, H., and Fontecave, M., (1992) *J. Biol. Chem.* **267** 20682-20688

31. Atta, M., Fontecave, M., Wilkins, P.C., and Dalton, H. (1993) *Eur. J. Biochem.* **217**, 217-223

32. Williams, R.J.P. (1982) *FEBS Letters* **140**, 3-10

33. Posey, J.E. and Gherardini, F.C., (2000) *Science* **288**, 1651-1653

34. Rae, T.D., Torres, A.S., Pufahl, R.A., and O'Halloran, T.V. (2001) *J. Biol. Chem.* **276**, 5166-5176

Chapter 4

Properties of a Novel Multicomponent Phenol Hydroxylase Encoded by the *dmp* Operon of *Pseudomonas* sp. Strain CF600

ABSTRACT

Phenol hydroxylase of *Pseudomonas* sp. strain CF600 is a multicomponent enzyme comprised of three components: DmpP is an FAD and [2Fe-2S] containing reductase, DmpM is a cofactorless activator protein and DmpLNO is the oxygenase made up of three copurifying polypeptides. Single turnover experiments confirm that DmpLNO contains the active site, but requires DmpM for efficient turnover. The maximum product yield obtained during single turnover in the presence of substrate and DmpM was 34 ± 10% suggesting the presence of inactive phenol hydroxylase in our preparations. DmpM increases the steady-state turnover rate reaching a maximum at 1.5:1 DmpM to DmpLNO molar ratio. Chemical cross-linking studies established that DmpM interacts with the large subunit of the DmpLNO oxygenase complex. Mössbauer, EPR and UV/vis spectroscopies were used to characterise the active site of the oxygenase component. Mössbauer data, demonstrated the presence of two types of binuclear iron center in DmpLNO. Treatment of the oxygenase with hydrogen peroxide and/or DTT was investigated in order to understand the basis for the observation that a significant proportion of the enzyme is not active.

INTRODUCTION

The versatility of aerobic microorganisms in degrading aromatic compounds is reflected in the wide array of oxygenases that are used to initiate metabolic processing of these molecules. Destabilisation of the aromatic ring is achieved by enzymatic insertion of one or more oxygen atoms, allowing further attack by ring-cleavage dioxygenases. The resulting non-aromatic products are transformed stepwise into central metabolites such as pyruvate and acetyl-CoA (1). The specificity and efficiency of the ring hydroxylating enzymes is therefore important in controlling the entry of potential growth substrates into metabolism.

While all oxygen-activating enzymes require redox-active metals or prosthetic groups, two broad categories of aromatic ring hydroxylases may be distinguished: those that consist of a single polypeptide, and those that are comprised of more than one polypeptide component. The single polypeptide oxygenases characterized to date contain FAD as the sole redox-active element responsible for insertion of one atom of oxygen from O_2 into the substrate, and reduction of the other oxygen atom to H_2O using electrons from NAD(P)H (reviewed in 2). All these enzymes act on mono-hydroxylated aromatics such as *o*-or *p*-hydroxybenzoate and phenol, or on aromatic amines. On the other hand, the chemically more difficult oxygenation of aromatic rings *lacking* electron-donating substituents (e.g. toluene, naphthalene and biphenyl) is carried out by microbial dioxygenases that contain non-heme iron cofactors (reviewed in 3,4). For these enzymes, one or more auxiliary polypeptides are required to transfer electrons in to the oxygenase active site. Non-heme iron prosthetic groups are also found in microbial oxygenases used to initiate degradation of various alkanes and alkenes (5,6,7).

A rather unique situation exists in the phenol degrader, *Pseudomonas sp.* strain CF600, which uses a multicomponent oxygenase for this activated aromatic compound (8). Sequence comparisons and biochemical studies indicate that the polypeptide components of this enzyme are related to the components of methane monooxygenase, which comprises: a binuclear iron center containing hexameric $(\alpha\beta\gamma)_2$ oxygenase; an FAD/[2Fe-2S]-center containing reductase; and a small activator protein lacking any redox cofactors (reviewed in 5). However, other than the putative iron centre ligands, the overall level of similarity between phenol hydroxylase components and those of methane monooxygenase is rather low (8). Sequence comparisons also indicate similarities with polypeptides involved in oxygenation of toluene at the 2- and 4-positions, as well as with phenol hydroxylase components from other bacterial strains (8, 9). Therefore, the study of the multicomponent phenol hydroxylase is of interest in that it is in widespread use by various bacterial strains, and in that it is a representative of a growing class of oxygenases of which only methane monooxygenase has been extensively characterized.

We have previously reported the purification and characterization of the reductase (DmpP), and activator (DmpM) components of this multicomponent enzyme, as well as DmpK, which appears to be involved in the assembly of the oxygenase (10, 11, 12). In this paper, we report on the purification and some properties of the oxygenase component, and compare the properties of its binuclear iron center with those of related proteins.

EXPERIMENTAL PROCEDURES

Chemicals and Materials

Fast-Flow DEAE Sepharose, Phenyl-Sepharose High Peformance, and Sephacryl S-300HR were purchased from Amersham-Pharmacia Biotech (Montreal, Que.). ^{57}Fe was obtained from Icon Services Inc. (Summit, NJ). The BCA Protein assay kit, and the crosslinkers EDC and sulfo-NHS were purchased from Pierce (Rockford, IL). All other chemicals were reagent grade or better.

Bacterial growth

Cultures of *Pseudomonas* sp. strain CF600 were grown in minimal medium with phenol as previously described (11) except that the pH of the growth medium was maintained at 7.0-7.5 by the addition of NaOH rather than NH_4OH. Frozen cell paste was thawed in 50 mM Tris-HCl pH 8, containing10% glycerol and 200 μM ferrous ammonium sulfate (2 mL buffer per g cell paste). A spatula tip of DNase was added, and after 5 min the cell suspension was sonicated for 10 bursts of 15 seconds each in 40 mL batches cooled by an ice salt-water bath. The temperature of the cell suspension during sonication was not allowed to rise above 10°C. After centrifugation at 70,400 x g for 60 min, the supernatant ("crude extract") was removed and used for further purification.

Purification of oxygenase (DmpLNO)

Crude extract was loaded onto a Fast-Flow DEAE-Sepharose column (30 x 2.6 cm) previously equilibrated with 50 mM Tris-HCl, pH 8, containing 10% glycerol ("TG buffer"). The column was then washed (1 mL/min) with 75mM NaCl in TG buffer (250

mL), and the oxygenase (DmpLNO) was eluted by applying a 75-275 mM NaCl gradient in TG buffer (1000 mL). Fractions (12 mL) containing oxygenase activity eluted approximately in the middle of the gradient. These fractions were combined and brought to 65% saturation with ammonium sulfate. After 30 min, the precipitate was collected by centrifugation at 15,300 x g for 30 min. The pellet was redissolved in TG buffer (30 mL) and the solution was clarified by centrifugation at 3,840 x g for 20 min before loading it onto the next column.

The preparation was loaded onto a Phenyl-Sepharose High Performance column (36 x 2.6 cm) previously equilibrated with TG buffer containing 0.15 M NaCl. The column was washed (1.5 mL/min) with the same buffer until the eluate was no longer yellow. A second wash with TG buffer only was applied until the absorbance at 280 nm dropped below 0.2. The buffer was then changed to 5 mM Tris-HCl, pH 8.0, containing 10% glycerol, whereupon the oxygenase component eluted. Fractions (12 mL) containing oxygenase activity were combined and concentrated by ultrafiltration with an Amicon YM30 membrane before proceeding to the next step.

The concentrated sample then was loaded (1 mL/min) onto a Sephacryl S-300HR gel filtration column (78 x 2.6 cm) equilibrated with TG buffer, and the oxygenase was eluted with TG buffer. Fractions (12 mL) were collected, and assayed for activity.

Active fractions eluting from the gel filtration column were combined and loaded (4 mL/min) onto a Fast-Flow DEAE-Sepharose column (18 x 1.6 cm), previously equilibrated with TG buffer containing 75 mM NaCl. Unbound protein was eluted with the same buffer (120 mL) before starting a 75- 200 mM NaCl gradient in TG buffer (500 mL): 5 mL fractions were collected. The oxygenase eluted near the end of the gradient.

Fractions with the highest specific activity were combined and concentrated by ultrafiltration using an Amicon YM 30 membrane. Aliquots of the concentrated oxygenase were stored at -80°C.

Preparation of ^{57}Fe-labeled oxygenase for Mössbauer spectroscopy

An ^{57}Fe metal chip (~15 mg) in a glass test tube was dissolved over several days in concentrated HCl (0.32 ml) maintained at 60°C. ^{57}Fe (13 mg) was added as $FeCl_3$ to sterile M9 medium (16L) in place of unlabeled iron (11): this medium was then used for growth of *Pseudomonas* sp. strain CF600 on phenol as described above. Purification of the oxygenase component from these cultures was carried out essentially as described above except that $^{57}FeCl_3$ (200 μM) and ascorbate (2 mM) were added to the crude extract in place of ferrous ammonium sulfate. After the last purification step, the oxygenase was concentrated using a Centricon YM30 and then diluted with TG buffer, to a protein concentration of between 83 and 116 mg/ml. Purified, concentrated samples (300 μL) were transferred to Mössbauer cups and frozen rapidly in liquid nitrogen.

Preparation of DTT inactivated oxygenase for Mössbauer spectroscopy

A sample of ^{57}Fe containing oxygenase was prepared as described above. DTT (75 mM) was added to the purified oxygenase (1 mM) and incubated at 4°C in TG buffer for a few days until oxygenase activity was completely lost. The DTT inactivated sample was transferred to a Mössbauer sample holder and frozen in liquid nitrogen. After Mössbauer analysis, the sample was thawed and dialysed against 1L TG buffer for 2 hr.

The buffer was changed to fresh TG and dialysed for an additional 2 hr before being re-frozen for additional Mössbauer analysis.

Analytical ultracentrifugation

Purified oxygenase was diluted to 0.32-1 mg/mL with 50 mM Tris-HCl, pH 8.0, in a volume of 500 μL and dialyzed against the same buffer for 1 hr. Some samples also contained 0.1 M NaCl. Sedimentation velocity experiments were performed at 20°C using a Beckman Coulter XL-A analytical ultracentrifuge with an An-60Ti rotor at 28,000 rpm. Data processing was done with DCDT Plus software (13).

Analytical methods

Protein concentration was estimated using the BCA assay according to the instructions given by the manufacturer (Pierce) for the 60° C protocol, with bovine serum albumin as the standard; additives that interfere in this assay were first removed using a modified procedure (14). Where noted, protein concentrations were also estimated using the spectrophotometric method of Gill and von Hipple (15). Iron concentrations were estimated using Ferrozine after removing the protein by TCA precipitation (16). SDS-PAGE was either performed on 10-20% gradient gels according to established procedures (17), or on gels using the Tricine buffer system (18).

Enzyme activity was quantitated using a coupled assay for the product, catechol, as described previously (12).

UV-visible spectra were obtained using Philips PU7415 or Varian Cary Bio50 recording spectrophotometers.

Single turnover experiments

Single turnover experiments were carried out in a modified anaerobic quartz cuvette (Hellma) fitted with a gas-tight syringe via a ground glass joint. The cuvette was loaded in an anaerobic glove box with phenol hydroxylase (8.9 μM monomer) and methyl viologen (1 μM) in 50 mM Tris-HCl pH 7.45, in a total volume of 2 mL. Phenol (12.5 μL of a 0.25 M solution) was contained in a side-arm. The oxygenase was titrated with sodium dithionite solution (~ 2.9 mM) which was prepared in 50 mM HEPES pH 8.0 and standardized by titrating into 0.25 mM potassium ferricyanide. Reduction was monitored by the decrease in absorbance at 350 nm, and was considered to be complete upon the appearance of the reduced methyl viologen peak at 395 nm. Once the sample was reduced, phenol was tipped into the cuvette from the side-arm to a final concentration of 1.5 mM. For product analysis, a 0.9 mL aliquot was transferred to a 1.5 ml cuvette and mixed several times to aerate the sample. The yield of catechol was determined by adding 4-5 Units of catechol 2,3 oxygenase (the next enzyme in the pathway) and monitoring the formation of α-hydroxymuconic semialdehyde, $\epsilon = 44\ 800\ M^{-1}\ cm^{-1}$ at 374 nm.

Inactivation of oxygenase by dithithreitol and hydrogen peroxide

Solutions of the as-isolated oxygenase (1.3-1.4 mg/mL) in 50 mM Tris-HCl, pH 7.5, containing 10% glycerol, were stored at 4°C in the presence of various additives, and samples were withdrawn periodically for activity assays. The following additions were made: dithiothreitol (1 mM); dithiothreitol (1 mM) and catalase (1000 U); catalase only (1000 U); dithiothreitol (1 mM) and DmpM (9 μM); dithiothreitol (1mM) and phenol (1.6 mM); DmpM only (9 μM); phenol only (1.6 mM) or hydrogen peroxide (100:1).

Inactivation of reduced oxygenase samples by peroxide was also examined. Anaerobic samples were prepared as described above for single turnover experiments. Reduction by DTT was examined by titrating DmpLNO (1 mg/ml) in TG buffer with an anaerobic solution of DTT (0.1 M), and monitoring bleaching of the 350 nm band. After the addition of DTT to 6 mM, no bleaching was immediately observed, but after 1 hr at 25°C under anaerobic conditions reduction appeared to be complete. A portion of the DTT reduced oxygenase was kept anaerobic, while another was exposed to air, and the two samples were assayed for activity periodically over several days.

Inactivation of DTT- or dithionite-reduced oxygenase by hydrogen peroxide was tested by adding a 100x molar excess of H_2O_2 to reduced DmpLNO. The DTT reduced oxygenase treated with H_2O_2 was exposed to air and activity was monitored at various times over several days. The dithionite reduced oxygenase treated with H_2O_2 was kept anaerobic, and also monitored for activity periodically.

Dialysis of the DTT inactivated DmpLNO sample and reconstitution with Fe^{2+}

The oxygenase reduced with DTT (6 mM) and inactivated by exposure to air for 24 hr (described above) was dialysed against 1L TG buffer at 4°C for 2 hr. The buffer was changed to fresh TG buffer and dialysis was continued overnight, after which the sample was assayed for activity. Reconstitution of activity was attempted by adding stoichiometric amounts of Fe^{2+} as ferrous ammonium sulfate to the dialysed DmpLNO sample (1mg/mL). Activity was monitored over a period of 30 minutes.

Chemical crosslinking with EDC and Sulfo-NHS

Chemical modification of DmpM (2.4 nmol) was carried out in 50 mM MOPS pH 7.0, with EDC (50 mM) and sulfo-NHS (50 mM) in a total volume of 50 μL. After incubation for 15 min at room temperature, the reaction was stopped by adding β-mercaptoethanol to a final concentration of 50 mM. Oxygenase component in TG buffer (2.4 nmol) was then added and allowed to react for 1 hr at room temperature. Control experiments were done in which either DmpM or the oxygenase component was omitted. Reaction products were analyzed by SDS-PAGE.

Mössbauer and EPR spectroscopy methods

For the reduction/reoxidation experiments the Mössbauer cup containing ^{57}Fe enriched protein was placed into a Schlenk line and at least six pump/refill cycles were performed while the sample was still frozen. After thawing the sample, 45 μl of a 3 mM dithionite solution, and 35 μl of 1mM methyl viologen, were added with a syringe through a single septum, and the sample was stirred gently for ca. 20 min with the syringe needle in the Schlenk line before freezing the sample with liquid nitrogen. Once frozen the sample was removed from the Schlenk line. After performing the Mössbauer experiments of the reduced protein, the sample was thawed in air, transferred into a microfuge tube, gently aerated for ca. 20 min by tilting the tube, transferred back into the Mössbauer cup, and then refrozen. This cycle was repeated twice.

RESULTS

Purification of the oxygenase component of phenol hydroxylase

Phenol hydroxylase activity has previously been shown to depend on the gene products of *dmpKLMNOP* (19). Purifications of the reductase (DmpP), activator (DmpM), and DmpK components have also been reported (10,11,12). The oxygenase component was purified as described in *Experimental Procedures*. Purification summaries for several representative preparations are shown in Table 4.1. Denaturing gel electrophoresis (Fig 4.1, Lane 1) shows that the protein contains three polypeptides with molecular masses of 39, 60, and 13 kDa, corresponding to DmpL, N and O, respectively (19). An unidentified contaminant migrating at 25 kDa consistently appeared in all preparations. Although the monomer unit appears to be DmpLNO, sedimentation velocity and gel filtration experiments are consistent with the existence of a DmpLNO dimer (data not shown).

Activity and iron measurements

When purified as described above and assayed under standard conditions (*Experimental Procedures*), the specific activity of the purified oxygenase was found to range between 780-1400 nmol/min/mg, and the iron content varied between 1-1.7 Fe per monomer. Initially, we purified the oxygenase with dithiothreitol present in the purification buffer, primarily because low molecular weight thiols are routinely used for purification of related proteins. For oxygenase purified in the presence of DTT, the specific activity was consistently lower, ranging from 557-923 nmol/min/mg, and the iron content ranged between 1.8-2.4 Fe/ monomer oxygenase. Thus, on average, omission of

Table 4.1 Purification of phenol hydroxylase

Purification Step	Total Activity* Preparation 38	Preparation 42	Preparation 43	Preparation 44
Crude Extract	10.8	8.9	11.5	31
DEAE-	393	833		
$AmmSO_4$ ppt	3161	5044	1895	3271
Phenyl-Sepharose	955	1513	906	2349
Gel filtration S-300	743	1409	882	1296
DEAE	484	441	567	1326
Final Specific activity (nmol/min/mg)	651	1158	981	1346

*Activity units are umol/min. Activities in crude extract and DEAE fractions could not be measured accurately because of the presence of α-hydroxymuconic semialdehyde metabolizing enzymes.

Figure 4.1 SDS-polyacrylamide electrophoresis of the oxygenase component of phenol hydroxylase. *Lane 1*, oxygenase component (10 μg)

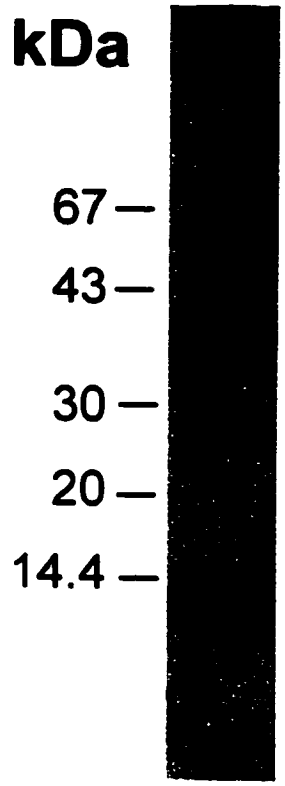
kDa
67
43
30
20
14.4

DTT from the purification buffer apparently resulted in higher specific activity but less iron. The nature of inactivation by DTT is examined further below.

UV/Vis spectra of the oxygenase component

Figure 4.2 shows the optical spectra of the as-isolated oxygenase component, and of the apo-oxygenase (protein lacking detectable iron). As reported elsewhere, the apo-oxygenase is inactive, which demonstrates the requirement for iron in active enzyme (E. Cadieux, Ph.D. Thesis, Chapter 3). Comparison of the spectra of holo- and apo-oxygenase indicates the presence of a shoulder between 320-400 nm associated with the presence of iron in the protein. The extinction coefficient at 350 nm ranged from 5000-6400 M^{-1} cm^{-1} per dinuclear iron centre depending on the preparation (Table 4.2). The nature of the iron centre was probed further using Mössbauer spectroscopy, as described below.

Dependence of steady-state turnover rate on DmpM concentration

The steady-state rate of phenol hydroxylase turnover is dependent on the DmpM concentration, with a maximum observed rate at 1.5 DmpM per oxygenase monomer: higher concentrations of DmpM inhibit phenol hydroxylase activity (Fig 4.3). This behavior is similar to that observed for methane monooxygenase, where MmoB was shown to inhibit methane monooxygenase activity at concentrations higher than 2 MmoB per oxygenase monomer (20).

Figure 4.2 Optical spectra of apo and holo oxygenase. Apo-oxygenase (—, 1 mg/ml protein, 9 μM protomer); holo-oxygenase (----, 1 mg/ml protein, 9 μM protomer)

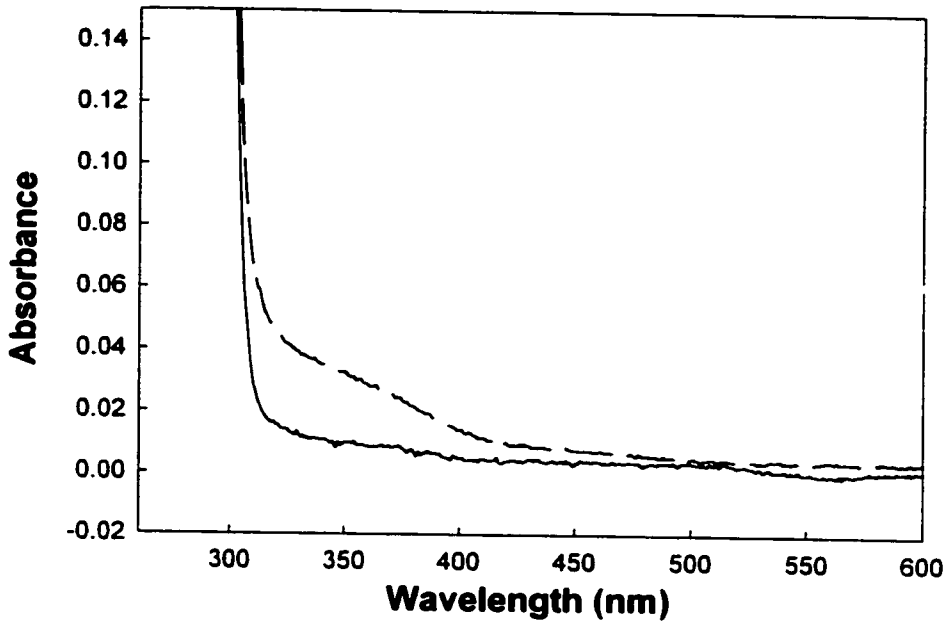
Absorbance
0.14
0.12
0.10
0.08
0.06
0.04
0.02
0.00
-0.02
300
350
400
450
500
550
600
Wavelength (nm)

Table 4.2 Properties of purified DmpLNO

Preparation	Protein conc. (mM αβγ)	Fe conc. (mM)	Fe/αβγ	A_{350}/A_{280}	ε350nm (M^{-1} cm^{-1})*	Activity/ binuclear center	Activity/ mg protein
48	0.35	0.63	1.8 (87%)	0.044	5000 (5750)	148	1205
44	2.4	3.3	1.4 (77%)	0.033	5300 (6900)	215	1297
Sample 1	1.0	0.91	0.93 (85%)	0.033	6400 (7500)	218	971

*per mol of binuclear iron cluster

Figure 4.3: The effect of ratio of DmpM to oxygenase on the steady state turnover of phenol hydroxylase. The steady state turnover rate of phenol hydroxylase was determined as described elsewhere (12) varying the ratio of DmpM to oxygenase component.

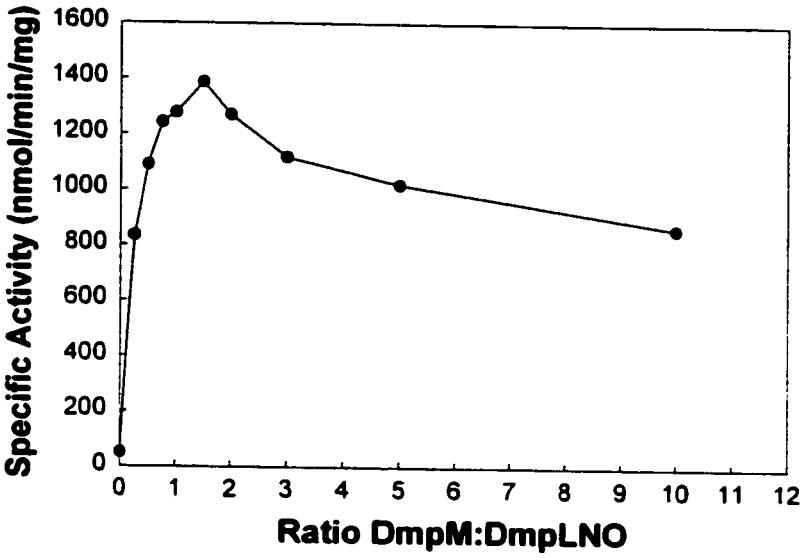
Specific Activity (nmol/min/mg)
1600
1400
1200
1000
800
600
400
200
0
0 1 2 3 4 5 6 7 8 9 10 11 12
Ratio DmpM:DmpLNO

Interaction of DmpM with the oxygenase revealed by chemical cross-linking

Chemical cross-linking studies of the methane monoxygenase system showed that the activator protein, MmoB, interacts with the largest subunit of the oxygenase component (20). Figure 4.4 shows the results of cross-linking experiments with the oxygenase and activator (DmpM) components of phenol hydroxylase. Incubation of oxygenase and DmpM with EDC and sulfo-NHS yielded products with molecular masses of 68 and 97 kDa (Lane 2) that were not observed in reaction mixtures containing DmpM (Lane 4) or oxygenase (Lane 3) alone. These cross-linked products are consistent with DmpM (10.3 kDa) complexed with DmpN (58 kDa) and DmpLN, respectively. DmpM in the presence of EDC alone did not yield any cross-linked products, while the oxygenase component treated with EDC yielded high molecular weight bands possibly corresponding to a dimer complex of the DmpLNO polypeptides (Lane 3).

Single turnover experiments

Anaerobic titration of the oxygenase component with sodium dithionite bleached the 350 nm shoulder in the visible spectrum (Fig 4.5) This spectral feature was restored by admission of oxygen (data not shown). Readmission of oxygen after adding phenol resulted in the formation of the product, catechol. Efficient product formation required the presence of DmpM, but not the reductase (DmpP) . Yields varied somewhat from preparation to preparation, with product yields in the absence of DmpM of 2.3 ± 1.3%, and of 34 ± 10% in its presence. These results indicate that the oxygenase is the site of product formation, although turnover is inefficient in the absence of the activator protein.

Figure 4.4 SDS-polyacrylamide electrophoresis of the cross-linked DmpM with the oxygenase component. *Lane 1*, DmpM (2 μg) and oxygenase component (20 μg) without EDC; *lane 2*, DmpM (2 μg) and the oxygenase component (20 μg) incubated with EDC; *lane 3*, Oxygenase component (20 μg) incubated with EDC; *lane 4*, DmpM (2 μg) incubated with EDC.

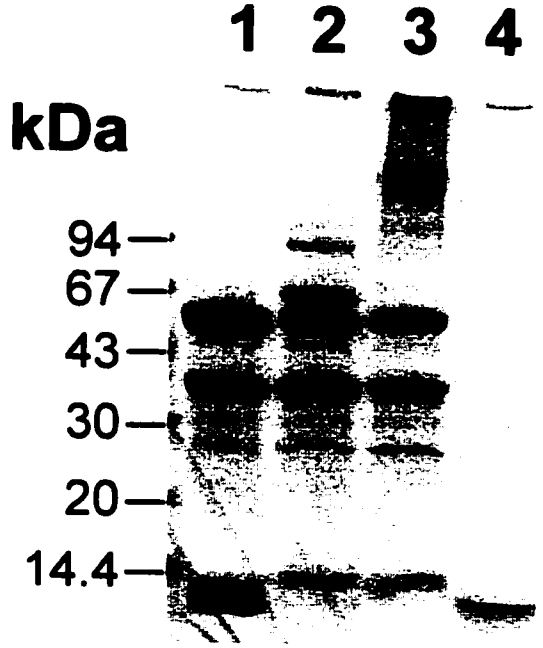
1
2
3
4
kDa
94
67
43
30
20
14.4

Figure 4.5 Reduction of the oxygenase component by sodiun dithionite titration. 8.9 μM protomer of oxygenase component and methyl viologen (1 μM) in 50 mM Tris-HCl pH 7.45, in a total volume of 2 mL. The oxygenase was titrated with sodium dithionite solution (~ 2.9 mM) which was prepared in 50 mM HEPES pH 8.0.

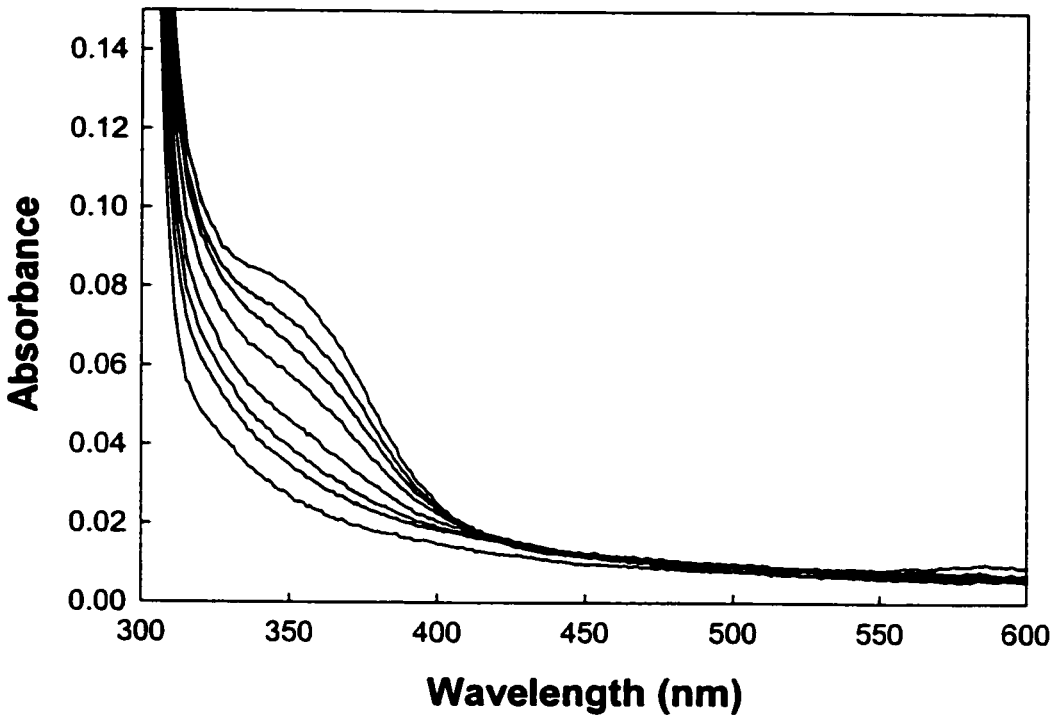
Absorbance
0.14
0.12
0.10
0.08
0.06
0.04
0.02
0.00
300
350
400
450
500
550
600
Wavelength (nm)

Anaerobic reduction of the oxygenase by NADH and a catalytic amount of DmpP was also attempted. Bleaching of the visible spectrum of the oxygenase was observed only in the presence of DmpM (data not shown). This suggests that DmpM alters the redox potential of the oxygenase, as has been reported for methane monooxygenase (21).

Mössbauer studies of the iron center

During the last five years we have studied eight preparations of the oxygenase component of phenol hydroxylase with Mössbauer spectroscopy. All samples exhibited two distinct spectral components with proportions that varied somewhat between preparations. Figure 4.6 shows 4.2 K spectra obtained from sample 1 (Table 4.2). The spectrum of Figure 4.6A exhibits two quadrupole doublets. The majority species, accounting for 85% of the Fe in the sample, has quadrupole splitting, ΔE_Q = 1.73 (3) mm/s, and isomer shift, δ = 0.54 (2) mm/s; we will refer to this spectral component as cluster form I. The remainder of the iron belongs to a doublet, representing cluster form II, with ΔE_Q = 0.79(3) mm/s and δ = 0.48(2). After addition of dithionite the spectrum shown in Figure 4.6B was observed. Its Mössbauer parameters, ΔE_Q = 2.80(10) mm/s and δ = 1.28(3) mm/s, are typical of octahedral high-spin ferrous sites with predominant O-coordination (carboxylate, water). The Mössbauer parameters and the cluster fractions are listed in Table 4.3.

The presence of quadrupole doublets in Figure 4.6A, coupled with the observation of high-spin ferrous sites generated by reduction with dithionite, indicates spin-coupled high-spin ferric sites similar to those observed in diiron proteins. The 8.0 T spectra shown in Figure 4.7 confirm this assignment. These spectra were obtained from a

Figure 4.6 Mössbauer spectra of *Pseudomonas* sp. strain CF600 phenol hydroxylase recorded at 4.2 K in the absence of an applied magnetic field. (A) hydroxylase as isolated; solid line is a spectral simulation for two doublets with intensity ratio 85:15; the minority doublet belonging to cluster form II is indicated by the bracket. (B) Sample of (A) after addition of dithionite. The solid line is a spectral simulation assuming one doublet with Voigt line shape. (C) Sample of (B) after re-oxidation in air. (D) Sample of (C) after an additional reduction/reoxidation cycle. Solid lines in (C) and (D) are simulations to two doublets with proportions listed in Table 4.3. The spectrum of the reduced sample contains unresolved contributions from the four iron sites of cluster forms I and II. We have described these unresolved contributions by using a Voigt shape with 0.55 mm/s gaussian width.

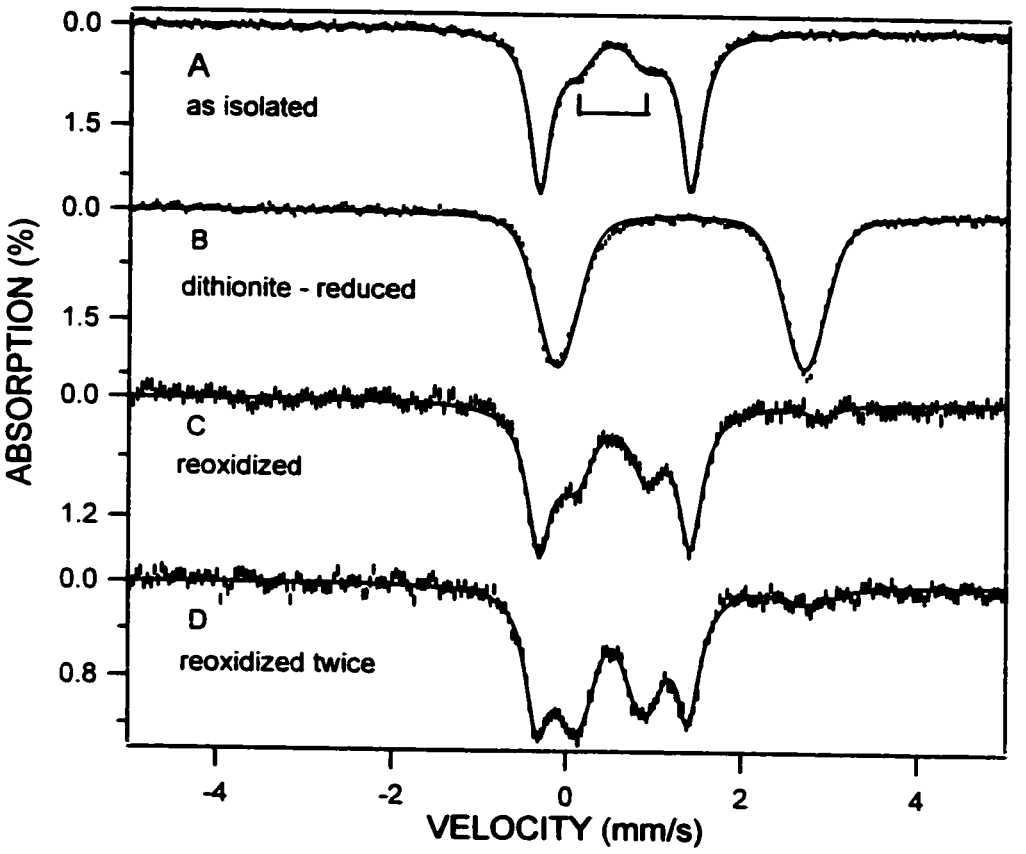
0.0
A
as isolated
1.5
0.0
B
dithionite - reduced
1.5
0.0
C
reoxidized
1.2
0.0
D
reoxidized twice
0.8
ABSORPTION (%)
-4
-2
0
2
4
VELOCITY (mm/s)

Table 4.3 Characterization of Mössbauer samples of Figures 4.6 and 4.12.

Sample	Diferric			Diferrous		
	ΔE_Q [a]	δ [a]	% [b]	ΔE_Q [a]	δ [a]	%
As isolated	1.73(3)	0.54(2)	85(3)			
	0.79(3)	0.48(2)	15(3)			
Dith-Reduced				2.8	1.28	100
One Red/Reox Cycle	1.73	0.54	62(4)	3.1	1.3	5
	0.79	0.48	33(4)			
Two Red/Reox Cycles	1.73	0.54	41(4)	2.8	1.3	8
	0.79	0.48	51(4)			
As isolated+DTT	1.92	0.39	46	2.8-2.9	ca. 1.3	8
	0.53	0.34	46			

[a] in mm/s

[b] Percent of total Fe in sample

preparation for which the zero field spectrum indicated a 70:30 ratio for the doublets of clusters I and II. The solid line drawn through the spectrum of Figure 4.7A is a theoretical curve generated by assuming that the iron of both cluster forms resides in diamagnetic sites; the good match of the theoretical curve with the experimental splittings confirms this assumption. The chemical nature of the ligands bridging the two iron sites can be assessed by estimating the exchange coupling constant J ($H = JS_1 \bullet S_2$). The spectrum shown in Figure 4.7B was recorded at T = 80 K in an 8.0 T parallel field. Close inspection of the data reveals that the spectrum of cluster I is the same at 4.2 K and 80 K, showing that excited states of the spin ladder are not measurably populated at 80 K. From analysis of the 80 K spectrum using a spin coupling model (the method has been described elsewhere; see text and Fig. 8 of ref 22). we conclude that $J > 120$ cm^{-1} for cluster I. In contrast, the spectra of cluster II change considerably between 4.2 K and 80 K. This is illustrated in Figure 4.7C which shows the 80 K spectrum of cluster II obtained by subtracting from the experimental spectrum the simulation of form I.

The shape of the 80 K spectrum of cluster II is actually quite similar to intermediate-relaxation spectra we have observed for the hydroxylase component of methane monooxygenase (MMOH). The observation of temperature dependent high-field spectra for cluster II indicates that low-lying states of the spin ladder are appreciably populated at 80 K (broadening is already seen at 30 K), implying that cluster II has a substantially smaller J than form I. The general features of the spectrum of Figure 4.7C suggest intermediate fluctuation rates of the electronic spin; under these conditions the spectra are exceedingly difficult to analyze for the present case.

Figure 4.7 Mössbauer spectra of an oxidized sample of phenol hydroxylase recorded in 8.0 T fields applied parallel to the observed γ-rays. For this sample 70% of the Fe(III)Fe(III) clusters were found to belong to form I and 30% to form II. The solid line in (A) is a spectral simulation assuming that the iron sites in each cluster forms are equivalent and that electronic ground state of both cluster forms is diamagnetic. For cluster form I we used ΔE_Q = -1.75 mm/s and η = 0.35 for the asymmetry parameter, and ΔE_Q = 0.80mm/s and η = 0.40 for cluster form II. The spectrum in (B) was recorded at 80 K. The solid line is a simulation of the spectrum for cluster form I (70% of Fe) assuming that only the S = 0 ground state is populated. The spectrum shown in (C) was obtained by subtracting the simulated spectrum of form I from the experimental spectrum of (B). The solid line in (C) is a simulation (same curve as shown above (A)) demonstrating that the 80 K spectrum of form II has contributions from excited states of the spin ladder (essentially S = 1 and S = 2 states).

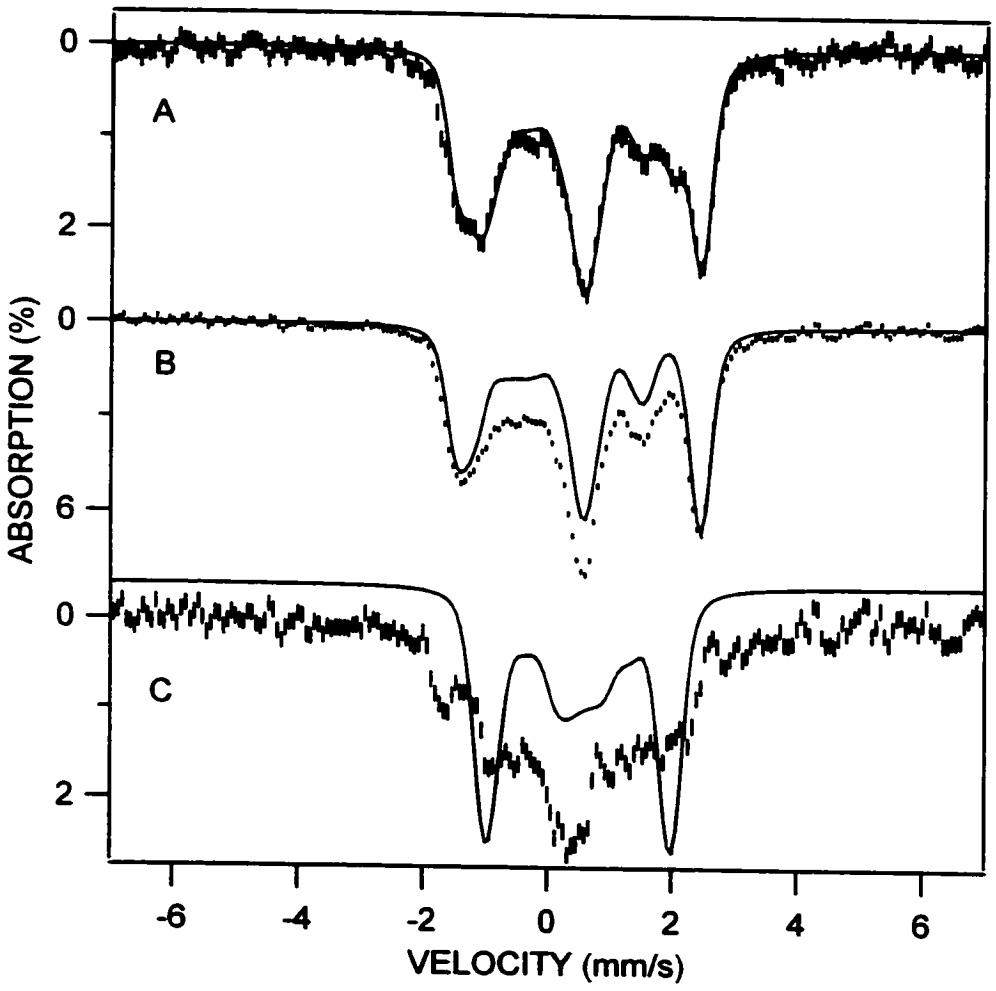
0
A
2
0
B
6
0
C
2
ABSORPTION (%)
-6
-4
-2
0
2
4
6
VELOCITY (mm/s)

To summarize, the spectra of the oxidized hydroxylase exhibit two spectral components. These components cannot originate from one cluster. First, their proportions vary between different preparations and, moreover, the spectral components are associated with sites that are constituents of spin-coupled Fe(III)Fe(III) clusters with substantially different J-values. Each cluster form contributes, in the absence of an applied field, *one* quadrupole doublet indicating that the two irons in each cluster form have very similar ligand structure. This is particularly true for cluster I which exhibits a sharp doublet with 0.30 mm/s line width (FWHM); our analysis indicates that the ΔE_Q-values of the two sites of the cluster can differ by at most 5 %, if they differ at all. Thus, the cluster binding sites of the hydroxylase dimer can accommodate two distinct dinuclear clusters. Because both irons in each cluster form are equivalent and because the sites in the two forms differ substantially, our data suggest different bridging ligands for the two cluster forms. The large J-value observed for cluster form I is consistent with a μ-oxo bridged structure whereas the smaller J-value of cluster form II is reminiscent of the hydroxo-bridged MMOH cluster.

In order to test whether both cluster forms are catalytically active, we have carried the sample of Figure 4.6 through two reduction/reoxidation cycles (see *Experimental Procedures*). The spectra of Figures 4.6C and 4.6D were recorded after one and two reduction/reoxidation cycles, respectively. It can be seen that a fraction of form I has been converted to form II after each cycle; after two cycles the proportion of Fe in cluster form I has decreased from 85% to 40%. As shown in Table 4.4, the catalytic activity as measured in the standard assay correlates quite well with the amount of cluster I present in the oxidized form of the enzyme.

Table 4.4 Activity of Mössbauer sample reduction, reoxidation cycled

	% Activity	% Cluster I
Sample 1	100	85
Reox 1	77	62
Reox 2	61	41

EPR spectroscopy of reduced phenol hydroxylase

The electronic spins of diferrous clusters ($S_1 = S_2 = 2$) are generally coupled by weak exchange interactions (J is smaller than the zero-field splittings of the two ferrous ions) to produce a system comprising 10 closely-spaced spin levels. If a pair of levels is separated by an energy, Δ, that is less than $h\nu = 0.30\ cm^{-1}$, one may observe at X-band an integer spin EPR transition. For reduced methane monooxygenase from *M. trichosporium* the integer spin EPR spectra have been analyzed in considerable detail, and Lipscomb and coworkers have used EPR to study the reaction of reduced MMOH with substrate and the effector protein component B (20). A similar integer spin signal has also been reported for T4MOH (23). In order to examine whether reduced phenol hydroxylase exhibits an EPR signal, we have reduced aliquots of the samples of Table 4.2 and Figure 4.6D. Figure 4.8 shows T = 2 K integer spin EPR spectra of the sample of Figure 4.7 recorded with the microwave field B_1 applied parallel (A) and perpendicular (B) to the static field B. At 2 K the signal saturates readily at microwave powers larger 2 μW, in particular for $B < 20$ mT (the shape of the signals indicates that the splitting parameter Δ is distributed; the portion of the signal below $B < 20$ mT originates from molecules whose Δ-values approach the microwave quantum). The observed signal declines strongly as the temperature is raised, showing that the EPR-active doublet is the ground state. At 8 K the signal can be observed at 200 μW without saturation, but its amplitude has declined by about a factor of 10 relative to the 2 K spectrum. Prior to reduction with dithionite, the sample of Figure 4.8 had circa 75 % of its iron in cluster form I, whereas the sample of Figure 4.6D, after passing through two redox cycles, had ca. 40% of its iron in cluster

Figure 4.8: EPR spectra of dithionite-reduced phenol hydroxylase recoeded at 2 K with the microwave field B_1 applied parallel (A) and perpendicular (B) to the static magnetic field. Protein concentration, 0.8 mM; Diiron cluster concentration, 0.57 mM. (prior to reduction 72% of the clusters were in form I). Instrumental conditions: microwave frequency, 9.26 GHz; modulation, 100 kHz at 0.98 mT (pp); gain, 10^5 dB/dt, scan rate, 0.33 mT/s.

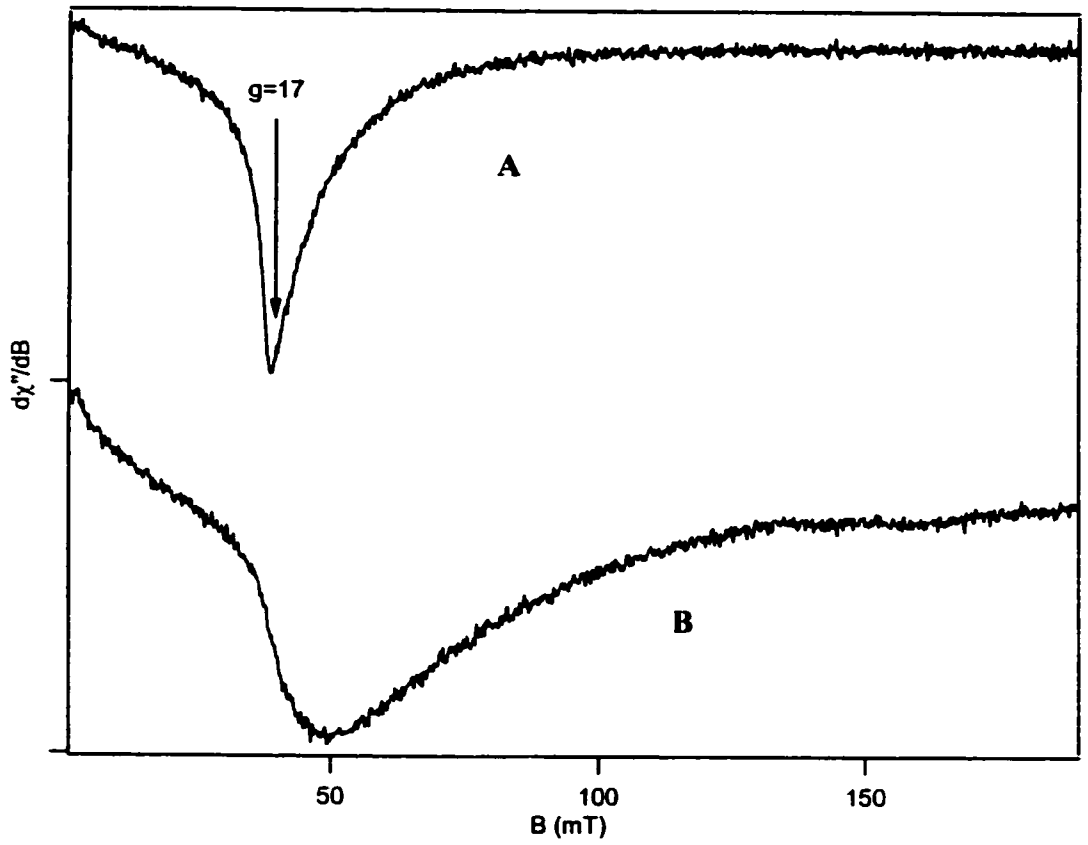
g=17
A
B
dχ"/dB
50
100
150
B (mT)

form I. The reader is reminded, however, that we do not know whether the conversion into form II occurs upon reduction or reoxidation; hence the amount of cluster form I is unknown in the reduced samples.

Inactivation of oxygenase by turnover and dithiothreitol

The variability in activity that is observed from preparation to preparation is not completely explained by the relative iron centre content of the oxygenase. The Mössbauer studies indicate the presence of variable amounts of two cluster forms, one of which appears to be inactive. However, the origins of the two forms are not known. We undertook to investigate what factors contribute to the inactivation of the oxygenase.

Steady-state turnover of phenol was accompanied by progressive loss of activity (Fig 4.9). Once product formation ceased, it was not regained by the addition of more coupling enzyme, catechol 2,3-dioxygenase (data not shown). However, inclusion of catalase markedly improved the linearity of these assays (Fig 4.9), suggesting that the enzyme is inhibited by the accumulation of hydrogen peroxide. Inactivation was also observed under single turnover conditions in the absence of substrate and DmpM. As the enzyme was cycled between reduced and oxidized forms, activity was progressively lost (Table 4.5). Inactivation may be related to formation of an activated oxygen intermediate, such as hydrogen peroxide, after turnover in the absence of substrate.

The observation that lower specific activity was associated with the presence of DTT in purification buffers suggested that DTT could also contribute to the generation of an inactive form of the enzyme. This possibility was examined more closely by incubating purified enzyme with DTT, and monitoring the activity over a period of time.

Figure 4.9 Steady-state turnover of phenol hydroxylase with and without added catalase. Phenol hydroxylase activity in the absence (A) and presence of 200 U of catalase (B). Activity assays were done as described elsewhere (12) except that the phenol concentration was 150 μM.

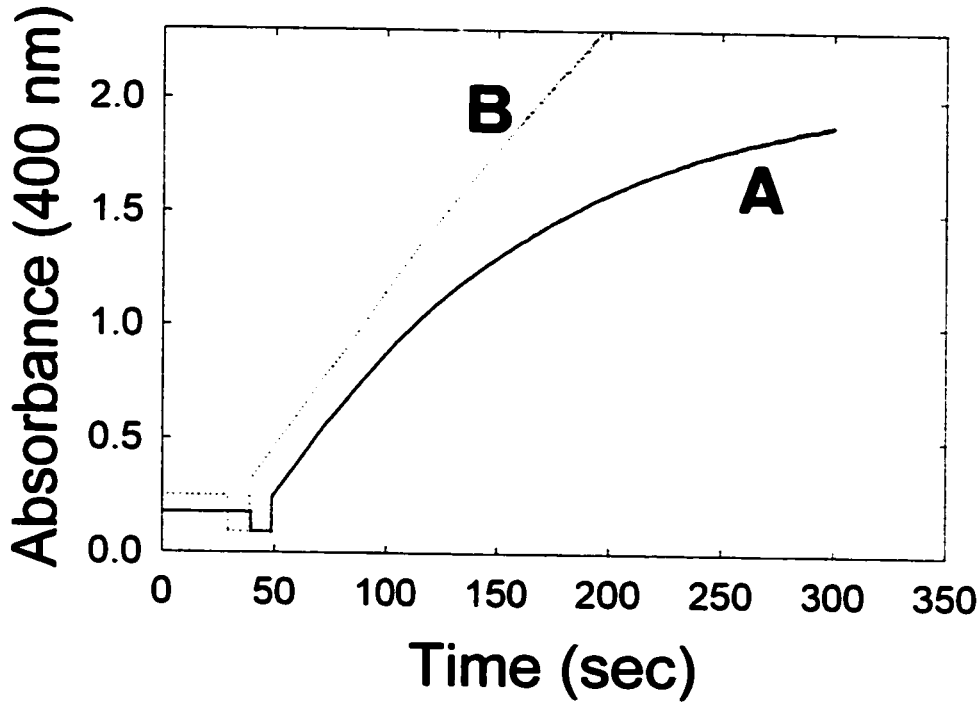
Absorbance (400 nm)
2.0
1.5
1.0
0.5
0.0
0
50
100
150
200
250
300
350
Time (sec)
B
A

Table 4.5 Reduction and reoxidation of DmpLNO

	% Activity			# electrons/Fe center		
	Reox1	Reox2	Reox3	Reduction1	Reduction2	Reduction3
Dithionite	97	82	66	2.5	2.9	3.1
NADH	Cannot be reduced without DmpM					
Dithionite + DmpM	95	87	75	2.2	3.1	4.7
NADH +DmpM	83	75	70	3.2	2.6	3.5

The presence of DTT caused large losses in the activity of the oxygenase: protection against these losses was afforded by the inclusion of catalase (Fig 4.10). Addition of DmpM or phenol to the sample containing DTT did not protect the oxygenase from inactivation (Fig 4.10). This suggests that DTT has its effect by acting as a peroxide generator, as has been previously described (24), although inactivation by DTT may also involve other factors, such as DTT's ability to act as a reductant or as a metal chelator. Interestingly, hydrogen peroxide itself did not inhibit the oxygenase when incubated with it under aerobic conditions (Fig 4.11A). However, incubation of the dithionite-reduced oxygenase with hydrogen peroxide under anaerobic conditions resulted in inactivation (Fig 4.11A).

These data suggest that inactivation by hydrogen peroxide occurs specifically with the reduced form of the enzyme. Since DTT may act as a peroxide generator, it is of interest to know whether the oxygenase diiron center can be reduced by it. When DTT was added to the oxygenase component under anaerobic conditions, bleaching of the 350 nm band indicated slow reduction of the binuclear iron center (data not shown). This sample was assayed periodically for activity over several days of storage under anaerobic conditions, and was found to retain it until O_2 was admitted (Fig 4.11B). These data suggest that inactivation of the enzyme with DTT involves reduction of the diiron center followed by a reaction with some form of O_2: protection of inactivation by catalase (see above) suggests peroxide formation is responsible. Consistent with this, addition of hydrogen peroxide to a dithionite-reduced oxygenase sample kept under anaerobic conditions resulted in loss of activity (Fig 4.11A).

Figure 4.10: Inactivation of the oxygenase component with dithiothreitol. Samples were prepared as described in *Experimental Procedures* and aliquots were periodically assayed for phenol hydroxylase activity. The concentrations of additives were : DTT, 1 mM, catalase, 1000 U, phenol, 1.6 mM, and DmpM, 9 μM.

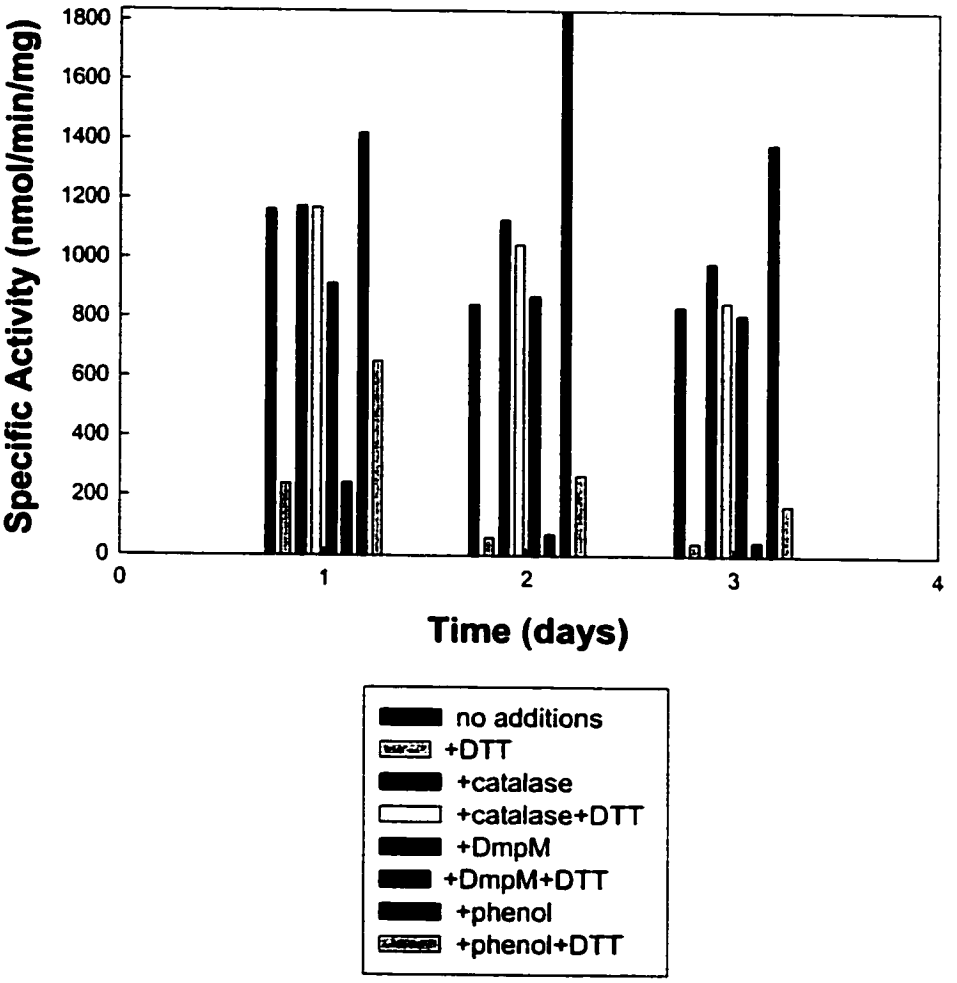
Specific Activity (nmol/min/mg)
1800
1600
1400
1200
1000
800
600
400
200
0
0
1
2
3
4
Time (days)
no additions
+DTT
+catalase
+catalase+DTT
+DmpM
+DmpM+DTT
+phenol
+phenol+DTT

Figure 4.11 Inactivation of DmpLNO by H_2O_2. (**A**): H_2O_2 (100:1 molar ratio of hydrogen peroxide to DmpLNO monomer) was added to oxidized DmpLNO (1 mg/mL) or anaerobic DmpLNO reduced with sodium dithionite (as described in *Experimental Procedures*). Phenol hydroxylase activity was monitored over time and assays were done in duplicate. Relative activity is the percentage activity relative to a fresh untreated DmpLNO sample. (**B**): DmpLNO (1 mg/mL) was reduced with excess dithiothreitol (see *Experimental Procedures*) and kept anaerobic. After 24 hrs, the sample was exposed to air and activity was monitored. [a] ND,not detectable.

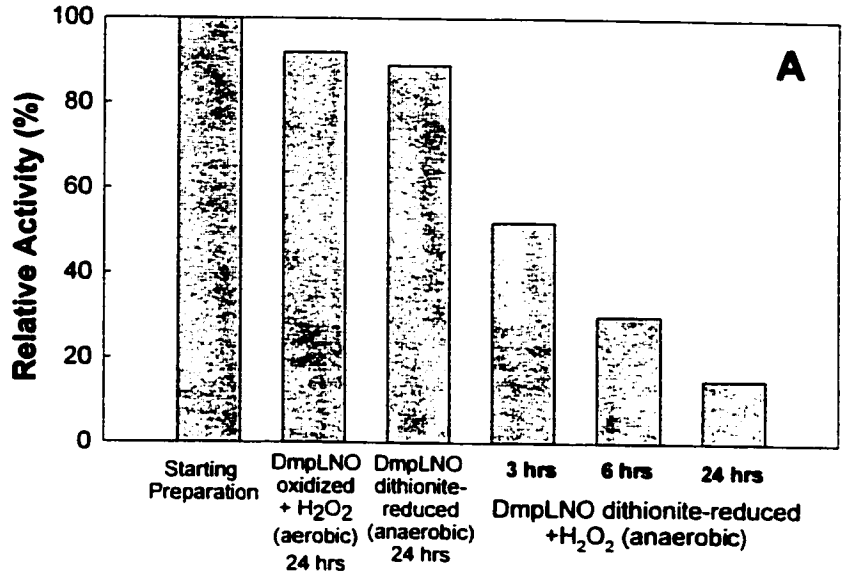
A
Relative Activity (%)
100
80
60
40
20
0
Starting Preparation
DmpLNO oxidized + H_2O_2 (aerobic) 24 hrs
DmpLNO dithionite-reduced (anaerobic) 24 hrs
3 hrs
6 hrs
24 hrs
DmpLNO dithionite-reduced +H_2O_2 (anaerobic)

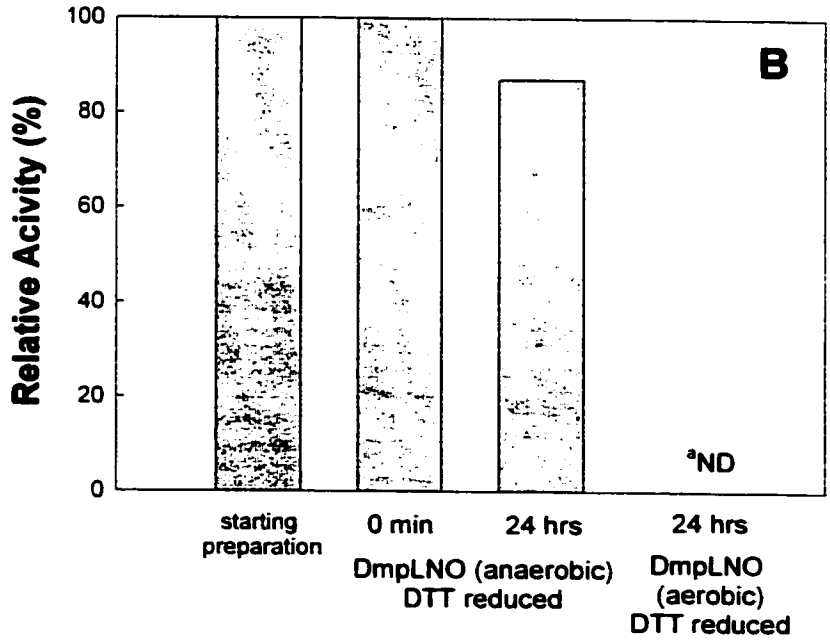
B
Relative Acivity (%)
100
80
60
40
20
0
[a]ND
starting preparation
0 min
24 hrs
DmpLNO (anaerobic) DTT reduced
24 hrs
DmpLNO (aerobic) DTT reduced

To test whether inactivation by DTT is related to chelation of the irons at the binuclear iron center, the DTT inactivated sample described in Figure 4.11B was dialysed against TG buffer to remove excess DTT and iron not bound to the protein. Activity was not regained after dialysis and addition of Fe^{2+} to this sample did not activate the enzyme. These data suggest that the DTT inactivated sample is not an apo form caused by removal of the binuclear irons by DTT. Consistent with this is the Mössbauer data described below.

Mössbauer spectroscopy of DTT-inactivated oxygenase

The DTT-associated inactivation mechanism was probed further by preparing a Mössbauer sample of oxidized enzyme in the presence of a large excess of DTT (see *Experimental Procedures*). Figure 4.12A shows a 4.2 K Mössbauer spectrum of this sample. The spectrum exhibits two major doublets and a minority species. Doublet a, representing ca. 45% of total Fe, has $\Delta E_Q(a) = 1.92$ mm/s and $\delta(a) = 0.39$ mm/s, while doublet b, also ca. 45% of Fe, has $\Delta E_Q(b) = 0.53$ mm/s and $\delta(b) = 0.35$ mm/s. The sample also contains a minor (6%) high-spin species with $\Delta E_Q = 2.9$ mm/s and $\delta = 1.3$ mm/s, reflecting either reduced dinuclear centers or adventitiously bound Fe. The isomer shifts of species a and b are substantially below those of the native diferric centers, suggesting thiolate coordination. Moreover, the observation of equal intensities for doublets a and b suggest that the two species are still constituents of a diferric center. That this is indeed the case is attested by the 7.0 T spectrum of Figure 4.12B which shows that species a and b are diamagnetic. Since monomeric ferric iron would yield spectra exhibiting paramagnetic hyperfine structure, the iron represented by species a and b must belong to

an antiferromagnetically coupled dinuclear center. Since both Fe sites have low isomer shifts, both must be coordinated to at least one thiolate. After completion of the Mössbauer study of the DTT-treated sample, the protein was dialyzed twice against TG buffer to remove excess DTT and iron not bound to the protein. The Mössbauer spectrum observed after dialysis was the same as that shown in Figure 4.12A, showing that the cluster observed in the spectra of Figure 4.12 is protein bound. Moreover, the data show that cluster-bound DTT is not removed by dialysis. The latter observation may explain why DTT inhibits the activity of the enzyme.

Figure 4.12 Mössbauer spectra of diferric phenol hydroxylase treated with excess DTT. The spectra were recorded at 4.2 K in zero field (A) and a parallel field of 7.0 T (B). The solid lines are spectra simulations using the parameters quoted in Table 4.3, and for the asymmetry parameter η the values $\eta(a) = \eta(b) = 0$.

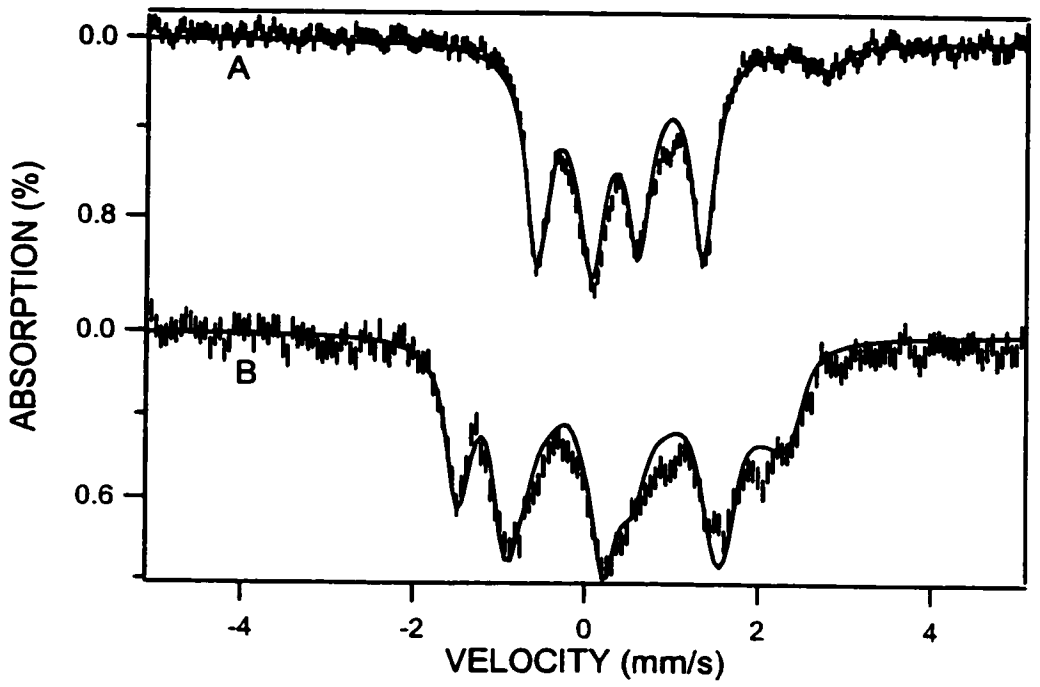
0.0
A
0.8
0.0
B
0.6
ABSORPTION (%)
-4
-2
0
2
4
VELOCITY (mm/s)

DISCUSSION

The present work has shown that the oxygenase component of phenol hydroxylase from *Pseudomonas* sp. strain CF600 is a dimeric protein composed of three subunits; DmpL, DmpN and DmpO, and containing a diiron center active site. Phenol hydroxylase is thus similar to other diiron cluster containing monooxygenases such as methane monooxygenase from *Methylococcus capsulatus* (Bath) or *Methylosinus trichosporium* OB3b (5), toluene-2-monooxygenase from *Burkholderia cepacia* G4 (25) and toluene-4-monooxygenase from *Pseudomonas mendocina* KR1 (23). The DmpN polypeptide contains the amino acid sequence motif assigned to the ligands of a diiron center. This motif was originally assigned in conjunction with various spectroscopic and X-ray crystallography data of the hydroxylase component of methane monooxygenase (26, 27). We have now confirmed the presence of a diiron cluster using Mössbauer spectroscopy.

Methane and toluene monooxygenases lack an optical spectroscopic feature between 300-800 nm, and several data suggest the presence of a hydroxo-bridged diiron cluster in these proteins (5, 23). In contrast, the oxygenase component of phenol hydroxylase exhibits a broad shoulder between 320-400 nm. This feature is reminiscent of the characteristic ligand to metal charge transfer interactions of the oxo-bridged diiron center present in ribonucleotide reductase (28) and stearyl-ACP Δ^9 desaturase (29). This optical feature along with the Mössbauer data suggest that the diiron cluster of phenol hydroxylase contains an oxo bridge. The mechanistic significance of the bridge variation in different oxygenases has not yet been defined.

DmpM shares amino acid sequence similarity with the well-characterised component B (MMOB) of the *M. capsulatus* and *M. trichosporium* OB3b methane

monooxygenases (30). MMOB has been shown to have multiple effects on methane monooxygenase including: increasing rate and yield in steady-state turnover (20,31); perturbation of the spectral properties of the diiron center (20); changing the redox potential of the diiron center (21, 32, 33); affecting the product distribution with isopentane as a substrate (34); and increasing the rate of association of the diferrous hydroxylase with O_2 (35). Chemical cross-linking with EDC showed that DmpM interacts with the diiron center containing polypeptide, DmpN, of the oxygenase component. Similarly, MMOB was shown to form a cross-linking product with the dinuclear iron centre bearing subunit of the hydroxylase component of methane monooxygenase from *M. trichosporium* OB3b (20). DmpM also had significant effects on both the multiple turnover rate and the product yield during single turnover reactions.

The single turnover experiments confirm that the site of phenol hydroxylation is on the oxygenase component of phenol hydroxylase, although product yields are very low in the absence of DmpM. Addition of DmpM dramatically increased the product yield, although it never exceeded 40% for any given preparation. Low yields during single turnover reactions have also been reported for toluene-4-monooxygenase from *Pseudomonas mendocina* KR1, where 8% product formation in the presence of activator protein was reported (23). Also, methane monoxgygenase from *M. trichosporium* yielded 40% product after single turnover in the absence of MMOB, increasing to 80% upon addition of MMOB (35). Low yields may result from the presence of inactive hydroxylase and/ or uncoupling reactions during turnover of the enzyme. In this work we have shown that all phenol hydroxylase preparations contain a proportion of apparently inactive species.

DTT is often used in purification buffers as a protective agent: thiols are often included in dinuclear iron center monooxygenase purification protocols. In the present study, we demonstrated that the presence of DTT is harmful to phenol hydroxylase activity, and the mechanism of inactivation was investigated. The protective effect of catalase in the oxygenase inactivation reactions with DTT suggests that the potent agent is H_2O_2, which has previously been shown to be generated by DTT (24). Addition of DTT to the oxygenase component under anaerobic conditions showed that DTT is able to reduce the diiron center and the enzyme remains active under these conditions until O_2 is added. Peroxide had no effect on the oxidized oxygenase but it was shown to inactivate the enzyme when incubated with an oxygenase sample that was reduced with dithionite. This suggests that peroxide by itself can inactivate the *reduced* oxygenase. Taken together, these data are consistent with an inactivation mechanism in which DTT first reduces the diiron center, followed by a reaction with O_2 to form H_2O_2. It is not clear whether H_2O_2 is generated by DTT or by the reduced diiron center reacting with O_2. The DTT thiolate ligand at the diiron site observed by Mössbauer spectroscopy must therefore be formed from a reaction involving H_2O_2.

A similar inactivation event is observed for the non-heme iron protein human 5-lipoxygenase (24). Purification of the lipoxygenase in the absence of DTT under aerobic condition resulted in higher specific activity compared to purification in the presence of DTT. The ferrous form of lipoxygenase was more sensitive to inactivation with hydrogen peroxide than the ferric form. From these data, the authors postulated that hydrogen peroxide is first generated by DTT and that the reaction of the active site Fe^{2+} with H_2O_2

generates an active oxygen species which could react with a side chain of an amino acid residue at the active site.

The Mössbauer studies unambiguously show that phenol hydroxylase contains dinuclear iron clusters similar to those observed in other diiron proteins. Thus, our studies have revealed a structure with antiferromagnetically coupled high-spin ferric sites that transform upon reduction with dithionite into high-spin ferrous sites. Furthermore, we have shown that the wild-type protein can accommodate two kinds of dinuclear clusters. The two iron sites in each Fe(III)Fe(III) cluster are indistinguishable by Mössbauer spectroscopy, but the quadrupole splittings for clusters I (ΔE_Q = 1.75 mm/s) and II (ΔE_Q = 0.80 mm/s) differ substantially. ΔE_Q-values larger than 1.5 mm/s have been found to be associated with μ-oxo bridged clusters such as those found in *E. coli* ribonucleotide reductase (36), *Ricinus communis* Δ^9 desaturase (37) and rubrerythrin (38), whereas ΔE_Q–values between 0.7 - 1.1 mm/s seem to be associated with hydroxo/water bridged clusters such as those observed in MMOH (see 5) and toluene-4-monooxygenase (23). Against this background cluster forms I and II represent μ-oxo and hydroxo (water) bridged clusters, respectively. This assignment is also supported by the estimated exchange coupling constants, J. Thus, from spectral simulations of the Mössbauer spectra of Figure 4.6 we have determined J = 120 cm^{-1} as a lower limit for the exchange coupling constant. J-values of oxo-bridged Fe(III)Fe(III) complexes fall into the 150-250 cm^{-1} range (39), and by combining our lower limit of J with ΔE_Q = 1.75 mm/s, we conclude that the iron sites of the ferric hydroxylase are most likely bridged by a μ-oxo group (perhaps supported by bridging carboxylate(s). This assignment is supported by the UV/visible spectra, which exhibit a broad feature centered around 350 nm. For three samples studied

extensively with Mössbauer spectroscopy the extinction coefficient at 350 nm varied between 5000-6400 cm^{-1} (or between and 7500 cm^{-1} if ε is solely attributed to the contribution of cluster I). These values compare quite well with ε(350 nm) $\approx$ 5000 cm^{-1} reported for $[Fe(III)_2O(Oac)_2(Me_3Tacn)_2]^2$ and ε(325-375 nm) $\approx$ 8000 M^{-1} cm^{-1} observed for oxidized ribonucleotide reductase (28). Based on magnetic circular dichroism and resonance Raman studies the latter transitions have been assigned to oxo-to-Fe charge transfer transitions. We are not sure why the ε_{350} varies so much between the preparations, but it should be noted that the extinction coefficient seems to increase as the amount of Fe per monomer decreases, suggesting that ε_{350} might contain a contribution from the tail of the absorption at 280 nm.

For cluster form II we found that excited S = 1 states of the spin ladder are already populated at 30 K, suggesting a substantially smaller J-value, consistent with a hydroxo-bridged cluster. The observation of two cluster forms in diiron proteins is not unprecedented. In fact, the two cluster forms observed here are very similar to those observed in Δ^9 desaturase for which a sample characterized by Mössbauer spectroscopy and EXAFS exhibited two doublets with ΔE_Q = 1.53 mm/s (μ-oxo form, 72%), ΔE_Q = 0.72 mm/s (μ-hydroxo form, 21%) and a minor form($\approx$ 7%) with ΔE_Q = 2.20 mm/s. For the desaturase the proportions of the two major forms were independent of pH between 6 and 10, showing that the cluster is sheltered from the solution pH and its state is not sensitive to the pH of the solution. Two species have also been observed for toluene-4-monooxygenase, with the hydroxo-bridged form (ΔE_Q= 0.93 mm/s, 85%) as the majority species; the minority species (15%) had ΔE_Q = 1.55 mm/s (23). However, it is interesting to note that single turnover reactions of toluene-4-monooxygenase resulted in only 8%

product yield, so in fact it may be the minority species that is active. Liu *et al.* have reported that MMOH isolated from *Methylococcus capsulatus* (Bath) contains two major forms of which only one (32% of Fe) was apparently active as assessed by kinetic studies (40).

It is well documented from crystallographic studies of methane monooxygenase that exogenous molecules such as acetate, methanol, ethanol and dimethylsolfoxide can serve as bridging ligands of the dinuclear center (reviewed in 5). It is generally not obvious whether a certain cluster form observed in the diferric state will be active because the cluster has to be reduced into the diferrous form before it reacts with oxygen and substrate. The X-ray structure of the Δ^9 desaturase shows a bis(carboxylato) bridged cluster in the reduced form (it has, however, not been established, whether this structure is also present in solution), and the bridging oxygen observed in the diferric cluster has been lost (41). Thus, one might suspect that it does not matter whether there was an oxo or a hydroxo bridge in the diferric state. On the other hand, the presence of a (hydrogen bonded) hydroxo bridge could impose a protein conformational state that might persist a considerable time. That hydroxylases can sustain altered conformations for a substantial amount of time has been shown by Lipscomb and coworkers (20).

In the present study we have found that the activity, as measured in the assay described in *Experimental Procedures*, is proportional to the concentration of the oxo-bridged cluster form. The observation that the activity, measured at room temperature, of a given preparation correlates well with the amount of cluster form I observed by Mössbauer spectroscopy at 4.2 K rules out the possibility that cluster form II is a freezing artifact. As pointed out above, we do not know at what step of the reduction/oxidation

cycle the conversion to cluster form II occurs. We may speculate that the conversion occurs in the reoxidation step that involves a step in the mechanism that differs substantially from the catalytic cycle followed in the presence of DmpM and substrate. In order to identify the root of the cluster transformation we have to learn to distinguish the two cluster forms in the reduced state of the protein. It would be interesting to learn how the cluster transformation can be reversed. Finally, given that the active form of MMOH contains a hydroxo-bridged cluster in the oxidized state, we were initially a bit surprised to learn that the catalytic activity of phenol hydroxylase is proportional to the amount of cluster form I. However, since little is known about to what extent a hydroxo bridge, observed in the diferric state of the cluster, affects the reaction steps that commence upon reduction, DmpM and substrate binding, we are not in a position to productively comment on this point.

ACKNOWLEDGMENTS

We thank Donald Tito for technical assistance. Elisabeth Cadieux was a recipient of a doctoral scholarship from Fonds pour la Formation de Chercheurs et l'Aide à la Recherche. This work was supported by a research grant from the Natural Sciences and Engineering Research Council of Canada.

REFERENCES

1. Dagley, S. (1986) in *The Bacteria* (Sokatch, J. R., and Ornston, L. N., eds), pp. 527-555, Academic Press, Inc. London.Ltd., London
2. Palfey, B., Ballou, D.P., and Massey, V. (1995) in *Reactive Oxygen Species in Biochemistry*, Vol II, Chapman and Hall, pp. 37-83
3. Lange, S.J. and Que Jr., L (1998) *Curr. Opin. Chem. Biol.* **2**, 159-172
4. Coulter, E.D., and Ballou, D.P. (1999) *Essays Biochem.* **34**, 31-49
5. Merkx, M., Kopp, D.A., Sazinsky, M.H., Blazyk, J.L., Müller, J., and Lippard, S.J. (2001) *Angew. Chem. Int. Ed.* **40**, 2782-2807
6. Gallagher, S.C., Cammack, B., and Dalton, H. (1997) *Eur. J. Biochem.* **247**, 635-641
7. Small, F.J., and Ensign, S.A. (1997) *J. Biol. Chem.* **272**, 24913-24930
8. Powlowski, J. and Shingler, V. (1994) *Biodegradation* **5**, 219-236
9. Teramoto, M., Futamata, H., Harayama, S., and Watanabe, K. (1999) *Mol. Gen. Genet.* **262**, 552-558
10. Powlowski, J., and Shingler, V. (1990) *J. Bacteriol.* **172**, 6834-6840
11. Cadieux, E. and Powlowski, J. (1999) *Biochemistry* **38**, 10714-10722
12. Powlowski, J., Sealy, J., Shingler, V., and Cadieux, E. (1997) *J. Biol. Chem.* **272**, 945-951
13. Philo, J.S. (2000) *Anal. Biochem.* **179**, 151-163
14. Brown, R.E., Jarvis, K.L. and Hayland, K.J., (1989) *Anal. Biochem.* **180**, 136-138
15. Gill, S.C. and von Hippel, P.H. (1989) *Anal. Biochem.* **182**, 319-326
16. Percival, M.D. (1991) *J. Biol. Chem.* **266**, 10058-10061

17. Laemmli, U. K., (1970) *Nature (London)* **227**, 680-685

18. Schagger, H. and von Jagow,G. (1987) *Anal. Biochem.* **166**, 368-379

19. Nordlund, I., Powlowski, J. and Shingler, V. (1990) *J. Bacteriol.* **172**, 6826-6833

20. Fox, B., Liu, Y., Dege, J.E., and Lipscomb, J.D. (1991) *J. Biol. Chem.* **266**, 540-550

21. Paulsen K. E., Lui Y., Fox B. G., Lipscomb J. D., Münck E., and Stankovich M. T. (1994) *Biochemistry* **33**: 713-722

22. Kauffmann, K. E., Popescu, C.V., Dong, Y., Lipscomb, J.D., Que Jr.,L., Münck, E. (1998) *J. Am. Chem. Soc.* **120**, 8739-8746

23. Pikus J. D., Studts J. M., Achim C., Kauffmann K. E., Münck E., Steffan R. J., McClay K. and Fox B. G. (1996) *Biochemistry* **35**, 9106-9119

24. Percival D. M., Denis D., Riendeau D., and Gresser M. J. (1992) *Eur. J. Biochem.* **210**, 109-117

25. Newman, L. M., and Wackett, L.P. (1995) *Biochemistry* **34**, 14066-14076

26. Lipscomb, J.D. (1994) *Ann. Rev. Microbiol.* **48**, 371-99

27. Rosenzweig A. C., Frederick C. A., Lippard S. J., Nordlund P. (1993) *Nature* **366**, 537-543

28. Sanders-Loehr, J. (1989) in *Binuclear Iron Center Proteins*, Loehr, T.M. (ed.) VCH, New York, pp. 375-466

29. Fox B. G., Shanklin J., Ai J., Loehr T. M., and Sanders-Loehr J. (1994) *Biochemistry* **33**, 12776-12786

30. Qian H., Edlund U., Powlowski J., Shingler V., Sethson I. (1997) *Biochemistry* **36**, 495-504.

31. Green, J., and Dalton, H. (1985) *J. Biol. Chem.* **260**, 15795-15801.

32. Liu, K. E., and Lippard, S. J. (1991) *J. Biol. Chem.* **266**, 12836-12839

33. Kazlauskaite J., Hill H. A., Wilkins P. C., and Dalton H. (1996) *Eur. J. Biochem.* **241**, 552-556

34. Froland W. A., Andersson K. K., Lee S. K. . Liu Y., Lipscomb J.D. (1992) *J. Biol. Chem.* **267**, 17588-97

35. Liu Y., Nesheim J. C., Lee S. K., and Lipscomb J. D. (1995) *J. Biol. Chem.* **270**, 24662-24665

36. Atkin, C. L., Thelander, L., Reichard, P., and Lang, G. (1973) *J. Biol. Chem.* **248**, 7464-7472

37. Fox B.G,. Shanklin J., Somerville C., and Münck E. (1993) *Proc Natl Acad Sci (USA)*, **90**, 2486-90

38. Ravi N., Prickril B. C., Kurtz D. M. Jr, and Huynh B. H. (1993) *Biochemistry* **32**, 8487-8491

39. Kurtz D. M. (1990) *Chem. Rev.* **90**, 585-606

40. Liu, K. E.; Valentine, A. M.; Wang, D. L.; Huynh, B. H., Edmondson, D. E.; Salifoglou, A. and Lippard, S. J. (1995) *J. Am. Chem. Soc.* **117**, 10174-10185

41. Lindqvist, Y., Huang W., Schneider G., and Shanklin J. (1996) *EMBO J.* **15**, 4081-4092

Chapter 5

Mutagenesis Studies on the Activator Protein, DmpM, of Phenol Hydroxylase

ABSTRACT

Site-directed and random mutagenesis were performed on DmpM to probe residues that might be involved in the interaction between DmpM and the oxygenase component. Although site directed mutation of 5 residues failed to affect activation of phenol hydroxylase in steady-state assays, the double mutant M37T/V77A, resulting from random mutagenesis, was unable to activate phenol hydroxylase. These results suggest that multiple substitutions are likely to be necessary to affect the interaction with the oxygenase component observed by steady-state activity assays.

INTRODUCTION

DmpM belongs to a family of activator proteins associated with non-heme iron containing multicomponent oxygenases (1-5). Phenol hydroxylase is the first enzyme in the phenol degradation pathway of *Pseudomonas* sp. strain CF600, and is comprised of three components: DmpP, DmpLNO and DmpM. DmpP is an FAD, [2Fe-2S]-centre containing reductase, DmpLNO is the oxygenase component containing a binuclear iron center, and DmpM is a cofactorless protein found to be essential for efficient catalysis in phenol hydroxylation (E. Cadieux, Ph.D. Thesis, Chapter 2). Chemical cross-linking data showed that DmpM interacts with DmpN, the binuclear iron center containing polypeptide of the oxygenase component. The steady-state turnover rate of phenol hydroxlase was shown to be dependent on DmpM concentration with a maximum rate observed at 1.5 DmpM per oxygenase. DmpM was also shown to affect single turnover reactions by increasing the product yield from 3% in the absence of DmpM to 40% in its presence (E. Cadieux, Ph.D. Thesis, Chapter 4).

DmpM shares sequence similarity with other proteins associated with multicomponent oxygenases including MMOB from *M. capsulatus* (Bath), component B of *M. trichosporium* OB3b, T4MOD from *Pseudomonas mendocina*, and TbmC from *Pseudomonas putida* (2-5). The best-characterised effector protein is MMOB associated with the methane monooxygenase system. MMOB has been shown to play several roles in catalysis, including: increasing the steady state turnover 150 fold (2); affecting the redox potential of the diiron center of the hydroxylase (6,7); modifying the regioselectivity of hydroxylation (8); and increasing the rate of O_2 reactivity with the

reduced form of the diiron center (9). Even though much data has been accumulated on MMOB, a mechanism for how this protein exerts its effects is still unknown.

Recently, a series of single, double and quadruple mutants of MMOB were made based on NMR, proteolysis, and sequence alignment data that suggested possible interaction sites with the oxygenase (10). All mutants studied exhibited no difference in steady-state turnover rates compared to wild-type MMOB although a few showed a slight effect on the formation and decay rates of some of the intermediates of the catalytic cycle during single turnover experiments.

In this study, site-directed and random mutagenesis were used to investigate residues on DmpM that may be involved in interaction and/or catalysis with the oxygenase component of phenol hydroxylase.

METHODS AND MATERIALS:

Materials: DTT and NADH were obtained from Roche Molecular Biochemicals; phenol, urea, guandinium hydrochloride and glycerol (Ultra Pure grade) were from ICN Biomedicals. Catechol 2,3-dioxygenase was purified as described previously (11). Purification of the oxygenase component (DmpLNO) of phenol hydroxylase is described in this thesis, Chapter 4, and the reductase (DmpP) was purified using a previously published protocol (12). All restriction enzymes were purchased from Promega.

Analytical methods: Protein concentrations were estimated using the bicinchoninic acid (BCA) method (Pierce) following the 60°C protocol supplied by the manufacturer. Interfering substances such as DTT were removed using a modification of this method (13). Circular dichroism spectra were collected using a Jasco J-710 CD spectrometer. Electrospray mass spectrometry was done using a Finnigan SSQ 7000 single quadrupole mass spectrometer. All samples were passed through a 1 cm C-18 small molecule cartridge (Michrom BioResources) interfaced to the mass spectrometer. Initially the cartridge was equilibrated with 95% water-5% acetonitrile-0.05% trifluoroacetic acid, and elution was with 35% water-65% acetonitrile-0.05% trifluoroactic acid. SDS-polyacrylamide gel electrophoresis was performed using a Tris-glycine buffer (14) or Tricine buffer system (15). Native gels were purchased precast from ICN (CAP-Gels, 10-20% Tris/Borate/ EDTA, pH 8.3, native format, 8 x 10cm), or from BioRad Laboratories (Ready Gels, 10-20% Tris-HCl, native format, 8 x 10cm).

DNA manipulations: DNA manipulations were done according to standard techniques (16). DNA was purified using Wizard Miniprep kits, and DNA sequencing was performed by McGill University Sheldon Biotechnology Center and the Center for Structural and Functional Genomics at Concordia University. The strategy for cloning *dmpM* into pET3a, a T7-polymerase based expression vector (17), was essentially as described previously (18).

Bacterial growth: The site-directed *dmpM* mutant genes were constructed in the T7-based plasmid, pET3a (Novogen), and expressed in *E. coli* BL21(DE3) using methods described for the recombinant wild-type DmpM (E. Cadieux, Ph.D. Thesis, Chapter 2).

Site-directed mutagenesis: Site-directed mutagenesis was done by following the Quickchange protocol (Stratagene). All mutant *dmpM* genes were sequenced to verify the construct. Mutations were also confirmed by electrospray mass spectrometry. Oligonucleotides used to make the mutations were E20A: 5'-CGTTACGTGGTGGCGG CGATCATCCAGG-3'and 5'CCTGGATGA TCG CCGCCACCACGTAACG-3', E55A: 5'-GGGAAACCG TGGA AGCGAACCTCGGCCGC-3' and 5'-GCGGCCGAGGTT C GCTTCCACGGTTTCCC-3', E55K: 5'-GCGGCCGAGGTTC TTTTCCACGGT TTCC C-3' and 5'-GGG AAACCG TGGAAAAGAACCTCGGCCGC-3', K44A: 5'-GGATCT CCAGGCGCGAATCGGCC TCG-3' and 5'-CGAGGCCGATTC GCGCCTGGAGA TC C-3', K44E: 5'-GGATCTCC AGGCGTTCCTCGGCCTCG-3' and 5'-CGAGGCCG AG

GAACGC CTGGAGATCC-3', T52Y: 5'-GGTTCTCTTCCACGAC GTATTCCCTGC GG-3' and 5'-CCGCAGGGA AT ACGTCGTGGAAGAGAACC-3', K89A: 5'-GTCCT CGAGTGGGCG AACTAGGAGA CAAGC-3' and 5'-GCTTGTCTCCTAGTTCGCCC ACTCGAGGAC-3', M37T: 5'-GCACCACCCGGCGACGATCC GTAT CGAGG-3' and 5'-CCTCGATACGGATCGTC GCCGGGTGGTGC-3', V77A: 5'-CCATCGGCGG CAAC GCGGA CGAGGACGAT GA CC-3' and 5'-GGTCATCGTCCTCGTCCGCGT TGCCGCCGATGG-3'

Random Mutagenesis: Introduction of random mutations into the *dmpM* gene was done using error prone PCR, as described by Juili L. Lin-Goerke *et al.* (19). Lowering of the $MnCl_2$ concentration to 0.05 mM, a slight alteration to the published method, was found necessary to yield an average of 2 mutations per gene. Error prone PCR was performed using pVI258 (20) as the template. Primers used for PCR were designed to also introduce *Nde I* and *BamH I* restriction sites at the beginning and at the end of the *dmpM* gene, respectively. The PCR product, containing a population of mutated *dmpM* genes, was then ligated into the pCRII vector (Invitrogen) and transformed into *E. coli* DH5. The transformants were resuspended in LB (5 ml), cells were centrifuged and the DNA was isolated. The population of mutated pCRII (*dmpM)* plasmid was cut with *Nde I* and *BamH I* restriction enzymes. The fragments were purified from agarose gels using a Sephaglas kit (Pharmacia) and ligated to pSBET3a vector cut with *BamH I* and *Nde I*. After ligation, the resulting plasmids were transformed into *E. coli* BL21DE3-pVI290Δ (already containing the pVI290Δ plasmid (21).

Selection and screening for soluble DmpM variants: First, pVI290Δ harbouring *dmpKLNOP*, was transformed into *E. coli* BL21(DE3) using carbenicillin selection (100 μg/mL). This plasmid expresses inactive phenol hydroxylase because it lacks the *dmpM* gene. Cells containing inactive phenol hydroxylase, when grown on LB supplemented with tryptophan and tyrosine, were found to form cream-coloured colonies whereas cells with active phenol hydroxylase form brown colonies. pSBET3a(*dmpM*) variants were transformed into the BL21(DE3) harbouring pVI290Δ using carbenicillin (100 μg/mL) and kanamycin (50 μg/mL) selection. These double transformants were grown on LB supplemented with tryptophan and tyrosine to screen for *dmpM* variants affecting phenol hydroxylase activity. Cream-coloured colonies were picked and inoculated in LB (5 ml) containing carbenicillin (100 μg/mL) and kanamycin (50 μg/mL). The cells were grown overnight at 37°C. Cells were then centrifuged, and resuspended in LB (5 ml). After dilution (1:100) into fresh LB containing carbenicillin (100 μg/mL) and kanamycin (50 μg/mL), cells were grown until OD_{600}= 0.8 at which point IPTG was added to 0.5 mM. Cells were allowed to grow for another 4 hours before harvesting. Cell pellets were stored at -20°C until use.

After resuspension in 50 mM sodium phosphate pH 7.5 + 10% glycerol , cells were broken by sonication and the solubility of the DmpM variant was verified by SDS-polyacrylamide gel electrophoresis of crude extracts and insoluble fractions.

Purification of DmpM variants: DmpM variants were purified as described previously for the recombinant DmpM (E. Cadieux, Ph.D. Thesis, Chapter 2).

Purification of Native DmpM: Purification of Native DmpM from *Pseudomonas* sp. strain CF600 has been reported previously (E. Cadieux, Ph.D. Thesis, Chapter 2).

Purification of the oxygenase: The oxygenase component of phenol hydroxylase was purified as described elsewhere (E. Cadieux, Ph.D. Thesis, Chapter 4).

Phenol hydroxylase activity assays: Multiple turnover reactions were done as described previously (11).

RESULTS

Steady-State Activity of Site-directed DmpM Variants. The site directed variants, S1A, E20A, E55A, E55K, in this study were chosen based on the conserved residues of the protein sequence alignment of DmpM with other non-heme oxygenase effector proteins shown in Figure 5.1. K89A, K44A, K44E were chosen from NMR experiments detecting DmpM residues that possibly interact with the oxygenase component (18).

Each variant protein was overexpressed and purified as described in *Experimental Procedures*, and checked by mass spectrometry to confirm the presence of the mutation. Since recombinant DmpM has been found to be expressed as an inactive dimer (E. Cadieux, Ph.D. Thesis, Chapter 2), the oligomerization state of all purified mutants was verified by native gel electrophoresis. Mutants that were found to be dimers after purification were converted to monomer using the activation techniques described previously (E. Cadieux, Ph.D. Thesis, Chapter 2). Most of the site-directed variants of DmpM showed no difference in activity compared to wild-type DmpM (Table 5.1). M37T variant had 70% activity compared to wild-type DmpM.

DmpM Variant generated by Random Mutagenesis. Since none of the site-directed mutant DmpM proteins exhibited a significant change in the stimulation of phenol hydroxylase activity, random mutagenesis was attempted. Error-prone PCR described by Lin-Goerke *et al.* was carried out under conditions to obtain an average of 2 point mutations per gene. Out of 76 colonies tested, 8 were selected because they failed to turn the characteristic brown colour of cells expressing active phenol hydroxylase. The 8 cream-coloured colonies were tested for expression, and 2 were soluble. DNA encoding

the soluble variants was sequenced to identify the mutations, which were then confirmed in the purified protein using ESI-MS. This technique resulted in one double mutant that could not activate phenol hydroxylase *in vitro*. The variant was identified as M37T/V77A. Native gel electrophoresis confirmed the oligomerization state as monomer (data not shown). Far-UV circular dichroism spectra of the double mutant and wild-type proteins were essentially the same (data not shown), suggesting no major secondary structural difference caused by introducing the two substitutions. In order to verify whether the double mutation was essential for inactivation, the site-directed mutants, of M37T and V77A, were generated. Both M37T and V77A single mutants were able to activate phenol hydroxylase activity as wild-type DmpM (Table 5.1).

Figure 5.1 Protein Sequence Alignment of DmpM with Other Non-Heme Oxygenase Effector Proteins. The protein sequences labeled are: PH3 from *A. calcoacaticus*, TbmC from *Pseudomonas putida*, T4MOD from *Pseudomonas mendocina*, component B from *M. trichosporium* OB3b, and component B from *M. capsulatus* (Bath). Sequences were aligned using MultAlin Software (F. CORPET, 1988, *Nucl. Acids Res.*, 16, 10881-10890).

```
                                                                1
DmpM    .......... .......... .......... ..MSSL.VYI AFQDNDNARY
PH3     .......... .......... .......... ..MTSK.VYL ALQDNDTSRY
TbmC    .......... .......... .......... ...MSQ.VFI AFQANEESRA
T4MOD   .......... .......... ....XTLADQ ALHNNN.VGP IIRAGDLVEP
B-OB3b  MSSAHNAYNA GIMQKTGKAF ADEFFAEENQ VVHESNAVVL VLMKSDEIDA
B-Bath  MSVNSNAYDA GIMGLKGKDF ADQFFADENQ VVHESDTVVL VLKKSDEINT

        18                                                      59
DmpM    VVEAIIQDNP ..H....AVV QHHPAMIRIE AEKRLEIRRE TVEENLGRAW
PH3     IIEAIEQDNP ..E....ATI QYLPAMIRVE STGELVVRAE TVSEKLGQNW
TbmC    VIEAIVTDNP ..E....AVV TYPTGLVKID APGRLTIRRE TIEEQTGRPF
T4MOD   VIETAEIDNP GKE....ITV EDRRAYVRIA AEGELILTRK TLEEQLGRPF
B-OB3b  IIEDIVLKGG KAK.NPSIVV EDKAGFWWIK ADGAIEIDAA EAGELLGKPF
B-Bath  FIEEILLTDY KKNVNPTVNV EDRAGYWWIK ANGKIEVDCD EISELLGRQF

        62
DmpM    DVQEMLVDVI TIGGNVDEDD DRFVLEWKN. .......... .
PH3     DIQELQLNMI TLGGNVDEDD DSFTLKWN.. .......... .
TbmC    DLQQLHVNLV TLSGHIDEDD DQLTLSWQH. .......... .
T4MOD   NMQELEINLA SFAGQIQADE DQIRFYFDKT M......... .
B-OB3b  SVYDLLINVS STVGRAYTLG TKFTITSELM GLDRALTDI. .
B-Bath  NVYDFLVDVS STIGRAYTLG NKFTITSELM GLDRKLEDYH A
```

Table 5.1 Relative Phenol Hydroxylase Activity in Steady-State Turnover[a]

DmpM variant	Relative Activity
S1A	90
K44A	94
K44E	96
E55A	96
E20A	84[b]
K89A	120
M37T	70
V77A	87
M37T/V77A	8

[a] Reaction conditions are described elsewhere (11). Activity is expressed in percentage relative to wildtype DmpM. 1.5:1 molar ratio of the DmpM variant to oxygenase component was used in activity assays. [b] E20A variant was partially purified (see *Experimental Procedures*) therefor the amount of variant used in the activity assay is not known.

DISCUSSION

DmpM is part of a family of activator proteins associated with binuclear iron center containing multicomponent oxygenases (1-5). Effector proteins have been shown to play several roles in hydroxylation of substrate, yet the structural interactions between the activator and the oxygenase that bring about the effects have not been determined. In this study, we attempted to identify specific residues on DmpM that are involved in activation of hydroxylase activity. Knowledge of the residues on DmpM important for catalysis will give insights into the mechanism by which DmpM functions.

Eight site-directed mutations on DmpM were made, but none of them significantly affected the steady-state turnover rate of the hydroxylase. Several possibilities can explain this observation. i) None of the residues investigated are involved in the interaction with the oxygenase or are important for catalysis. ii) Several residues are involved in the interaction with the oxygenase component and more than one residue change is required to observe a significant difference in multiple turnover rate. iii) The mutations may affect steps in the catalytic cycle that are not rate limiting.

The third possibility has in fact been reported in a study of the effector protein of methane monooxygenase from *M. trichosporium* OB3b (10). Two conserved residues were mutated to determine their function and were found to have very little effect on multiple turnover rate compared to the wild-type: however, both mutants affected different steps in the catalytic cycle. The experiment demonstrates that MMOB exerts regulatory effects throughout the catalytic cycle since the variants affected different steps in the catalytic cycle. In the same study, a quadruple mutant N107G/S109A/S110A/T111A was made in the core of the MMOB protein to determine

if a polar loop was involved in interaction with the oxygenase as was suggested in NMR experiments. The authors predicted that this mutation would inhibit catalysis, but the opposite was observed. The turnover rate for methane was not changed and when larger substrates were used, the turnover rate doubled. When the kinetics of formation and decay of the intermediates of the catalytic cycle were examined, the quadruple mutant was found to affect different steps in the cycle depending on the substrate used. Without detailed knowledge of the intermediates in the catalytic cycle of phenol hydroxylase, it is difficult to demonstrate which of the three possible explanations listed above represents the true effect of the mutants.

Random mutagenesis was used to screen DmpM mutants that had an effect on phenol hydroxylase activity. This method was successful in identifying a double mutant, M37T/V77A, that could not activate phenol hydroxylase activity. Sequence alignments show that neither of these residues is conserved amongst other effector proteins. Site directed mutations were made of each residue separately, and the variants were overexpressed, purified and tested for activity. The single mutants were active thus confirming that the double mutation is essential for affecting catalytic activity. Further experiments are required to reveal the basis for inactivity. It may be worthwhile to carry out random mutagenesis of DmpM with a higher error frequency. MmoB with four mutations (3), and our DmpM mutants of conserved residues, were all active suggesting that the structures of these proteins can tolerate multiple substitutions. Since protein-protein interactions between DmpM and the hydroxylase are likely to involve many residues on the protein surfaces, it is likely that multiple mutations would be necessary to affect the interaction enough to change the rate-limiting step in steady-state turnover.

REFERENCES

1. Powlowski, J. and Shingler, V. (1994) *Biodegradation* **5,** 219-236
2. Fox, B.G., Froland, W.A., Dege, J.E., and Lipscomb, J.D. (1989) *J. Biol. Chem.* **264**, 10023-10033
3. Newman, L., and Wackett, L. (1995) *Biochemistry* **34**, 14066-14076
4. Green J, Dalton H.(1985) *J. Biol. Chem.* 260, 15795-801
5. Pikus J.D., Studts J.M., Achim C., Kauffmann K.E., Munck E., Steffan R.J., McClay K., Fox, B.G. (1996) *Biochemistry* **35**, 9106-19
6. Paulsen K.E., Liu Y., Fox B.G., Lipscomb J.D., Munck E., Stankovich M.T. (1994) *Biochemistry* **33**, 713-22
7. Gassner G.T., Lippard S.J. (1999) *Biochemistry* **38**, 12768-85
8. Froland W.A., Andersson K.K., Lee S.K., Liu Y., Lipscomb J.D. (1992) *J. Biol. Chem.* **267**,17588-97
9. Liu Y., Nesheim J.C., Lee S.K., Lipscomb J.D. (1995) *J. Biol. Chem.* **270**, 24662-5
10. Wallar B.J., Lipscomb J.D. (2001) *Biochemistry* **40**, 2220-33
11. Powlowski, J., Sealy, J., Shingler, V., and Cadieux, E. (1997) *J. Biol. Chem* **272**, 945-951
12. Powlowski, J. and Shingler, V. (1990) *J. Bacteriol.* **172**, 6834-6840
13. Brown R.E., Jarvis K.L., and Hyland K.J. (1989) *Anal. Biochem.* **180,** 136-138
14. Laemmli, U. K., (1970) *Nature (London)* **227**, 680-685
15. Schagger, H. and von Jagow,G. (1987) *Anal. Biochem.* **166**, 368-379

16. Sambrook, J., Fritsch, E.F., and Maniatis, T. (1989) *Molecular Cloning: A Laboratory Manual*, 2nd ed., Cold Spring Harbor Laboratory, Cold Spring Harbor, New York

17. Rosenburg, A.H., Lade, B.N., Chui, D.-S., Lin, S.W., Dunn, J.J., and Studier, F.W. (1987) *Gene (Amst.)* **56**, 125-135

18. Qian, H., Edlund, U., Powlowski, J., Shingler, V., and Sethson, I. (1997) *Biochemistry* **36,** 495-504

19. Lin-Goerke L. J., Robbins D. J., and Burczak J. D. (1997) *BioTechniques* **23**, 409-412

20. Bartilson, M., Nordlund, I., and Shingler, V. (1990) *Mol. Gen. Genet.* **220**, 294-300

21. Nordlund, I., Powlowski, J., and Shingler, V. (1990) *J. Bacteriol.* **172**, 6826-6833

ACKNOWLEDGMENT

We thank Mark Krasny for technical assistance on the DmpM random mutagenesis experiments.

Chapter 6

Summary

In the process of characterising the interaction of DmpM with the oxygenase component of phenol hydroxylase, recombinant DmpM was found to be inactive (Chapter 2). The inactive form was found to be a dimer, unlike wild-type DmpM which is monomeric. The inactive form was activated by treatment with trifluoroethanol, urea, or heat, and activation was shown to be concomitant with dimer dissociation. Very little is known about the way in which stimulatory proteins interact with the oxygenase components. Information about this interaction is critical to an understanding of the activation process. It was therefor essential to have an active wild-type recombinant form of DmpM in order to construct the site-directed variants described in Chapter 5.

Chapter 3 describes an investigation of the role of DmpK in iron insertion into the oxygenase component of phenol hydroxylase. In this study it was shown that DmpK increases the rate of iron insertion into the oxygnase component, and causes displacement of Mn^{2+} by Fe^{2+} at the binuclear site. DmpK does not seem to be an iron donor to the oxygenase, since it does not stably bind Fe^{2+}, but it appears to stimulate a conformational change at the metal binding site to decrease the Mn^{2+} binding affinity and facilitate iron insertion. Further studies on the mechanism of protein assisted binuclear iron center assembly necessitates finding of the physiological iron donor. The work done on DmpK provides the first evidence of a protein involved in assembly of a binuclear iron center.

In Chapter 4, characterisation of some key features of the oxygenase component of phenol hydroxylase was reported. The oxygenase comprises three polypeptides, DmpLNO. Single turnover studies provided evidence that the oxygenase contains the

site of phenol hydroxylation: in the absence of DmpM the yield of product from a single turnover was 2.5%, while in its presence a 40% product yield was observed. Mössbauer spectroscopy showed the presence of a binuclear iron center in DmpLNO. Two major species of binuclear iron center differing in bridge structure were identified, with the proportion of each varying somewhat between preparations. These species were identified as oxo-bridged and hydroxo-bridged diiron centers. Other oxygenases such as methane and toluene monooxygenase have been shown to contain a hydroxo-bridged diiron center (1,2). The significance of these various diiron bridges in different oxygenases is not known. Investigation into whether the low product yield after single turnover was related to the two species of binuclear iron center led to the finding that dithiothreitol, often used as a protective agent, inactivates phenol hydroxylase by forming a thiolate ligand to the binuclear iron center. This inactivation probably involves reduction of the iron center by DTT and production of hydrogen peroxide that participates in thiolate-iron bridge formation.

Chapter 5 described site-directed variants of DmpM that were made based on conserved residues amongst activator proteins associated with multicomponent oxygenases and NMR experiments on DmpM (3). None of the site-directed variants differed in their ability to activate phenol hydroxylase as monitored by steady-state turnover, which was somewhat surprising. Random mutagenesis provided a double mutant, M37T/V77A, that was apparently properly folded but inactive. Further characterisation of the double mutant is necessary to determine why it is inactive. Site-directed mutagenesis of selected MmoB residues was previously shown to have no effect

on the steady-state turnover rate of methane monooxygenase, but the variants did have effects on various intermediates in the catalytic cycle (4). In order to fully characterise the site-directed and random DmpM variants, it would be necessary for the intermediates in the catalytic pathway of phenol hydroxylase to be determined before such studies could be done.

REFERENCES

1. Fox, B. G., Liu Y, Dege, J. E., and Lipscomb, J. D. (1991) *J. Biol. Chem.* **266**, 540-550

2. Pikus, J. D., Studts, J. M., Achim, C., Kauffmann, K. E., Münck, E., Steffan, R. J., McClay, K. and Fox, B. G. (1996) *Biochemistry* **35**, 9106-9119

3. Qian, H., Edlund, U., Powlowski, J., Shingler, V., and Sethson, I. (1997) *Biochemistry* **36,** 495-504

4. Wallar, B.J. and Lipscomb, J.D. (2001) *Biochemistry* **40**, 2220-3